DOT AND STRIPE ARRAYS AS SURFACE ACOUSTIC WAVE REFLECTORS:

A Thesis for the Degree of Doctor of Philosophy

by

ANDREW STOVE,

St. Catherine's College.

Michaelmas 1980.

"Then I saw a new heaven and a new earth, the
"first heaven and the first earth had disappeared
"now, and there was no longer any sea."

Revelation of St.John
the Divine, 21:1.

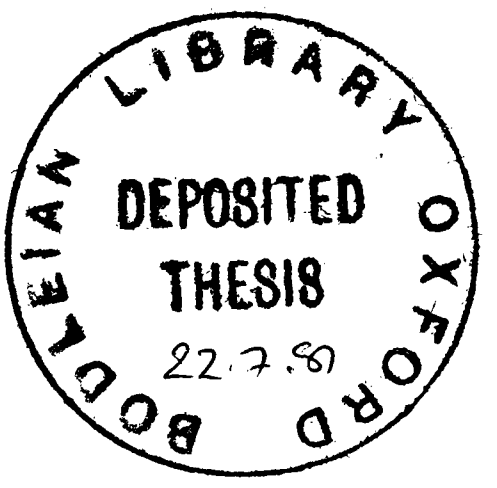

DOT AND STRIPE ARRAYS AS SURFACE ACOUSTIC WAVE REFLECTORS

A Thesis for the Degree of Doctor of Philosophy

by ANDREW STOVE
St. Catherine's College
Michaelmas Term 1980

ABSTRACT

Reflective dot arrays represent a promising innovation in the field of surface acoustic wave devices. This work has investigated a simple model for uniform rectangular dot arrays. From this model the reflection coefficents of the dots and the correct angle for the array's reflectors can be deduced. Experimental results for these parameters are reported for some specific types of metal dot array using aluminium dots on Y-cut lithium niobate. Several different arrangements of dots within the arrays have been investigated, and their different advantages and disadvantages are contrasted. The use of specific array patterns to suppress undesired reflection modes has been investigated, and it has been shown that such suppresion can be achieved by this means.

Some information has been gathered on the reflection properties of different shapes of metal dots and with different thicknesses of metal. The properties of these different dot types have been compared and their implications on a theory for the behaviour of reflective metal dots have been discussed.

Experimental results have been obtained for the reflection of surface waves on YZ lithium niobate by thin metal strips at normal incidence. These results have been shown to agree with the available theoretical models for the problem. The effect of the mutual capacity of the strips on their behaviour has been shown to be important if several of them are grouped together. This part of the work is seen as a preliminary to the possible development of a model for the reflection properties of metal dots.

Two inline reflective dot array devices have been made. The results reported show that the principle of these devices has been sucessful, but that more work is still needed if they are to fulfil their full promise.

ACKNOWLEDGEMENTS

I must first acknowledge the help of my supervisor, Professor E.G.S. Paige, without whose help, advice, knowledge and encouragement this work just could not have been done at all. I would also like to thank Dr. L. Solymar for his interest in my work and for his helpful comments. Dr. P. Bloch must be similarly thanked, as well as for his help with computing.

I must thank Brian French for his constant practical help and patience, and especially for making many of the devices used in this work. I must thank Mike Wagg for many deep and useful discussions.

Thanks must also be due to the Ministry of Defence Committee for Valve Development for supporting this work, and to Drs. F.G. Marshall and G.L. Moule for acting as its sponsors.

Many thanks are also due to Dr. D. Snell and to Mr A. Young of R.S.R.E. Malvern for much help in the manufacture of masks and devices.

If I were to adequately express the help and support which I have received over three years from so many other people, this section would begin to exceed in length the rest of this thesis, so I must just thank also those Catzpersons, past and present with whom I have spent evenings drinking coffee and at Catz. bar,for trying to keep me sane and cheerful.

INDEX

LIST OF SYMBOLS AND ABBREVIATIONS

a.c.	alternating current
d.c.	direct current
f	frequency
i.f.	intermediate frequency
ILRAC	In Line Reflective Array Compressor
k^2	Piezoelectric coupling coefficent
l.o.	local oscillator
Q	Electrical Quality factor
r.f.	radio frequency
R.S.R.E.	Royal Signals and Radar Establishment
RAC	Reflective Array Compressor
RAD	Reflective Array Device
RDA	Reflective Dot Array
TB	(usually) Time-Bandwidth Product (of a Disperser)
U.C.L.	University College, London
U.H.F.	Ultra High Frequency
v	velocity
V.H.F.	Very High Frequency
δf	frequency deviation
$\delta \lambda$	change in wavelength
δv	change in velocity
λ	wavelength
θ	array reflector inclination to incident wave.

CHAPTER 1

INTRODUCTION

1.1: Properties of Surface Acoustic Waves

Surface acoustic waves are propagating mechanical disturbances on the surfaces of solid or liquid media. They are characterised by the fact that they are almost entirely confined to the surface of the medium along which they are propagating, with essentially no disturbance in the bulk of the material. They are ideally non-dispersive and lossless. Ripples on the surface of water are an example of surface waves propagating on a liquid medium.

The behaviour of surface waves on isotropic substrates was first investigated by lord Rayleigh about a hundred years ago[1], but it was only about fivteen years ago that surface waves began to be exploited for the production of signal processing devices[2]

The substrates used for surface wave devices are normally monocrystalline piezoelectrics. The characteristics of the surface waves on such substrates are, of course, anisotropic. This anisotropy is an important factor in the design of certain types of surface wave devices, and is responsible for a major part of the complexity of the work to be described in this thesis. It is in any case always necessary to choose the propagation direction of the waves with care in designing a surface wave device.

The most common materials used for the substrates of surface wave devices are Y-cut lithium niobate and ST-cut quartz, the preferred propogation directions on these two substrates being

in the Z- and X- directions of the crystal repectively.

The surface waves thus used have velocities of the order of three kilometres per second, which is very low for a signal in an electronic system, hence the original interest in surface wave delay lines. The wave is essentially lossless and dispersionless below one gigahertz or so. The loss is proportional to the square of the frequency of the wave, and on lithium niobate is about one decibel per microsecond at one gigahertz, a respectibly low figure. The losses on quartz are slightly lower. This low loss of the surface wave allows the fabrication of very high-Q resonators at U.H.F., and is another advantage of surface waves.

Two other important properties of the surface wave substrate which are important in the manufacture of part of an electronic signal processing system are the temperature coefficent of the wave velocity, dv/dt, and the piezoelectric coupling to the wave, k^2. The first of these is obviously important for the temperature stability of any device, and the second, measuring the efficency of coupling between the acoustic device and the rest of the electrical system, controls the relationship between the maximum attainable bandwidth of the device and its insertion loss. It will be shown in part three of this chapter that it is to some extent possible to trade between bandwidth and insertion loss in a surface wave device.

It is on the question of whether bandwidth and insertion loss or temperature stability is more important that the choice is normally made between lithium niobate and quartz for substrate material. The properties of the two materials in this regard are

compared in table 1.1 below.

	Substrate and Propogation Direction	
Property:	Y-cut, Z-propogating Lithium Niobate	ST-cut, X-propogating Quartz
k^2	4.5%	0.16%
dv/dt	85ppm/K	0

Table 1.1: Trade-Offs Between Quartz and Lithium Niobate

It can be seen from the table that lithium niobate has the higher value of k^2, and that higher performance devices can be made from it that can be made with quartz. It has, however, got a temperature coefficent which can be unacceptable for many applications, for which quartz will be preferred. The latter's performance is not , however, entirely independent of temperature because it does possess a second order, parabolic, dependence of velocity on temperature, but its performance in this regard is muah better than lithium niobate. It will be observed that the 'ideal' surface wave substrate, which would combine the coupling efficency of lithium niobate with the temperature stability of quartz, without introducing any other problems due to its anisotropy, problems of which the latter two substrate materials are free, has yet to be found.

As all the devices which will be described in this thesis are 'test piece' devices, rather than devices designed to try to meet a pre-existant specification, and thus have no constraints of temperature stability upon them, they have all been made on lithium niobate rather than quartz, becuase of its better coupling.

1.2: Surface Wave Devices.

The relatively low velocity of surface acoustic waves, together with their low loss at high frequencies, makes them very suitable for use in making a variety of signal processing devices, operating broadly in the V.H.F. / U.H.F. part of the electromagnetic spectrum, between about 10MHz and 1GHz. The lower limit is imposed by the size of any device which can perform a worthwhile signal processing function. Several review papers have been written detailing the range of surface wave devices.[3,4]. Such devices include delay lines with delays measured in tens of microseconds, dispersive delay lines, convolvers, resonators and complex bandpass filters. A surface wave device with a delay of ten microseconds will be about three centimetres long, and it was for the construction of compact, low loss, nondispersive, U.H.F. delay lines, for use in radar systems, that interest was first turned to surface wave devices. Although surface waves are intrinsically non-dispersive, a variety of techniques exist whereby they can be used in the design of dispersive devices. Dispersive delay lines operating at U.H.F. are an area in which surface wave devices have been particularly sucessful, having no serious competitors in such fields as dispersive matched filters for radar systems.

The versatility of surface wave devices is due principally to the ease with which the progress, including the launching and detection, of the surface wave on its substrate can be controlled by structures, metal patterns or etched grooves, on the surface

along which it is propogating.

Another important application of surface wave devices is in the field of bandpass filter design. Proven design techniques exist whereby it is relatively easy to design filters with quite complex characteristics which employ surface acoustic waves. A good example of this is in the design of the video i.f. filters for television receivers. Surface wave bandpass filters are subject to the same constraints of causality as are all such filters, although the fact that they are not minimum phase devices means that there is a degree of freedom allowable between the specifications of the amplitude and phase responses of the devices.

There is now an extensive technology which is based upon surface acoustic waves, and the above-mentioned types of devices, delay lines, dispersers and bandpass filters, have all been manufactured successfully commercially and in considerable numbers.

Surface wave resonators, which can be used as frequency-stabilising devices in oscillators or as very narrow band filters are also well-established devices.

Surface acoustic wave devices have intrinsically high dynamic ranges, but despite this a lot of work has gone into the design of surface wave convolvers, more because surface waves are one of the better available technologies than because they are ideal for the purpose.

The work which will be described in this thesis is intended to provide some information for the design of arrays of dots

which can be used as elements in dispersers or bandpass filters.

1.3: The Interdigital Transducer.

The launching and detection of surface waves is now almost universally done with a structure known as the interdigital transducer[5], which is shown in figure 1.1. The electrical signal is fed between the two interleaved patterns of metal which have been laid on the substrate using standard photolithographic techniques. These patterns would normally be either of aluminium or of gold. The piezoelectric nature of the substrate means that a strain field which corresponds to the electric field due to the applied signal is set up in the region of the transducer. If this signal is an alternating voltage, the strain field will propogate as a wave in both directions away from the transducer. This bidirectionality of the transducer is the source of 3dB loss per tranducer in a device using only two simple transducers. It can be reduced, but the reduction is seldom worth the effort, and this loss limits the minimum loss of a surface wave device with an input and an output tranducer to 6dB. The wavelength of the launched wave, λ, is such that

$$\lambda = v/f,$$

where v is the wave velocity in the direction of propogation and f is the frequency of the electrical signal. The transducer will obviously be most efficent at the frequency where λ corresponds to the period of the transducer, and the bandwidth of the transducer will clearly be inversely proportional to its length, for a long

transducer. The bandwidth of a short transducer is limited, however, by its static capacity, which must be tuned out with an inductor to match the transducer to the source from which it is being fed. This imposes an electrical constraint on the bandwidth of the transducer, The shorter the transducer, the lower its capacity and thence the higher its electrical Q. The capacitance per finger for a transducer of a given radiation resistance is controlled by the electromechanical coupling coefficent, k^2, of the substrate. The maximum obtainable bandwidth of the transducer is determined by a compromise between these two factors, and is thus itself a function of k^2. Hartmann et al[6] give a formula for the fractional bandwidth of a transducer, $\delta f/f_o$, as

$$\delta f/f_o = \sqrt{4k^2/\pi}\,.$$

Hence fractional bandwidths of 25% can be obtained on lithium niobate without increasing the insertion loss above 6dB per device, whilst the corresponding figure for ST-cut quartz is around 4%.

The full analysis of a surface wave transducer is very complicated[7], especially if its ability to launch waves other than the surface wave must be taken into account. A first-order design of a surface wave filter can be accomplished, however, using the fact that the transducer's impulse response is fundamentally the same as the pattern of its fingers, the amount of their overlap giving the relative amplitude of the impulse response at a given point[6]. The filter characteristic, if specified as a frequency response, can be fourier transformed to express it as an impulse response, and the impulse response can then be used as the 'pattern' to design the transducer. This process is illustrated simply in figure 1.2. The dotted line in figure 1.2b

illustrates the desired 'top-hat' filter response. The fourier transform of that response is an envelope of the form sin(x)/x around a sine wave corresponding to the centre frequency of the passband, the width of the lobes of the envelope being inversely proportional to the bandwidth of the filter response. Figure 1.2a shows this envelope, and the transducer which would be made using this pattern. The frequency response of the transducer would inevitabley tend to follow a line such as the full line in figure 1.2b, however, rather than the ideal, because the full impulse response of the ideal filter is infinitely long, and that of the transducer must inevitabley be truncated. This is an example of the filter's having to obey causality, as must all physically-realisable filter designs.

Figure 1.3 shows how an interdigital transducer can be used to make a dispersive delay line. The two transducers both have periodicities which vary along their length, so that waves of different frequencies will be preferentially launched and detected at differeent parts of the transducer. Signal components of different frequencies will thus travel different distances along the device, and it will thus be dispersive as its delay time will be a function of frequency. Hence, although the wave itself is still non-dispersive, a dispersive device has been made. This form of transducer is known as a chirp transducer[8], and is a good example of the versatility which can be obtained in surface wave devices, where a complicated signal processing function can be carried out by a simple pattern of metal on the surface of the substrate. This versatility is due in large part to the fact that the surface wave, travelling along the top of the substrate can be easily 'got at'.

An unfortunate side-effect of this is that the surface wave devices must be well packaged in order to prevent inadvertant contamination of the surface of the substrate.

The chirp transducer is not the ideal way in which to make a surface wave disperser, however, because the form of the chirp transducer means that it tends to have characteristics which make it difficult to drive efficently[9], and its performance becomes uncomfortably sensitive to defects in its manufacture, which is a particular disadvantage in a surface wave device, because surface wave devices are usually quite tolerant of such faults.

A figure of merit of a disperser is its time bandwidth product, the product of its bandwidth and the differential time delay across that bandwidth. A typical value of time-bandwidth product for a chirp filter using interdigital transducers would be 300. The maximum that has been obtained is about 1000 [10], with some considerable difficulty.

The limitations on the performance of dispersers using interdigital transducers are due to the fact that the transducers are being used for two distinct functions at once. They are being used to try to launch the wave onto the substrate, and also to try to control its dispersion, and these two functions have become incompatible. If these functions can be seperated an order-of-magnitude improvement in performance, as well as a greater ease of design, can be gained, as will be seen in the next section of this chapter.

1.4: Reflecting Array Devices.

A surface wave reflecting array device can be defined as a device in which the signal processing functions of the device are performed by means of some structure,other than the launching and detecting tranducers, which selectively reflects the surface wave.

The work of this thesis is involved in the design of dot arrays for such functions.

A classic example of a reflecting array device is the RAC.[11] This name is an acronym for reflective array compressor, the term compressor being derived from their used as matched pairs in pulse-compression radar syatems.

Figure 1.4 illustrates the general form of a RAC. It consists of two simple transducers which are not directly looking at one another, the bandwidth of each being the total bandwidth required from the device. A reflecting structure is then used to deflect the surface waves through a 'U' path by two ninety-degree reflections to turn the signal from the input to the output transducer. In the classic surface wave RAC the reflectors are banks of grooves milled into the surface of the substrate. The grooves are each weak reflectors, and their periodicity varies along the length of the device, so that signal components of different frequency will travel different-lengthed paths before returning to the output transducer.

By this method dispersive devices have been made with time-bandwidth products up to 10000[12]. If the period of the reflectors is made

constant along the length of the array, bandpass filters can be similarly made with very good freedom from spurious signals, because the input and output transducers are not looking at one another.

The reflectors are generally ion-beam etched grooves of the order of 1000Å deep in the substrate. Such grooves have a suitable reflection coefficent for the purpose, and the reflection coefficent of the grooves can be varied along the array by varying their depth. These grooves produce only a minimal alteration in the velocity of the waves, which is an important advantage they possess over metal reflectors, because the correct operation of such devices depends, as will be seen, upon the correct alignment of the reflectors so that they reflect the wave through exactly ninety degrees on the substrate on which the wave velocity will be a function of direction, so that the reflector will not in general be at 45 degrees to the incident wave.

1.5: Reflective Dot Arrays.

The principal disadvantage with grooved RACs is the time and effort which must be expended in milling the grooves, so that it would be much better if the reflecting structures could be made with coatings of metal in the same way, and at the same time, as the transducers are made.

If the grooves are replaced by metal strips problems srise because the reflection coefficents of the individual strips are found to be too high, and to be uncontrollable, being fixed by the electrical properties of the conductor over the piezoelectric substrate.

If the metal strips can be replaced by rows of metal dots, however, the reflection coefficent can be controlled at will by altering the density of the dots, and the whole pattern can be made at the same time as the transducers, in one photolithographic step. Such a device would seem to be the ideal way in which to make dispersers and high performance surface wave bandpass filters, and the work described in this thesis is directed towards this end.

Solie[13,14] has already done a considerable amount of work, over some years, on reflective dot array devices, or RDA's.

He has produced a variety of quite sucessful devices, mostly bandpass filters in which the filter characteristic has been obtained by weighting the density of the dots in the reflecting array. Part of one of the arrays he has used[13] is shown in figure 1.5. He has demonstrated one such filter[14] with sidelobe and spurious levels 90dB below the main lobe, which is an impressive achievement, and indicative of the potential of dot array devices (figure 1.6).

1.6: Aims of This Work.

In the work in which he has done and in the devices which he has made Solie appears to have tried to avoid the problems of the electrical effects associated with his metal dots, and has tried to minimise these effects. He has not published any design rules for dot array devices, prehaps as a result of his failure to tackle the electrical effects of the dots. Whilst he claims sucess in designing dot array devices by merely replacing the grooves in the equivalent groove device with rows of dots, others[15] have found problems with using such a simple approach.

Solie claims to be able[13] to use the free surface values of the wave velocities in order to calculate the correct angles for the rows of dots. It is known however that the presence of metal on the substrate alters the wave velocities, and that, because of the anisotropy of the substrates, it alters it by different amounts in, for example, the Z- and X- directions of Y-cut lithium niobate, on which most RDA's are made. It has been established that these perturbations can affect significantly the correct angle at which the reflecting planes must be placed in a dot array device, especially if it is wished to use arrays in which the electrical effects will be more significant than they are in those made by Solie.

It is also by no means clear how the dots should be placed along the reflecting planes, and whether or not they should be arranged in two-dimensionally regular patterns. Solie at one stage mentions the use of randomization along the planes[16]. He has also published no data on the actual reflection coefficents of the individual dots which he has used.

It is the aim of this work to try to develop some design rules for dot array devices, and in order that this may be done there are at least three questions to which answers should be sought.

First: how does the presence of metal dots slow the wave, and how does this affect the correct angle at which the rows of dots must be placed in such a device, and what is that angle in specific cases?

Second: To what extent, and how, does the pattern in which the dots are placed in the arrays affect the performance of the devices?

Third: What is the reflection coefficent of the individual dots, and how does it vary as the shape and size of the dot and the thickness of metal used all vary.

This work provides information to help answer the first of these questions, and shows how the correct array angle can be found for any specific case. It shows that the pattern of dots used can be very significant, and shows examples of suitable and of unsuitable patterns. It also provides information on the reflection coefficents of the dots in specific cases and of the variation of the reflection coefficent as the metal thickness is varied.

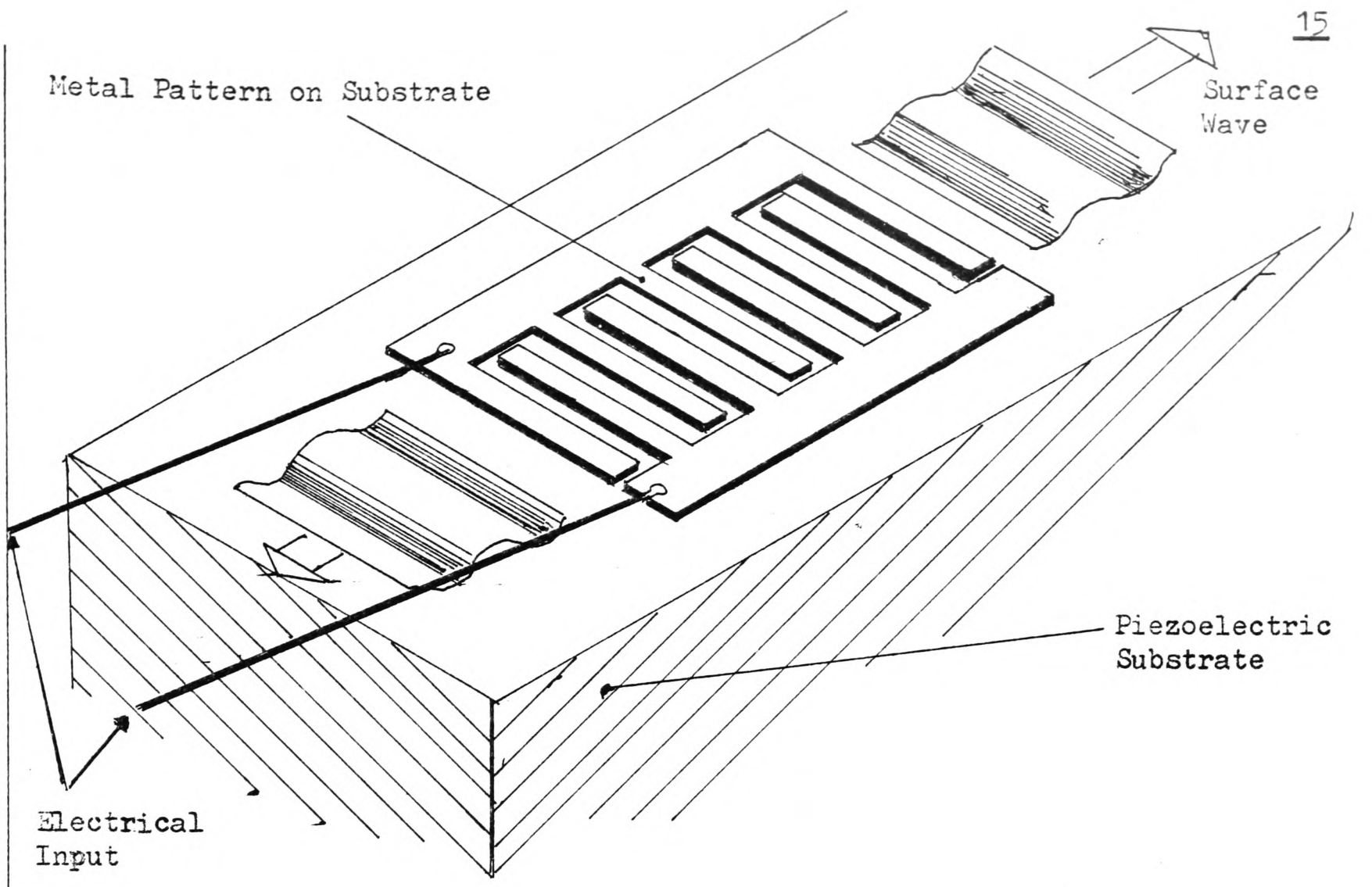

Fig 1.1a: The Interdigital Transducer.

Fig 1.b: Electric Field Pattern on an Interdigital Transducer

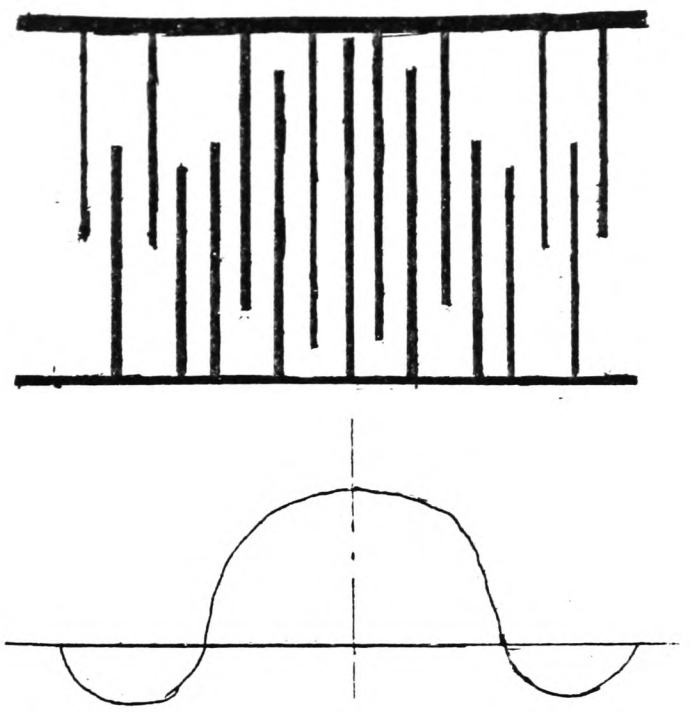

Fig 1.2a: Weighted Transducer.

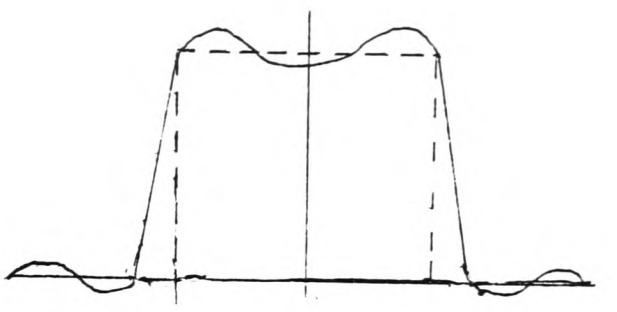

Fig 1.2b: Frequency Response of Weighted Transducer.

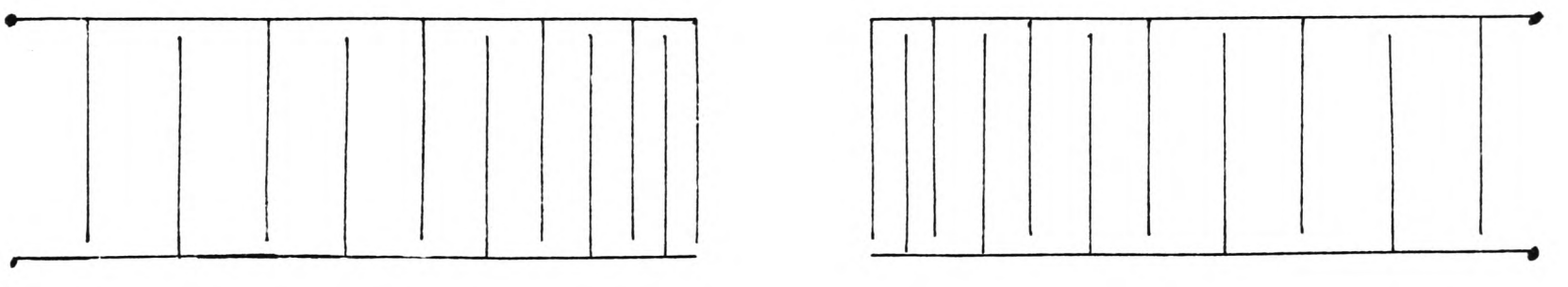

Fig 1.3: Dispersive Delay Line Using Chirp Transducer.

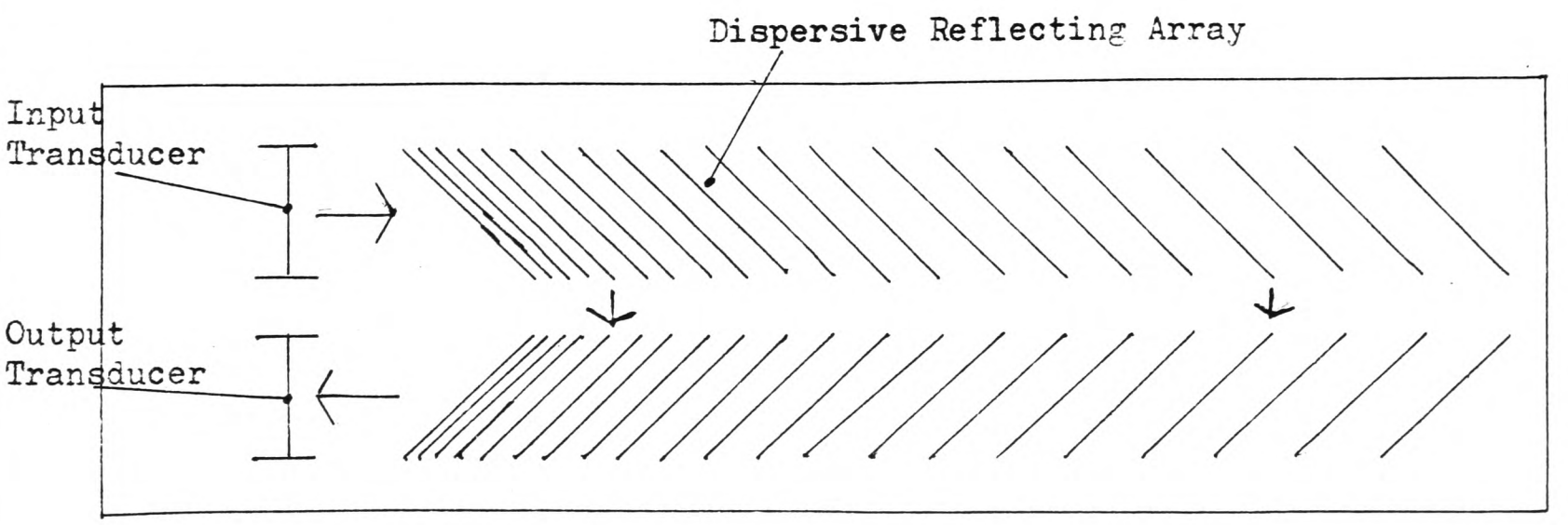

Fig 1.4: Reflective Array Compressor.

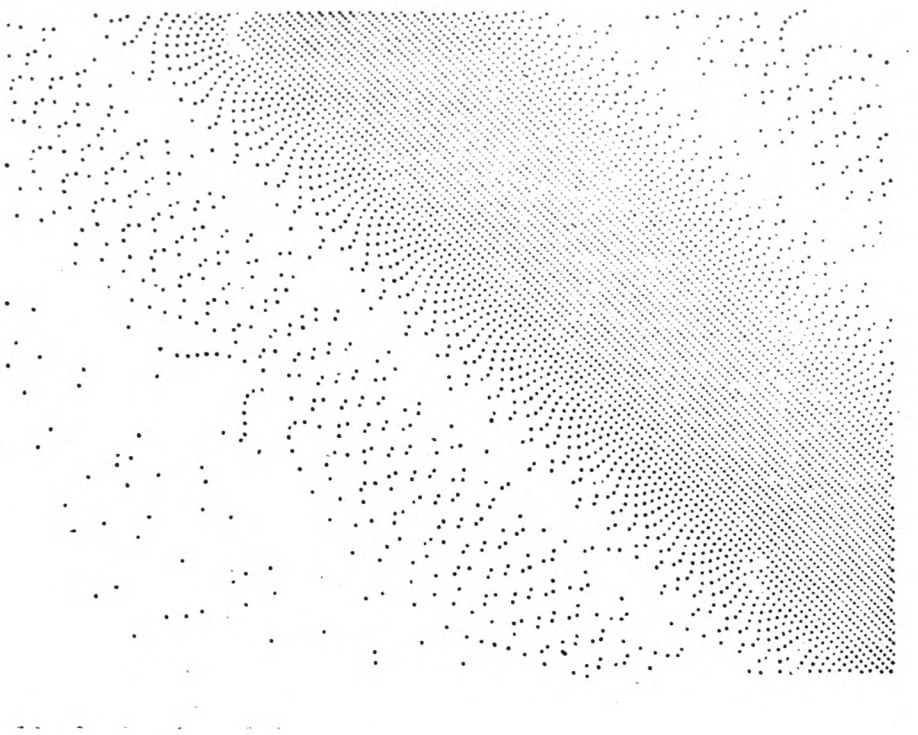

Fig 1.5: Part of a RDA made by Solie

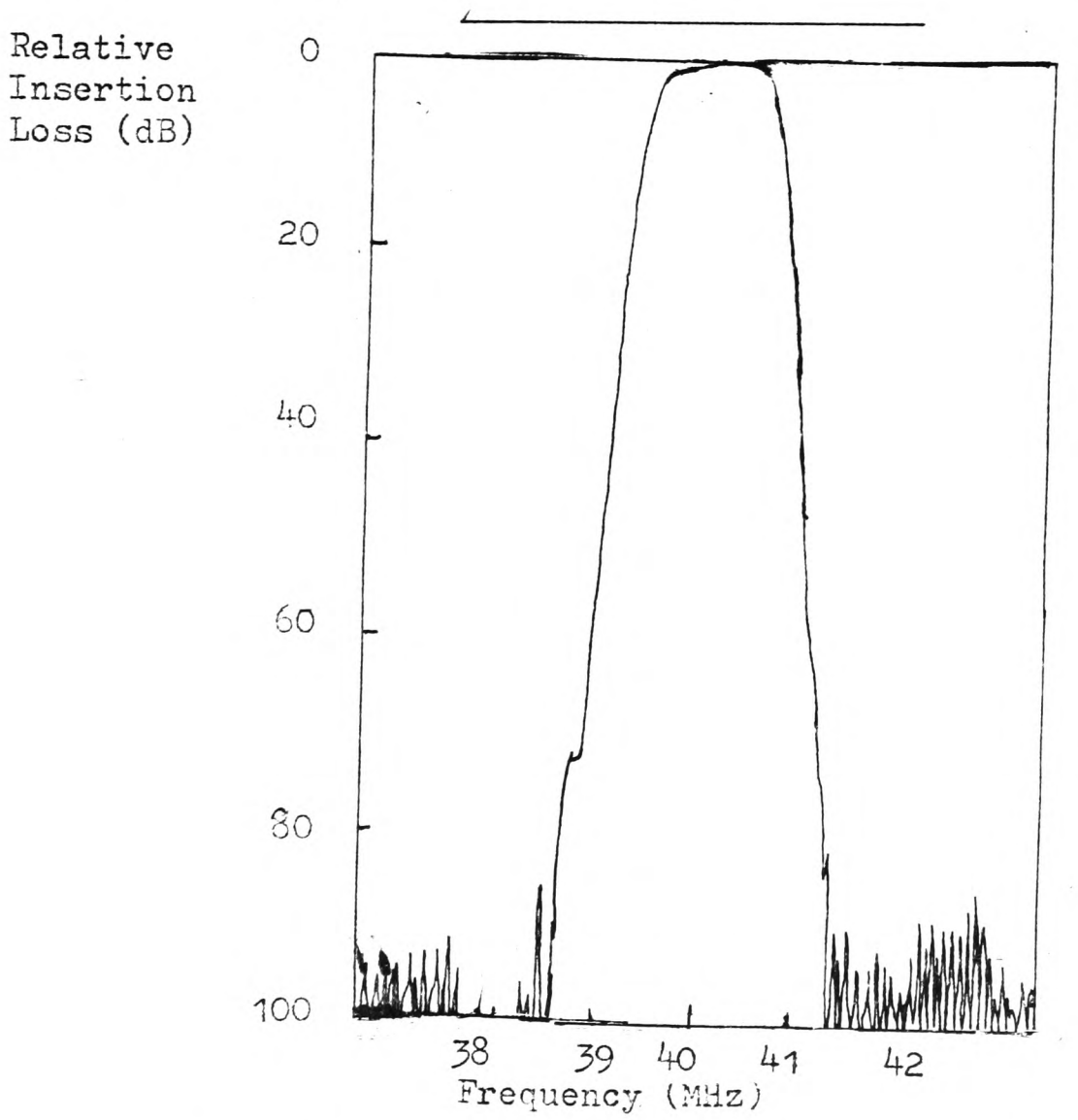

Fig 1.6: Response of a RDA filter made by Solie, Showing Nearly 90dB Sidelobe Rejection.

CHAPTER 2

REFLECTIVE ARRAY DEVICES

2.1: Types of Reflective Array Devices (RAD's).

It was said in the previous chapter that the great advantage possessed by surface acoustic wave reflective array devices over the simpler devices using only transducers is that by using separate structures to launch and detect the wave and to process it the inevitable compromises associated with trying to do two jobs with the same structure are avoided.

Prehaps the simplest reflective array device is the resonator[17]. Here two banks of reflectors are used to construct a resonant cavity within which the transducer is placed. The good U.H.F. characteristics of surface waves allow very high Q-factors (greater than 1000) to be obtained with these devices. The reflectors are usually either grooves or metal strips, although metal dots have been used[18] to simplify the multi-moding effects which can occur within arrays of metal strips. The work in this thesis was not entered into with any intention of its being of use in the design of resonators, and the results presented herein are of only minor importance to the design of such devices. The work does, however, concern itself with the design of bandpass and dispersive filters using RADs. These devices work by using the reflective arrays to send the signal from the input to the output transducer, processing by the selectivity of the reflectors en route. A recently-announced device, the inline RAC[19], uses only one propagation direction for the whole of the wave's path, as does the resonator, and like it is almost immune to the effects of the anisotropy of the substrate. Most filters, however, reflect the wave

through two turns of 90 degrees each, so using two perpendicular propagation directions. The anisotropy of a typical substrate, lithium niobate for example, is such that the wave velocities in two such directions can differ by about 10% or so, and the effects of this on the reflection angle are very important, so that the variations of wave velocity need to be well-known to design high-performance devices.

Dispersive filters are used principally in pulse compression radar systems, and also in fast spectrum analysers. In both of these applications the figure of merit of the device is the time bandwidth product, TB, which is the product of the bandwidth of the device, B, and the differential delay across that bandwidth, T. This determines the amount of processing gain available in the radar system or the number of discrete channels in the spectrum analyser. It is also important to be able to weight the amplitude response of the devices, as it is possible by this means to greatly reduce the sidelobes on the output pulses of the system, improving its usuable dynamic range. The performance of these systems is dependent on the accuracy of the amplitude and delay characteristics of the filters used.

The performance requirements of a bandpass filter are the accuracy of its frequency setting and the shape of its response, which depend on the accuracy of the calculations of its working frequency from the array periodicity and the surface wave velocity, and upon the accuracy of the amplitude weighting within the passband which determines the filter characteristic. The design of reflective arrays for use in devices of either of these types thus requires and accurate knowledge of the wave velocity through the array, to get the array angle and the operating frequencies right, and of the reflection characteristics of the individual reflectors in order to define the amplitude response properly.

2.2 Surface waves and Reflective Array Design.

It was shown in the previous chapter that surface wave devices are very well suited to the manufacture of high-performance dispersive and bandpass filters . It was seen that the factors which contributed to this were that the surface wave is intrinsically almost dispersionless for frequencies below about 1GHz, and has correspondingly low loss. It was seen furthermore that the velocity of the wave on a typical substrate allowed the easy fabrication of devices with delays of the order of 10 microseconds, but that the ability to launch the wave onto a piezoelectric substrate meant that it could be easily and efficently coupled to the rest of an electronic system. It is a point prehaps worth making in passing that whereas surface wave devices are electrical devices, they are not strictly speaking electronic in most cases, because ,except for the occasional devices which launch the wave onto semiconducting substrates, their operation and analysis does not rely on the electronic nature of electrical conduction, the electrical nature of their properties being entirely described by classical electromagnetism.

The foregoing remarks apply also to devices which use bulk acoustic waves, such as conventional crystal resonators and bulk delay lines, but the great advantage of surface wave devices, which allows their use in dispersers, is that the behaviour of the wave can be easily controlled by simple alterations to the nature of the surface along which it propagating, because the wave is confined to that surface. On a typical substrate almost all the energy carried by the wave travels within one wavelength's depth of the surface.

In order to obtain the low loss and low intrinsic dispersion possible with good surface acoustic wave devices at frequencies above 100MHz, it is necessary to use single crystal substrates, because the grain boundaries in polycrystalline materials will obviously present sources of disruption to the wave.

This use of single crystal substrates is the cause of the anisotropy of the behaviour of the waves, which has been mentioned before as being important to the design of devices. The wave characteristics are functions of the elastic and piezoelectric constants of the material, which are necessarily anisotropic for a single crystal. This limits the range of materials and orientations upon which surface waves can usefully be launched.

If a surface wave travels with arbitrary propagation direction on an arbitrary substrate, the flow of power in the wave will not necessaily be perpendicular to the phase fronts. In fact this desirable property can only be gaurenteed to be satisfied when the wave is propagating along a symmetry axis of the crystal. A further important constraint on the substrate is the efficency of the piezoelectric coupling to the wave, which, as was said in chapter 1, relates the attainable bandwidths and the insertion losses of the transducers. Considerations which are also taken into account are the possibility of launching unwanted bulk waves from the transducers and the temperature coefficent of the surface wave velocity.

Y-cut lithium niobate satisfies most of these considerations quite well, except that of temperature coefficent. However the velocities in the Z and X directions track very well with temperature, which is not the case with the X direction and perpendicular to it

on ST quartz, which is a disadvantage with the latter substrate material for devices, like most array devices, which need to use waves travelling in two different directions.

The X-propagation direction tends to be avoided if possible on Y-cut lithium niobate, because the behaviour of transducers coupling to surface waves in this direction can be upset by coupling to bulk acoustic waves as well as to the surface wave. The Z-direction however does not suffer from this problem, and like the X- direction it is a symmetry direction of the crystal, and so avoids the possibility of problems due to the phase and energy velocities of the wave not being collinear, this effect being known as beam steering.

Lithium niobate has, moreover, another advanatge which is itself caused by the anisotropy of the material. If the phase velocity of the surface wave in a particular direction is greater than it is in neighbouring directions on the same substrate, then the power will tend to flow along that direction, even when the phase velocity is in other nearby directions.(20)

The practical consequence of this is that the rate at which diffraction spreads the energy of a wave launched in such a direction is reduced compared with the corresponding case on an isotropic substrate. Both the X- and Z- propogation directions on Y-cut lithium niobate show this effect, but it is particularly strong in the Z-direction, giving a reduction of diffraction of four times compared with the isotropic case. This can be very useful when long devices are to be made, in which cases diffraction can become a significant source of losses in them.

There are also some disadvantages suffered by surface wave devices in their suitability as dispersive delay lines. One is that a substrate has not yet been found which will satisfy all the requirements described above. At present lithium niobate and quartz are the two most generally suitable, although the former suffers from a temperature coefficent of velocity which can be excessive for many purposes (-85 p.p.m. per kelvin for a Z-propogating wave on a Y-cut substrate), and the latter from a low piezoelectric coupling coefficent, such that wide bandwidth devices with low insertion loss cannot be made with it. For some applications in which the greatest possible temperature stability is required, even quartz surface wave devices are not ideal, their temperature stability being inferior to that of the best bulk wave devices.

The other principle limitation on surface wave devices arises from the sensitivity of the wave to the condition of the surface upon which it is propagating. This sensitivity is, of course, the great advantage of surface waves, but also means that the devices must be carefully packaged if they are to perform predictably outside a research laboratory. For example the presence of any moisture on a surface wave device, such as the condensation from breath, will completely damp out the wave. This packaging obviously increases the cost of the devices, and together with the expense of having to use carefully-grown monocrystalline substrates is the factor limiting the wider use of surface wave devices in electronic equipment to be sold in price-conscious markets.

One aspect of the behaviour of surface waves of obvious importance to the design of RADs is their reflection by obstacles on the surface.

There are in general three possible mechanisms by which surface waves are reflected by the sorts of discontinuities at present introduced onto the substrates used. The simplest of these is called the topological effect, where the wave is reflected by a sudden change in the shape of the surface, such as occurs in the grooved RAC (figure 2.1a). This is probably the simplest reflection mechanism. Away from the actual edges of the step the wave behaviour is the same whether it is travelling through one of the higher or one of the lower parts of the free surface. The reflection is thus an effect which occurs only at the discontinuities of level, enabling the overall behaviour to be modelled purely by the behaviour at the seperate discontinuities. In this model, since the wave velocity is the same over all the surface, the presence of the grooves does not perturb the velocity of the wave from its free surface value.

The reflection coefficent for a quarter wavelength wide groove is approximately $\frac{2}{3}$ h amplitude, where h is the depth of the groove in wavelengths. This can be easily controlled by varying the depths of the grooves. A groove 1000Å deep will have a reflection coefficent of 0.2% at 100MHz, which is a suitable value for use in RADs. An accurate model for the behaviour of the groove reflector has been developed by Farnell[21].

This simple model is quite effective at explaining the behaviour of the grooved RAC, but is not perfect, because there is some disturbance to the wave's velocity caused by the presence of the step[22].

This arises because the step is able to vibrate in modes of its own, and to absorb energy from the surface wave which it can then

re-radiate in quadrature with the incident wave. This ability to store the energy in the wave for a quarter cycle has led to the phenomenon's being called the stored energy effect.

The consequence of this on the wave is that a certain amount of the wave is in quadrature with the incident wave, altering the phase of the reflected wave, and slightly retarding the transmitted, so altering its velocity through the reflector.

The other two reflection mechanisms are called mass loading and electrical shorting. Mass loading arises when some dense material is placed over selected parts of the substrate (figure 2.1b), so as to perturb the boundary conditions subject to which the wave is propogating, and hence in general altering its velocity and the acoustic impedance of the surface. It behaves similarly to the topological effect in that the reflections are localized at the discontinuities. Its perturbation of the wave velocity will, however, be a first order effect, rather than of second order as it was in the topological effect.

The strength of the mass loading effect is proportional to the material used for the loading and to its depth. On YZ lithium niobate aluminium will give a reflection coefficent of approximately .23h, where h is the depth of material in wavelengths, for a quarter-wavelength wide strip. The corresponding electrical shorting reflection coefficent will be about 1% amplitude, independent of the type and thickness of metal used, provided its resistance can be neglected.

The accurate description of electrical shorting is very complicated, and theoretical predictions of reflector behaviour have only been made for the case of reflection straight back through 180 degrees, in an essentially one-dimensional case.[23,24]

To describe even the case of a single isolated reflector requires the use of a computer to solve by numerical methods the non-analytic equations which describe the problem.

The general behaviour of this reflection mechanism can be understood however, by considering its implementation by placing thin conducting plates onto the substrate to act as the reflectors.

As the wave travels under the plate the piezoelectric nature of the substrate will set up electric fields in the plate in accordance with which the free charges in it will move to ensure that the potential on the plate remains constant. The re-arrangement of charge will be subject to two constraints. Firstly the potential everywhere on the plate must be the same at any instant, and the total charge on the plate must be always the same.

This rearrangement of charges will then react back to launch acoustic waves into the piezoelectric substrates, in general launching both surface and bulk waves. The problem is further complicated by the possible interactions between the charges on neighbouring reflectors in an array. The relative importance of electrical shorting as a reflection mechanism is obviously related to the strength of the piezoelectric coupling in the substrate material.

The electrical shorting phenomenon has a first-order effect in slowing the wave. The conductor on the surface 'shorts out' the piezoelectric stiffening of the elastic constants of the material, which normally act to increase the velocity of the wave. The removal of this effect is called electrical slowing. The magnitude of this effect, $\Delta v/v$, is approximately equal to $\frac{1}{2}k^2$, where k^2 is the strength of the piezoelectric coupling. On YZ lithium niobate it has the substantial value of 2.35%.

Unlike topological reflection, which is used in grooved RACs, no devices have been made which use either pure electrical or pure mass loading as their reflection mechanism, although one or other can dominate in a particular device. Reflectors of both types are made by depositing metal on the surface. This obviously means that electrical shorting is always to some extent present in such devices, and because the metal cannot be made infinitely thin and massless, mass loading is also always present. If thin strips of aluminium are used on lithium niobate the reflection mechanism is predominantly electrical, if gold dots are used on quartz, (a much denser metal on a less strongly piezoelectric substrate,) mass loading predominates. The strengths of the general, two dimensional, scatterings due to these two effects vary with the size and shape of the reflectors, so that when the first RDAs were made it was not known which, if either, reflection mechanism was dominant when aluminium dots were used on lithium niobate. It will be shown later (in chapters 4 and 5) that electrical shorting dominates in this case, and that the electric fields due to the

individual dots can interact significantly.

It is probably fair to comment that RAC devices have generally been sucessful without the need for sophisticated models for the reflection mechanisms which are applicable to the cases actually encountered (especially regarding reflections through angles other than 180 degrees). Those parameters which have needed to be known having been found by experiment rather than from the accurate analysis of the behaviour of the surface wave itself, this being due in part to the intractable nature of the mathematical description of its behaviour on an anisotropic substrate.

2.3 Design of Surface Acoustic Wave RADs.

RAC devices can be made using four different types of reflectors. The reflectors can either be continuous or divided into dots, and can be made either by ion-beam etching into the substrate or else by deposition of aluminium onto the surface. The first and most common method is to use continuous strip reflectors etched into the substrate. As has been said before, this method has produced some very sucessful devices. The analysis of these devices is relatively simple, due to the simple reflection mechanism and to the low reflection efficency of each groove, which stops multiple reflections within the reflective arrays from building up to become a problem. Any residual errors in the phase response of the final device can be removed by the use of a phase plate, shown in figure 2.2.[12] To design a phase plate for a RAC, its phase errors are measured, and the plate is then designed as a metal pattern which can subsequently be

added to the mask which produces the transducers. Its width in the direction of the wave propagation between the two arrays is made variable so that the total amount of electrical slowing which the wave receives through travelling under the metal plate is sufficent to cancel out the measured phase error at the frequency corresponding to the distance down the array at that point. It is possible by this stratagem to reduce the remaining phase error to about $\frac{\phi}{2}$ r.m.s..

The metal strip array, unlike the groove array, has never really been sucessful. In contrast to the latter, it has a high reflection coefficent for each strip (greater than one percent, as has been mentioned in the previous section), which taken with the fact that the effective length* of a dispersive array, for example, is frequently of the order of 100 strips, means that one is getting into the régime where multiple reflections of the wave within the array are becoming significant. This makes the sucessful design of such arrays a very much more complicated matter than it is for a groove array. Another problem with such arrays is the difficulty in weighting them. The method used with groove arrays, of varying the groove depth, is inapplicable here. The simplest weighting method would be to vary the lengths of the strips, so that they intercepted that portion of the incident beam required to give the correct weighting. This, however, is not as simple as it seems because the reduction in the wave velocity under the metal strips makes the pattern tend to act as a waveguide, severely disrupting the amplitude and phase profiles of the wave as it travels through the array.

An ingenious attempt to overcome this difficulty is the chevron-weighted

*The effective number strips whose reflections are coherent at any one frequency. It is equal to $N/\sqrt{TB}$, where N is the total number of strips.

array[26], shown in figure 2.3. Here the total amount of metallization is kept constant, but parts of the array are designed to reflect the wave away from the second array rather than towards it. This technique has recently been used to make a weighted grooved RAC with constant depth grooves[27], in an attempt to simplify its manufacture. The technique has nor been particularly sucessful in metal RAD's, however, because the waveguiding effects still cause problems within the arrays, and metal dot arrays, in which the wave guiding effects are much less strong, provide a better weighting method.

The use of metal dots keeps the advantage of using one process to make the whole device, but without introducing the severe problems associated with metal strip arrays. It is usually possible to design these devices without having to worry about multiple reflections, as the reflection coefficent can now be freely chosen. It is a function of the number of dots used to replace one strip of a grooved array and of the reflection coefficent of each dot. It is worth noting that this function is only a simple product if the dots act independently, which need not necessarily be the case if they are close together, when their mutual capacity can become significant.

Solie[13,14] has had great sucess in designing RDA's using simple assumptions about their operation, whilst others[15] have had difficulty in such work, because of such problems as the correct angle for the reflectors. It is noticable that Solie has always tried to use the mass loading effect as the reflection mechanism, frequently using heavy gold dots, in the RDAs which he has designed. Some of his best devices have been made on quartz, with its weak piezoelectric coupling, despite the adverse consequences which this would have on the possible design of wide bandwidth devices. It is also noticeable that he has tried to use small dots relatively widely seperated, which

tends to reduce the importance of the electrical shorting effects and of the mutual capacity of the dots.

It is also Solie[14] who has made the only example of the fourth type of reflective array, using etched dots. To date only one such device has been reported, the value of the technique being uncertain except for experimental comparisions, because needing ion beam milling to produce the etched pits, it would appear to have few significant advantages over the proven-sucessful grooved array.

As there are several different possible types of reflector, so there are many different possible ways of arranging them into arrays and of placing the arrays relative to one another and to the input and output transducers. Several of these ways are illustrated in figure 2.9. Such arrangements are identified for the most part by letters of the alphabet the shapes of which the paths taken by the waves seem to resemble.

Conceptually the simplest type is the L-path (figure2.4a), where the wave undergoes a single reflection to turn it from one transducer towards another. The angle through which the wave is defected need not necessarily be 90°, so long as the output transducer is aligned correctly to intercept the reflected wave.

In general this device can suffer two drawbacks which restrict its usefulness. The first is that of finding two directions on the substrate which are suitable for the operation of surface wave transducers, and the second is that of ensuring that

the incident and reflected beamwidths are both such that efficent transducers can be designed to intercept all the energy in the wave. This is obviously impractical if, for example, the array is used in a long RAC using 90° reflection, in which case the aperture of the output transducer will be so large that its electrical impedance will be too low to be useful.

One very specialised application for such a device, although with less than 90° reflection angle, was in a correlator made by Solie[28]. This was a specialised application for an RDA, where the waveform coding was in the form of phase reversals on a constant frequency signal, which had to be decoded by correctly reversing the phase of parts of the signal as it travelled through the device. The abruptness of the changes in weighting (the phase reversals) meant that the spreading of the wave which would occur in a two-array structure, such as the U-path, due to the finite aperture of the beam of any frequency component as it leaves the first array, would be unacceptable. Hence the use of the single-bounce structure.

The U-path (figure 2.4b) is made by constructing two L-path devices back to back, so that the signal returns to the output transducer travelling back along the same crystal direction as that in which it was launched, with the energy spread across the same aperture. The problems associated with the L-path design are thus avoided, so that the only requirement on the direction perpendicular to that of the incident wave is that the surface wave should propogate along it without excessive problems. This requirement is now relatively easy to satisfy.

The new configuration introduces a much greater sensitivity of device performance to accuracy of alignment of the arrays. Misalignment manifests itself most severely not in the energy of the output wave missing the aperture, but in its arriving with its phase fronts not parallel to the transducer fingers, which, in view of the wide aperture of a typical transducer (about 50 to 100 wavelengths) can have a very severe effect on the amplitude of the detected signal. If the device can be designed with sufficently accurate knowledge of the wave velocity in the two directions, however, this need not be a problem, but rather an advantage. In bandpass filters it will aid the roll-off of the response out of band, as the angle of reflection of a wave from an array varies as the periodicities of the wave and of the array diverge. It also means that any spurious modes of operation of the array, such as the launching of bulk modes, are unlikely to have a significant effect on the overall response of the device, as waves launched unintentionally are unlikely to satisfy the demanding angle criteria for their being detected at the output transducer.

The relative orientations of the two transducers on a U-path device also mean that any spurious waves launched from the transducer are unlikely to make their way to the receiving transducer by any possible means, further protecting the device against the effects of spurii, such as the spatial sidelobes of the transducer response, which would travel unaffected through the reflective arrays.

The physical proximity of input and output transducers means however that, unless care is taken with packaging, devices are likely

to suffer from excessive electromagnetic breakthrough between input and output, which can disrupt the performance of the device.

This is rightly looked upon, however, as a packaging problem which is by no means insoluble, rather than as a matter to significantly affect the design of the surface wave structures, so that the U-path is by far the most popular configuration for RACs and bandpass filters.

The Z-path configuration, shown in figure 2.9c, has the two transducers seperated so that electromagnetic breakthrough is a much less significant problem. The transducers are now nearly looking at each other however, especially if the reflective arrays are long, so that acoustic spurii are likely to more significant than in the U-path. More importantly the reversal of reflection sense of one of the arrays has meant that the device is now self-compensating for errors in the array angle. If the error built into both arrays is the same, and small, then any error in wave direction after reflection from the first array will be corrected rather than worsened by the second. Bulk waves launched at angles other than the desired surface wave direction will similarly be corrected in direction and contribute to the overall signal seen at the output transducer. The roll-off in the frequency reponse of a bandpass filter due to the variation of wave angle with frequency will also be compensated for, giving the device a relatively broader response than an equivalent U-path device.

Z-path devices are generally in fact only used as experimental structures, but sucessful s.a.w. bandpass filters using the Z-path configuration have been made[29].

Solie has demonstrated a four-bounce device[14], shown in figure 2.4e, which consists of two U-path devices end to end.

This device, like the Z-path, is insensitive to the array angle, but is without the diadvantage of having the transducers looking at one another. In general the extra space on the substrate and the extra complexity of having to have four arrays cannot be justified if it is only required to correct for an erroneous array angle, it being better to get the angle right. The purpose of this device, however, was to demonstrate compensation for changes in reflection angle with temperature. As was said in the previous section, this is not a problem with lithium niobate, becuaes the velocities track well between the Z and X directions, but it is a problem on ST quartz.

An interesting configuration which has recently been reported is the inline RAC, or ILRAC[19], shown in figure 2.4d.

As was pointed out in section one of this chapter, this device uses what is conceptually the simplest reflection mode, straight back through 180 degrees. It is a mode which has

not been used before however, because of the obvious difficulty of distinguishing the input and output waves, so that the latter only is detected at the output transducer. Here the multistrip coupler[30] is used to seperate the two waves. This device consists of a series of metal strips across the aperture of the wave, and of such a period as not to reflect the incident wave, which can change the track along which the output power flows. Its exact behaviour depends on the number of strips used, but in this device their are sufficent of them to split the energy coming from the input transducer equally between the two reflective array tracks, but with a quadrature phase shift between them. The waves reflected straight back are then combined so that all the power returns to the output transducer. The placement of the transducer will of course, mean that the device will have a similar sensitivity to electromagnetic interferance and freedom from spurious transducer modes as the U-path. Its behaviour with respect to spurii created by the arrays will depend on how these pass through the coupler. In general those from the lower RAC will come straight back to the output whilst those from the upper will miss it.

The ILRAC can suffer however from reflections straight back from input to output caused by faults in the coupler, which removes or at least reduces the RACs advantage of insensitivity to localized device faults. Against this is the considerable advantage that the wave always travels along the same crystal direction, entirely removing the problems caused by the anisotropy of the substrate.

The first ILRACS reported used groove strips as the reflectors, but placed normal to the wavefronts, of course. **Instead of weighting** the device by varying the depths of the grooves, weighting was achieved by varying the relative positions of equivalent grooves between the two arrays. This has the effect of introducing a phase shift between the two signals returning to the multistrip coupler, which diverts the ouput energy back into the input transducer rather than to the output, thereby effecting the weighting.

This weighting suffers from the disadvantage that the relationship between groove position and weighting is an inverse cosine, which is not a well behaved function, so that if large weightings are to be accurately introduced, great care must be exercised in the design and fabrication of the arrays. This is a severe disadvantage to these devices with the weighting implemented in this manner. Despite this, however, the first reported devices performed well, so that it seemed to be worth investigating the possibility of making such devices using metal dot arrys as the reflectors, which would remove this over-sensitivity of the weighting to such errors.

2.4: Devices to Study The Performance of Reflective Dot Arrays.

Most of the devices reported in this thesis will be reflective dot array bandpass filters, or at least they will behave as such. They were designed as regular, uniform, patterns of dots in order to simplify the analysis of the devices so produced. In order to test the effect of weighting the array, a whole new array would be made which was still regular, but with the dots arranged more sparesely than in the comparable fully-reflective array.

A standard transducer and array configuration was used, as shown in figure 2.5, which allowed the arrays to be used in both U- and Z- path configurations, and which also allowed the signal passing straight through the array to be observed. The transducer labelled '4', although not strictly necessary, was generally used because it provided a certain degree of redundancy which could be useful for checking the results obtained, or it could be brought into service if one of the other transducers were faulty or damaged.

As has been said, the arrays could be used in either the U- or the Z- path configuration. On some devices the pattern of dots was made so as to allow the array to work, it was hoped, equally well in either mode, adding to its overall symmetry, whilst in others it was made so as to attempt to suppress the Z- path reflection and with it the corresponding problems which it appeared would inevitably occur in an array which was capable of operating in both modes.

The size and shape of the dots used was also varied between different devices in an attempt to determine more about the behaviour of the individual dots, and one device was made using full metal strips as reflectors, in order to compare its response both with those of the dot devices and with some theories which had been developed for such arrays[31]. As these devices were made with regular rectangular arrays, it follows that if they are weakly reflective their expected frequency responses would be of the form of a product of sine(x)/x- like terms.

Two ILRAC devices were also made. The first of these has as its reflectors a series of blocks of dots of regular apacing, similar to those of the U- and Z- path devices. Each of these blocks should have behaved as a sin(x)/x-like bandpass filter, and they should have been non-interacting, so that the overall response of the device should have been a series of narrow passbands spread across the passband of the transducers, with different weights in the different passbands.

The other ILRAC was designed to imitate exactly the responses of of the device using groove reflectors which was reported by Chapman et al[19]. It was a disperser with 20 microseconds dispersion over a 50MHz bandwidth centred around 150MHz, giving a time-bandwidth product of 1000. The device was intended to have a 40dB Taylor weighting[32], which was implemented by varying the density of the dots along each reflecting line.

These latter two devices were, however, not very sucessful.

The performance of the devices made was measured either by observing their frequency responses between various transducers, or else by plotting the actual amplitudes and directions of travel of the waves along the surface of the devices using a potential probe system[33,34]. The apparatus which was used for these measurements is described in the next chapter, and the results obtained in chapter 4. These results give information on the correct angles at which the arrays should be placed, and on the reflection strength of the reflectors used, and on the types of array pattern which have been found to be most suitable for dot arrays, in order to provide some rules for the design of these devices.

Other designs, which are not specifically array devices at all, were made to the design shown schematically in figure 2.6, in order to be able to obtain some more fundamental information about the properties of s.a.w. metal reflectors which could be compared with the theories which have been put foreward[23,24].

In operation these devices were given a short burst of r.f. waveform into the input transducer, which would travel under the output transducer before being reflected from the metal strip reflectors placed normally across its aperture. The output transducer would then see a burst corresponding to the input pulse, and a series of later pulses corresponding to the reflected pulses coming back from the different reflectors. This device enabled information to be gathered about the behaviour of different numbers of metal strips of different widths and separations as s.a.w. reflectors.

By re-making the device several times with different thicknesses of metallization the relative contributions to the overall reflectivities of the electrical shorting and mass loading effects could be gauged, because the former is insensitive to the metal thickness, whereas the latter depends upon it for its operation.

The results of the measurements made upon these devices are described in chapter 5, and compared with the predictions of the theories mentioned above, and with the reflection coefficents of metal dot reflectors of various shapes and metal thicknesses.

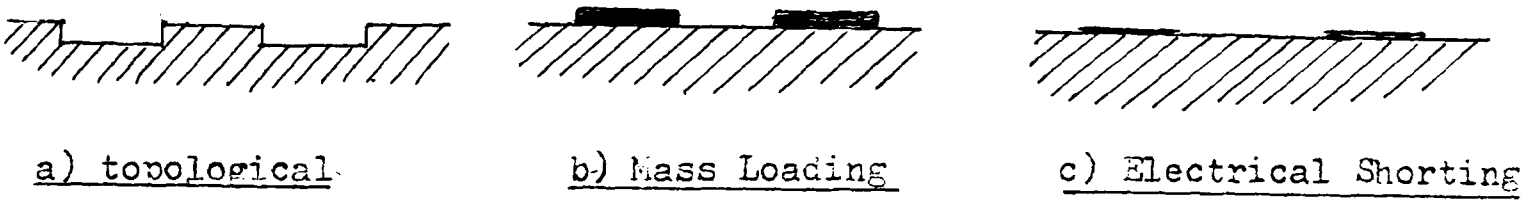

a) topological b) Mass Loading c) Electrical Shorting

Figure 2.1: S.A.W. Reflector Types

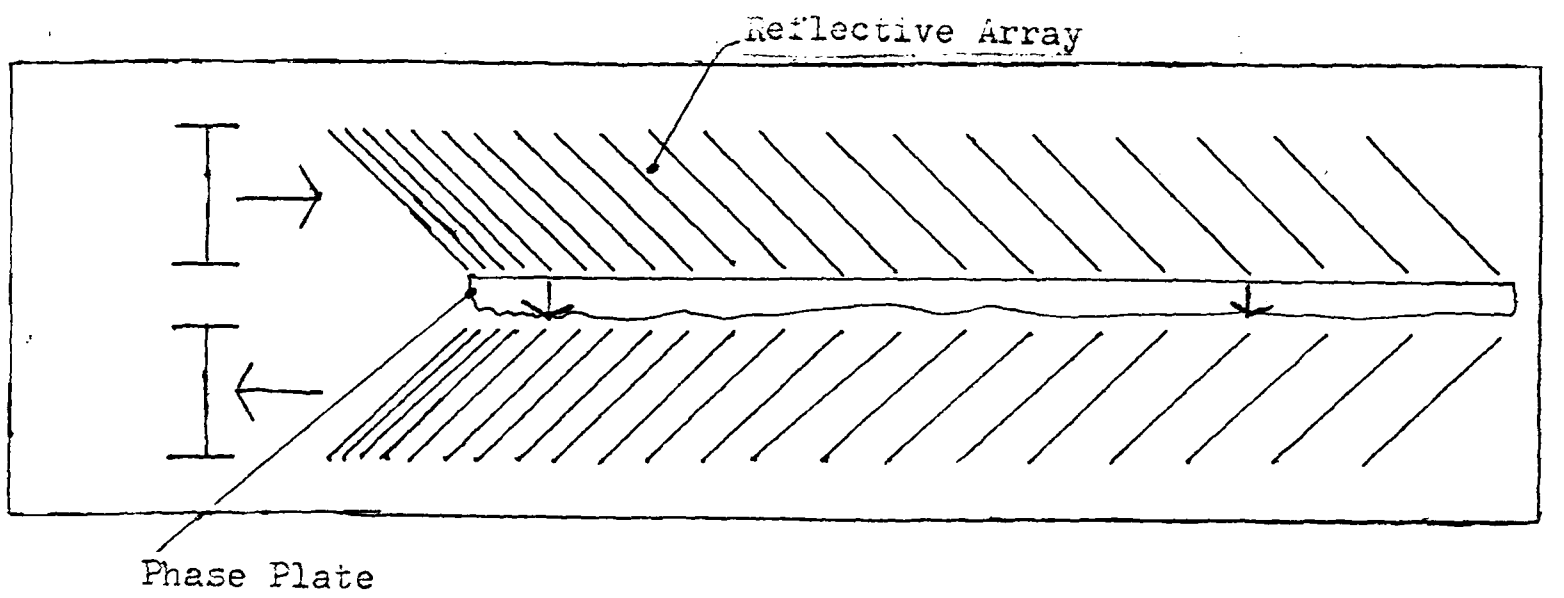

Figure 2.2: Reflective Array Compressor, showing Phase Plate

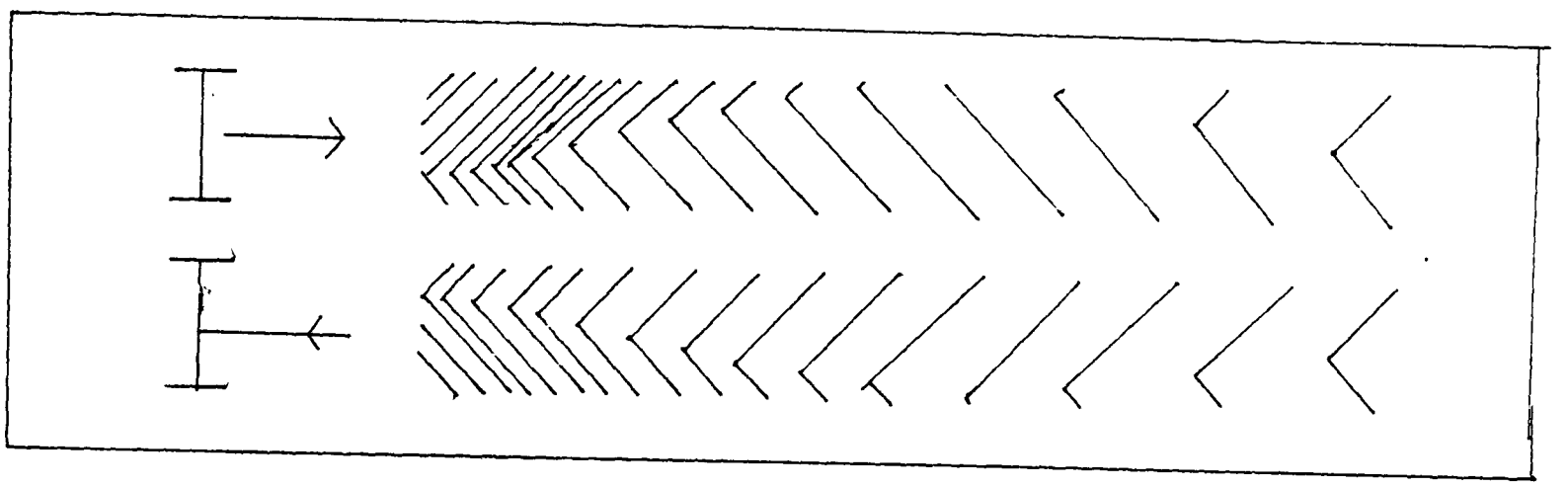

Figure 2.3: Chevron Weighted RAC

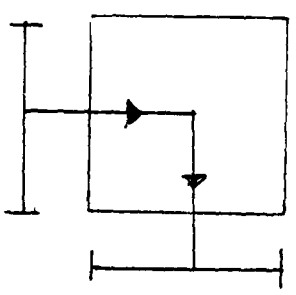

a) L-path

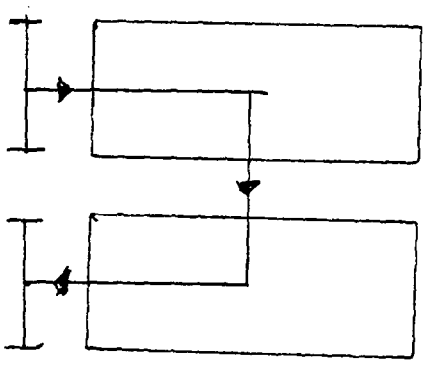

b) U path

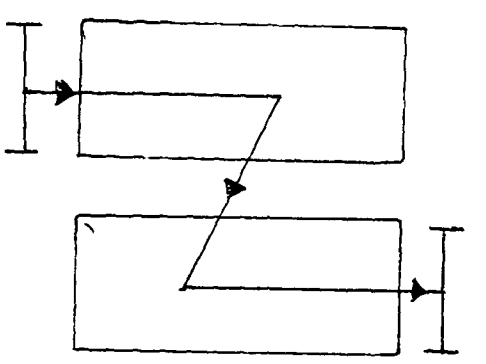

c) Z-path

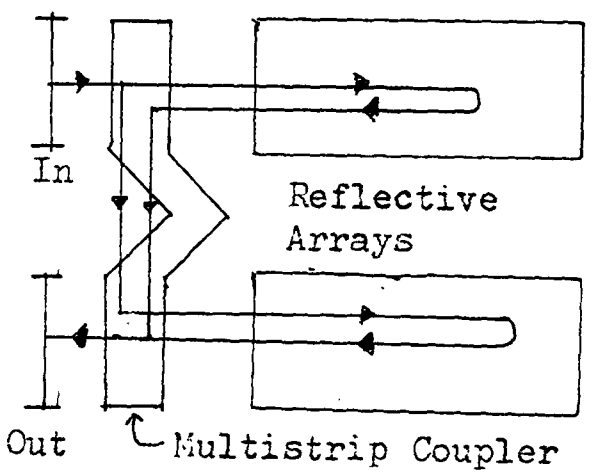

d) In-Line RAC

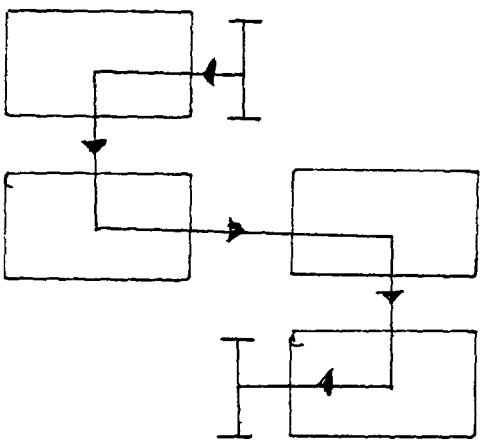

e) 4-Bounce RAC

Figure 2.4: RAC Designs

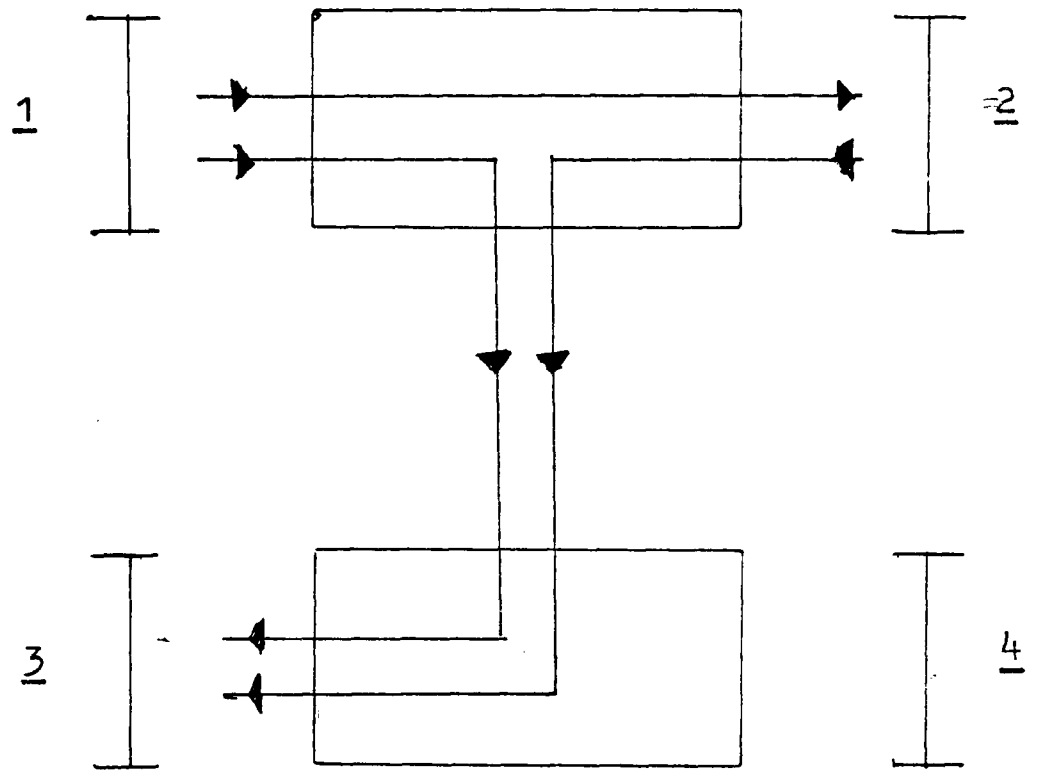

1,3 U-path 2,3 Z-path 1,2 Straight-through Response

Figure 2.5: Laycut of Experimental RDAs

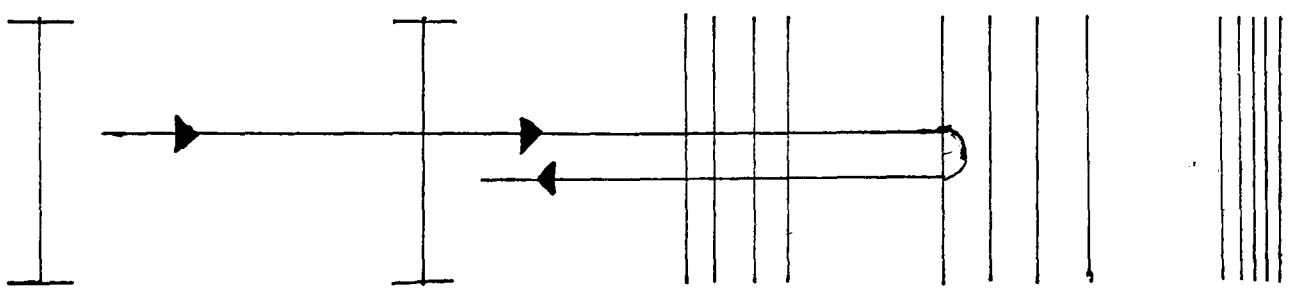

Figure 2.6: Outline of Devices to Examine Reflection of S.A.W. from Metal Strips

CHAPTER 3

MEASUREMENT TECHNIQUES.

3.1 Introduction.

This chapter will describe the equipment which was used to measure the behaviour of the experimental dot array devices were described at the end of the last chapter. It will also mention some techniques used to suppress unwanted waves on the experimental devices.

The two main pieces of equipment which were developed were a fully automatic pulsed potential probe system, and a pulsed insertion loss measuring system. The former will be described in particular detail, because it is a fully automatic system which was developed, as part of this work, from a partially automatic system which is used at the Royal Signals and Radar Establishment (R.S.R.E.), at Malvern.

The operation of the insertion loss system will also be described in detail. Its hardware has many components in common with the potential probe system, and it too is a development, done as part of this work, of a system in use at R.S.R.E. Malvern, and operates approximately ten times as fast as the latter.

3.2: The Potential Probe System

In order to obtain direct information about the behaviour of reflective dot arrays it is necessary to be able to observe the surface wave as it is travelling on the surface of the device. Results from measurements of the response of a device obtained at its transducers can only be interpreted to yield information about the behaviour of the reflective arrays themselves if a suitable model for the arrays is available. When the work was started no suitable models existed, and even when they began to be developed it was useful to be able to compare their predictions with direct observations. The method used to observe the waves directly was an electrostatic potential probe[33]. This device, which is illustrated schematically in figure 3.1, detects the potential asssociated with a stress wave which is travelling along a piezoelectric substrate. It consists of a tungsten needle, etched to be much smaller at its tip than the wavelength of the wave. The needle is connected by a length of coaxial cable to amplifying and detecting circuits. The probe tip is at the local potential of the surface of the device, which will be different from that of the surrounding material, such as the various earthed pieces of metal, because of the stresses associated with the acoustic wave. The travelling wave thus creates an alternating potential between the probe tip and the earth of the input amplifier to

which it is connected, The probe thus appears to the amplifier as a voltage source, the impedance of which is the capacity between the probe tip and the near end of the screened lead to the detector amplifier. This capacity is of the order of a picofarad, which gives the device a source reactance of about 1000 ohms at 100 MHz, a typical operating frequency. This reactance is much greater than the 50 ohms input impedance of the amplifier into which the signal will be fed, and a certain amount of signal gain can be obtained by using a step-down transformer between the probe and the input amplifier to get a somewhat better match. This gave no practical advantages, however, as there was no problems with lack of signal, while there were problems with spurious pick-up from the probe, which could also be increased when the match of the probe to the amplifier was improved. The metal screening container in which the surface wave device was housed contributed very little to the source capacity of the probe, as was determined when the earth connection between the launching transducer and the probe amplifier was reduced to a 100 microhenry choke at the end of a long power supply lead. The shape and amplitude of signal picked up by the probe when this was done differed not at all from that observed when the earth connection was made by two inches of thick wire. The earth connection at d.c. had to remain in order for the system to work, for reasons presumably connected with the operation of the rest of the complex system, probably small d.c. currents flowing into the oscilloscope on which the traces were observed, but the a.c. earth path appears to

be totally uncritical. This confirms what would be expected from a detailed analysis of the probe, such as that produced by Williamson[34], but is not what would have been expected from a simple model which would consider that the source susceptance of the probe was due to the capacity between it and the metal screening under the substrate.

The probe tip itself was mounted vertically, like Williamson's[34], and not inclined, like Kino and Richardson's[33], because it was intended that it should be equally sensitive to waves travelling in all directions within the device, as far as was possible considering the anisotropy of the piezoelectric coupling coefficent, k^2.

An a.c. electrolytic etch method was developed to prepare the probe tips, using saturated sodium hydroxide solution as the electrolyte. This is a relatively weak electrolyte, and a direct current etch soon polarizes it strongly, greatly reducing the etch rate for a given applied voltage. An alternating voltage was therefore used to etch the probe tips. One electrode of the electrolytic cell was the tungsten needle to be etched, and the other was a piece of copper.

The etching mechanism in this case is unclear, but the net result is that tungsten is oxidized to form some sort of complex ion in solution, resulting in an efficent etch of the probe tip. An alternating supply of 12 volts will easily provide a current in excess of the 50 milliamps or so which will etch

a probe tip to a suitable shape in a couple of minutes. The high etch rate may be partially responsible for the shape of the resulting probe end, illustrated in figure 3.2. The diameter of the bulk of the probe is about 1mm, tapering gently to about 500 microns or so, and then to the etched 'point' which is an ellipsoid of about 800 microns major radius. The rounded end of the probe is desirable because it is mechanically stable. It does not deform much and is unlikely to scratch the surface of the device under examination. The ultimate diameter of the tip is about ten microns, which is about a third or a quarter of the wavelength of the surface wave at 100 MHz.

The other end of the needle was electroplated with copper for about 5 miuntes with a current of about 10 milliamps in a solution of approximatly molar copper (II) sulphate. This produced a sufficently thick and sufficently cohesive coating of copper to enable the probe needle to be soldered into a standard miniature coaxial connector, allowing it to be plugged into the probe arm and removed at will if necessary, for example in order to re-etch its tip. Etching is normally only necessary when the tip is first prepared and occasionally later, as the shape of the probe tip does not appear to deteriorate significantly in normal use. All the electrochemical details mentioned above are quite uncritical to the actual fabrication and performance of the probe system.

The probe tip has about the same area as the smaller of the dots in the reflective arrays, and it is interesting to note

that its effectiveness as a detector of surface waves is similar to the effectiveness of a similar-sized dot as a reflector. Its efficency was approximately .005 watts detected per watt per wavelength incident power density (≙-26dB wavelengths).

Besides being, of course, unable to be used to detect waves on a metallized substrate, the potential probe suffers from several other defects as a detector of surface waves of which one must be aware if it is to give relaible results. The most fundamental of these is that it relies on the piezoelectric coupling of the substrate material in order to detect the waves, so that quantitative comparisions between the amplitudes of different waves travelling in different directions can only be made with care. Accurate knowledge of the probe dimensions will be required if any absolute measurements of power densities are to be made at all with the probe[34,35], but this is seldom, in fact, necessary.

A more insidious trouble, which does not appear to have been reported before, can arise from the fact that the probe's source susceptance seen by the input of the amplifier arises from its general capacity to it surroundings. It can arise in certain dot array devices that this capacity is dominated by the proximity of a relatively large dot array. In certain cases the potential of all these dots is in phase, so that the relative "ground" is not at a constant potential, which can give rise to the probe's detecting a separate electrical signal from that due to the wave beneath it. The complexity of the probe's

operation can be judged from the fact that this effect is extremely hard to remove, and appears to enhance the strength of the detected signal, whilst giving rise to spurious standing-wave like effects, i.e. the observed power flow appears to vary in the direction of travel of the wave. This effect is shown in figure 3.3, where the lower trace shows the power flow detected by the probe moving along the direction of travel of the wave. The upper trace shows the signal picked up by the probe before the acoustic signal began to reach it, i.e., the electromagnetic signal radiated by the array. The length of the array meant that there was still a degree of electrical signal reaching the probe from further down the array by the time the acoustic signal from the array had reached the probe, so that time resolution of the acoustic signal was impossible.

The arrays is off the left of the figure, and the acoustic wave is travelling to the right. It is observed that the electromagnetic wave decays rapidly as the probe moves away from the array, and with it the amplitude of the oscillations in the apparent intensity of the acoustic wave. As the electromagnetic wave is so much faster than the acoustic that its phase is almost constant over the distance observed (about 2000 microns), it would be expected that the wavelength of the observed oscillations is the same as that of the acoustic wave, which is indeed the case. Indeed it is this effect which identifies the interfering wave as being electromagnetic, because the period of the interference shows that the interfering wave must be much faster than any possible acoustic wave.

This phenomenon is, then, only of importance in the vicinity of

structures such as dots arrays in which all the dots are excited in phase by the incident surface wave.

A related though much better known phenomenon from which the potential probe suffers is electromagnetic pickup from the launching transducers of the wave and from the leads thereto, but this, although normally very large, can be removed by time-gating the signals, as will be explained later. Significant electromagnetic pick-up can also occur from other transducers which intercept the surface wave, if these are of the correct period to be excited by it. For work on dot arrays, however, this is generally less of a problem than is radiation from the arrays, if the latter occurs. because one is more likely to want to probe near an array than near a transducer. These latter signals cannot be gated out like direct radiation from the launching transducer because they are regenerated from acoustic waves, and, like the signal of interest, are delayed with respect to the excitation of the input transducer.

The overall design of the probing system which was used was determined by the need to remove electromagnetic breakthrough to the probe, and by the need to accurately probe relatively large areas of the substrate and to process the results thus obtained in order to obtain from them the information sought, such as the correct direction of travel of the wave. To these ends a pulsed, fully automatic, probe system was set up.

The system is a development of a partially automatic system, developed at R.S.R.E., Malvern, which was similar to one subsequently described by Williamson[34]. This development was made feasible by the continual advances in the power and cheapness of digital

computing systems. The probe stage used was itself, in fact provided on loan from R.S.R.E. Malvern. A photograph of it is shown as figure 3.5. It is provided with two stepping motors which move the stage underneath the probe with a resolution of half a micron, which was more than adequate for the requirements of this work. Thus in order to probe over an area of a device, it would be placed on the stage and moved under the probe. The probe arm itself was similar to that with which the stage had been provided when received, but re-designed to stiffen it laterally so that the stage could be moved backwards and forewards freely in the whole horizontal plane without excessive backlash due to bending of the probe arm. The balancing of the arm was uncritical provided there was sufficent tracking force on the tip to avoid its leaving the surface of the substrate whilst probing and moving was in progress, this problem being aggravated by the discontinuous manner in which this digitally-controlled system operated. Our work confirmed Williamson's observation[34] that a tungsten probe tip shows no evidence of damaging lithium niobate substrates.

The digital control of the system was effected by a Hewlett- Packard 9825A desk-top calculator system, which had been obtained for the National Coal Board and to which access was available for this work. This calculator also proved sufficently powerful to analyse the results obtained by the probe and to do most of the theoretical modelling to which this work has led, as well as a lot of other incidental computing.

The signals which the system observed were pulsed, in order to be able to distinguish different signals which reached the probe with different time delays. Continous-wave operation could be simulated by running the system with long enough pulses for all the acoustic paths from input transducer to probe to come into effect.

The timing sequence used by the system is shown in figure 3.6. If the electrical excitation is then stopped the electromagnetic pickup from the input transducer to the probe stops almost instantaneously (within a few nanoseconds)(a), whilst the end of the acoustic pulse has to propogate to the probe at the surface wave velocity of about 3 millimetres per microsecond. If the probe is three millimetres from the transducer (it is frequently further), the pure, pseudo-continous, acoustic signal will be received for a further microsecond (b). After this the observed signal will change. The presence of multiple paths for the signal may mean that it will not end altogether, and the system can thus give indications of the extent of such effects (c). It can also be used with short input pulses in order to accurately distinguish the different signal paths and, if applicable, the different modes, acoustic or otherwise, whereby signals reach the probe. In this case the pulse width is reduced until it is less than the differential time delay between the different modes, so that the different signals can be distinguished.

In order to do this and to retain the ability to use the system automatically, the pulse generator and linear gate were introduced. The pulse generator had three outputs. One was a

reference signal which was used to trigger the oscilloscope on which the behaviour of the system was observed. One output was used to chop the input signal to the probe system, and the third was used to open the sample-and hold gate of the linear gate to produce a steady direct voltage corresponding to a particular part of the video waveform which was obtained after the system's detectors and their associated low-pass filters. This direct voltage could then be read asynchronously by an analogue-to-digital convertor controlled by the calculator. The relative timings of the chopping and sampling outputs of the pulse generator could be adjusted so that the required part of the video signal which entered the linear gate could be sampled to appear as the direct voltage at its output. The video waveform was monitored on the oscilloscope in order to do this.

The r.f. signal to the transducer input came initially from a Hewlett- Packard 8660C synthesized signal generator, the frequency and amplitude of the output of which could be controlled by the calculator. This was then chopped by two double-balanced mixers in series, Anzac type MD108's. Two were used as one alone had insufficent isolation at the higher end of the system's designed operating frequency range of 50 to 400MHz.

The chopping signal was applied to the i.f. ports of the mixers, these being the only ones which were direct-coupled The r.f. signal was applied from the r.f. to l.o.† ports, this arrangement being sufficently satisfactory because of the balanced nature of the mixers. The output of the the chopping mixers was then amplified to give a maximum power to the device input

†l.o.= local oscillator.

transducer of around 3 watts. The signal picked up by the probe was applied to an Avantec AMG 502 amplifier, the output of which was subsequently itself amplified through a chain of four further amplifiers. After the first two of these were placed a pair of manually switchable attenuators, to prevent overload of the later amplifiers or of the detectors by strong signals. This positioning proved optimum to give a compromise between amplifier overload characteristics and degradations of signal-to-spurious ratio.

Thermal noise was not in itself a problem in the system. The presence of a strong v.h.f. broadcast band transmitter nearby accounted for most of the observed spurious signals in the broadband r.f. amplifier stages. After the detectors, at video frequencies, other spurious signals made their contributions from the general electrical environment in which the system had to be used, and after the analogue-to-digital convertor quantizing noise could make a significant contribution to the resultant uncertainties in the detection of weak signals. The system proved quite effective however despite these sources of noise, largely because of the excellent ability of the linear gate to reject spurious signals.

Three types of detector could be employed in the system. The first was a phase-sensitive detector, made by feeding the r.f. signal into the appropriate port of another double-balanced mixer whilst feeding a constant-amplitude reference signal from the synthesizer into the local oscillator port and taking the output from the i.f. port.

Of course the reference from the synthesizer must be taken before

the r.f. signal is chopped if it is intended that delayed acoustic signals are to be detected. The output from this detector is proportional to the amplitude of the input signal multiplied by the cosine of its phase delay relative to the reference. If an area of the substrate is probed, then the resulting data can be displayed to give a 'frozen' picture of the wave (see figure 3.7a).

The second detector is a diode square-law detector. It is accurately calibrated, but its maximum allowable output is limited, so that it tends to limit the dynamic range of the system. It also has the disadvantage that spurious signals produce a d.c. output from it, which will interfere with the desired output signal. If such signals differ in frequency from the reference to the phase-sensitive detector, however, as they generally will, they appear as a.c. signals at its output and can therefore be removed by adjusting the video bandwidth after the detector.

If the square-law detector used was overloaded, it took several microseconds to recover, which was a long time within the scales within which the system operates, and this, together with the inevitable noise on the output signal, reduced the dynamic range of the detected signal. It will be realised that although the electromagnetic breakthrough to the probe is removed from the signal recorded by the calculator by the linear gate, it is present at the detector, and this acts with the limitations of the square law detector to reduce the sensitivity of the system in the presence of breakthrough if it is wished to use this detector.

It was to remove this limitation that the third detector, which

is also a square-law device, was built. It consisted of a 3dB power splitter,the outputs of which were fed to the r.f. and l.o. inputs of another mixer, the output of which should be literally the square of the voltage at the input of the splitter. In fact mismatches between the various ports of the devices, all of which, however, are nominally matched to 50 ohms, together with the inevitable losses of total symmetry within the device, mean that its square law response is not particularly accurate. Its frequency response also varies by about 4dB over the 50-400MHz bandwidth of the system. It is however of use where great accuracy is not required and where all the signals in which one is interested are within a relatively narrow bandwidth. Its great asset is that its maximum output is about 200mV, as against 5mV for the more accurate square law detector, and its sensitivity is almost the same, so that it is much freer of problems due to overloading than the latter.

After the detector comes the low pass filter. This serves to remove the second harmonic of the input which is present from all the detectors, and to limit the overall bandwidth of the signals observed on the oscilloscope. The former task is easy, meaning that all it has to do is to reject signals at frequencies above about 100MHz whilst passing those below about 5-10MHz, which is the required video bandwidth. 10MHz bandwidth implies a risetime of the order of 100nS, which corresponds to a distance along the substrate of 300 microns, which is closer than it is normally wished to resolve the operation of surface features, such as transducers, which will have lengths of typically 1mm.

The restriction of the system bandwidth, to remove spurious products produced by the detectors, is harder, requiring, ideally, the narrowest possible bandwidths. This conflict has led to the provision

of three separate low-pass filters. The first is an eight-pole 50 ohm low-pass filter designed to cut off at around 30MHz, to ensure the faithful reproduction of the fastest features of the video waveforms. The second is a similar filter which cuts off at 0.8MHz, to give the narrowest possible bandwidth at the expense of resolution. The third filter, the most used, is a compromise designed to cut off at around 5MHz and subsequently 'tweeked' to cut off nearer 4MHz by trading off steepness of roll-off for a better square-wave response below cutoff.

The signal after the low-pass filter is monitored on the oscilloscope, together with the chopping and sampling pulses, before going to the linear gate. It should be emphasized that the role of the low-pass filters is purely to allow the video waveform to be seen more accurately on the oscilloscope, the bandwidth of the signal reaching the analogue-to-digital convertor being controlled by the linear gate. It is necessary to be able to see the video waveform however in order to correctly position the sampling pulse and to measure acoustic propogation delays as time delays after the end of the r.f. pulse.

The time constant at the output of the linear gate is normally set at 10mS, so that the noise coming from the system is comprable to the analogue-to-digital convertor's quantization noise of 0.5 mV. This relatively short time constant allows relatively fast settling of the output signal level after the probe has been moved, speedingup the probing of large areas.

The analogue-to-digital convertor is a 12 bit device, with a range of ± 1 volt. In order to save memory space in the calculator, however, only the 8 least significant bits are used, giving it a useable range of ± 63.5 mV at the output of the linear gate, which is equivalent to about 16mV useable signal at the detector. Note that the electrical breakthrough no longer contributes to the maximum signal level after the linear gate.

The calculator controls the system by setting the synthesizer frequency and level via and IEEE bus connection[36], and the stepping motors through a multi-purpose interface device known as a multiprogrammer,and made by Hewlett-Packard. This provides pulses which drive the stepping motors through power amplifiers. The resolution of the stepping motors is 0.5 microns on the probe stage. The controller can thus move the probe at will across the device, by moving the device under the probe, and can then measure and store the signal level at any point as seen by the analogue-to-digital convertor, which is also part of the multiprogrammer and which measures the voltage at the output of the linear gate. The general area in which it probes, and the part of the video waveform which it sees at the output of the linear gate are set up before the experimental run either by hand in the case of the latter or by another calculator programme in the case of the former.

The data taken by the probe system was displayed by the calculator in forms which could be interpreted in order to provide information about the propagation of the waves in the region which had been probed.

The results were presented as plots on a graph plotter which were chosen to represent aspects of the behaviour of the wave. A series of such plots is shown in figures 3.7, 3.10 and 3.11.

Figure 3.7 gives examples of plots of data taken with the phase sensitive detector of a simple travelling wave.

Figure 3.7a shows an isometric plot of the detected signal levels recorded and stored by the calculator. This gives a good idea of the general behaviour of the waves present. It was first used by Richardson and Kino[33], and shows the phase sensitive detector's ability to obtain information about both the phase and the amplitude of the wave. It is however difficult to obtain quantitative information from it, and there are other methods of portraying the information which are more easily quantifiable.

Of these the simplest is one used by Williamson[34] in his semi-autpmatic system, in which the sense of the detected signal (greater or less than zero) was used to raise and lower the pen on an x-y plotter. This method of displaying the information is of course suitable for a system without any power to analyse its data in a digital manner, but can be simulated by one, as was done by the fully automated system used for this work. It produces plots similar to figure 3.7b. It can be appreciated that this method is more suited to giving quantitative information about the wave's propagation than is the isometric plot, but at the cost of having suppressed the amplitude information which was present in the original data.

This method can give information about the direction of travel and about the wavelength of a wave detected on the surface.

The former information can be judged from the inclination of the wavefronts and the latter from their seperation. Information about the wavelength of the wave at a given frequency can be used to determine whether the wave at which one is looking is a surface wave or not, which is a useful check on the operation of reflective structures which can, in principle, scatter energy into modes other than that incident onto them.

The accurate determination of the direction of travel of a surface wave requires some reference relative to which the direction of travel can be specified, the determination of which depends on the alignment of the device relative to the probe stage which moves it. This cannot be done to better than about one degree, whilst higher accuracy is wanted in this work for the determination of the direction of travel of the waves reflected by dot arrays. This absolute direction was obtained by propagating the wave from each of the arrays (in figures 2.10 and 3.8) in turn into the space between them. The wave will be reflected through the same angle by each of them, be it greater or less than 90 degrees (see figure 3.8) , and the angle between the waves travelling from each array, which can be measured accurately is twice the deviation, θ, from 90 degrees of the reflection angle of each array. In this way the angle of reflection of the array could be resolved to within about one tenth of a degree. The

resolution is limited by the consistancy with which the directions of the phasefronts can be measured from the plots in the presence of the various spurious signals which are present and which reduce the clarity of the plots of the phasefronts.

This method of detecting the direction of travel of the waves works well in simple cases where there is only one wave present, but the plot shown in figure 3.7b becomes difficult to interpret when there are other waves present than that in which one is interested. The measurements on dot arrays must always be made in the near field of the array, because of the size of the array relative to the total space available on the substrate, so that the pattern of waves present will always be more complicated than a far-field assumption would suggest. In this case the distribution of areas where the detected signal was positive or negative becomes complicated, and another technique is required to distinguish the direction of the wave of interest.

The problem is made worse in the accurate determination of wave directions from an array, because one needs to probe over an area about a hundred wavelengths long across the wavefronts and about a couple of wavelengths deep. In order to obtain a suitable resolution whilst keeping the amount of data produced within the analysis range of the calculator, the probed points will be about a wavelength apart along the wavefront of the desired wave, so

that any interfering waves will be undersampled and will reduce the plot of the zero-crossings to unintelligibility.

A third analysis technique, illustrated in figure 3.7c, was used to overcome this problem. In essence it consisted of looking at the eight nearest neighbours of each point and trying to work out from these whether the point was at a saddle point of the detected data field. The principle is shown in figure 3.8. Each point's nearest neighbours are taken in pairs, and if the value at the point is higher than either of its neighbours a line is drawn at that point in the appropriate direction. The idea is that if the point is part of a continuous crest of a wave, even if it is on the slope of a wave in a different direction, the lines will join up to draw a wavefront, as shown in figure 3.7c. The technique is somewhat crude in its analysis, and susceptible to noise errors, but was found to be a suitable compromise between the complexity of more sophisticated techniques and the presence of difficulties produced by the simpler methods. One necessary refinement was the ability to suppress the plotting of lines which were obviously nothing to do with the wavefronts of interest. Attempts were also made to suppress all points which were not connected to lines at adjacent points in the same directions, but there were unsucessful because the desired line could itself be broken up somewhat, by the peaks being displaced sideways by one point, and the desired line would also then be suppressed.

The technique was useful, however, in determining the direction of the wavefronts in cases beyond the ability of the simpler analysis. Figure 3.10a shows the zero-crossing plot for such a case, and figure 3.10b shows the corresponding plot of the peaks of the wave of interest, showing the wavefronts considerably more clearly than does the zero-crossing plot.

The plots are shown with the scale much compressed along the wavefronts, giving wavefront slopes on the graph of about sixty times those occuring in the actual device. Quantitative measurements were made by estimating the actual positions of the wavefronts on the plot, measuring their slope and converting back to the actual angle of travel of the wave on the device by taking account of the changes of scale of the plotting. It was found to be impossible to develop a calculator routine which would do the job in the presence of noise better than it could be done by eye.

It can be seen in the development from the zero-crossing plots to those which seek out the peaks of the wave that the additional complexity has made use of more of the information in the data, which necessarily increased the sensitivity to noise and other unexpected features in the data, which must be taken into account when devising the analysis routines, to ensure that they can cope with the problems these will introduce. This is the limiting factor which stopped the development of any more complicated methods of analysis.

Full use of the amplitude information in the data has not been

made however, and once the direction of a wavefront has been established it is better gained from direct use of the square law detector than by analysis of the data produced from the phase sensitive detector. This is best used by moving the probe along a line parallel to the wavefronts and plotting the intensity of the power along that line. This technique also was first used by Richardson and Kino[33]. It gives information about the amplitude distribution along the wavefronts of a wave. The example shown in figure 3.11 shows the power distribution along the wavefront of a wave leaving a reflective array, showing that most of the energy is scattered from the front of the array. This gives useful direct information about the wave and needs no further analysis. Again the calculator system is here merely used to imitate operations which can be carried out by purely analogue systems, which would use helical potentiometers to produce an analogue signal corresponding to the position of the probe stage. In this system the probe position is known because the calculator can count how many pulses have been sent to the stepping motors.

The probe system is, overall, capable of probing with resolutions down to a micron or so. It can take up to 10000 points in one run and is able to take the measurements in a matter of 5 minutes or so and to analyse them in a similar length of time.

One of its disadvantages, however, is the need to take so many readings in order to produce its results, which, although practical with a modern digital system, is somewhat inelegant.

3.3: Insertion Loss Measuring System.

A system was also set up to measure the insertion loss of the devices made between their transducers, so that measurements could be made of the overall performance of the devices made. The system is ahown schematically in figure 3.12.

It is a pulses system, like the probe system, and ,as can be seen from the system diagram,it has many components in common with the latter. A conventional network analyser could not be used effectively for this purpose, because the response it would have seen would have been dominated by electromagnetic breakthrough due to the simple packaging used for the experimental devices.

The electrical circuit of the insertion loss system differed from that of the probe system between the power amplifier and the input pre-amplifier, in that the signal was passed either through the device, from transducer to transducer, or else through two programmable attenuators. The principle of the system is that the attenuators should be adjusted so that the signal level through them was the same as that through the device, so that the device attenuation would be of the value programmed into the attenuators. In practice attenuator pads of known characteristics, of 6 or 10dB loss, were used before the transducers to reduce the effects of any possible mismatches between the transducer impedances and the 50 ohm characteristic impedance of the rest of the system. The signal was detected using the accurate square law detector, accuracy being the prime detector requirement in this application.

The system was calculator controlled, as it was possible thereby to control the synthesizer, and also to control the programmable

attenuators through the multiprogrammer. The system was run pulsed, like the probe system, usually with long pulses to imitate pseudo-continous working. This was done because in experimental devices electromagnetic breakthrough between the device transducers can be problem, and this work was done to analyse acoustic rather than electromagnetic effects, so the system was run to simulate the acoustic behaviour of the device with a continuous-wave input, but without the electrical breakthrough effects (see figure 3.6). In order to do this the pulse generator needed to be modified to be partially controlled by the calculator. This is because the gating pulse to the linear gate needs to be sampling the delayed acoustic signal when the system is looking at the signal through the device, but when the signal is coming through the programmable attenuators there is no delay, so the sampling gate must be moved back. This was done by using the multiprogrammer to produce a d.c. voltage which could be added into the delay circuitry inside the pulse generator to alter its behaviour as required .

In use the calculator first of all altered the output level of the synthesizer until the signal level out of the device was such as to produce a level at the detector at the top of its square-law range, so reducing the effects of noise. This in itself could yield a value of the device attenutaion accurate to within one or two decibels.

The value obtained would thus be used as a 'first guess' for the attenuator setting. This whole system behaved somewhat as a digital control system operating to keep the signal level constant at the output of the square law detector.

The use of this comparative method of measuring attenuation . means that the stability of everything except the attenuators over periods longer than that required to take a reading (about half a second) doesn't matter, and results can easily be obtained which are accurate to better than one decibel with a dynamic range of about seventy to eighty decibels. The dynamic range is practically unlimited at low attenuations, and is limited at high attenuations by the available gain of the system, it being necessary to have sufficent signal at the detector for spurii not to be a worry and for the quantizing of the analogue-to-dogital convertor and the offset at the output of the linear gate not to be problems.

This system gives a simpler impression of how a given array device would behave as a frequency filter than does the probe, because its filter response can actually be plotted by measuring its insertion loss over a range of frequencies. The information which this gives about the behaviour of the reflective arrays themselves is less accesible than that given by the probe and requires some sort of model for the device for it to be possible to interpret the device's filter response in terms of the characteristics of the array. Such a model was, however, developed and will be discussed in the next chapter with the results produced by this system.

The system was able to give good results, although, by virtue of its complexity it could sometimes misbehave due to the presence

of spurious signals. It could however take 1000- point measurements of the frequency-response of devices to within better than one decibel accuracy in less than ten minutes, and could plot out the results as it took them, besides being able to store them on the floppy disk system for future retrieval.

3.4: Other Measurement Techniques

The two previous sections of this chapter describe measurement techniques which were designed principally in order to try to understand the behaviour of the reflective arrays. Other measurement methods were also required on occasion in order to gather more information about the reflectors within the arrays. The reflection coefficent through 90 degrees for dots in arrays could be deduced from the modelling and fitting described above to analyse the data produced by the insertion loss measuring system, but further information could be obtained by more direct experiments. The further information which was frequently felt to be useful was the 180 degree reflection coefficent. In the case of the devices designed purely for the measurement of this property of metal stripes, which were desribed at the end of the previous chapter and illustrated schematically in figure 2.6 , this was easily done. As described in that chapter they were given a short burst of r.f. into the input port and the reflection coefficent could be deduced from the relative amplitudes of the direct and reflected signals

appearing at the input port. For these measurements the system common to both probe and insertion loss measurements was used, up to the power amplifier, which fed the input transducer of the device. The signal from the output port passed through the preamplifier and then directly to the oscilloscope. This gave reflected signal levels of about 20mV at the oscilloscope which were sufficently free of noise and spurious to allow the reflection coefficents to be measured with accuracies up to about 5%.

As the frequency responses of such devices varied only slowly, only a relatively small number of measurements needed to be made, so that there was accordingly no need to make use of the various facilities for calculator control in these measurements.

The above technique could also be applied to the measurement of the 180 degree dot reflection coefficent on some dot array devices which had transducers suitably placed to act as the ouput transducer in figure 2.6 . On one case where no such transducer was available the input transducer itself was used, being connected to both power amplifier and oscilloscope through a 3dB coupler (figure 3.13b), which was intended to isolate the incoming signal from the power amplifier from the line to the oscilloscope. The degree of this isolation was in practice limited by the deviation of the transducer's input impedance from 50 ohms , but proved sufficent to stop the breakthrough from overloading the oscilloscope input to make measurements impossible, which would have happened had it not been used.

The amplitude of the observed reflected signal was calibrated against that which was produced when the output of a similar transducer was observed after having been passed through a power divider with its third port terminated by a fifty ohm load (see figure 3.13a).

When electromagnetic radiation from the arrays was not a problem, however, the straight-back reflections from the array could be measured by the simpler method of using the potential probe to detect the reflected wave. This technique could be used for 180 degree reflections because the anisotropy of the piezoelectric coupling would not enter into the relative amplitudes of the signals seen by the probe, because both the incident and the reflected waves will be travelling in the same direction.

This simpler method, where applicable, also removes the neccesity for seperate calibration introduced when the coupler method is used.

The methods which were used to try to suppress spurious electromagnetic signals have been described above, but it seems worth while at the end of this chapter to describe the methods used to suppress unwanted surface waves.

The edges of the substrates of all the devices made were angled so as not to be perpendicular to the prinicipal propagation direction of the waves, in an attempt to reduce problems due to waves being reflected back from these edges. This meant that the substrates were trapezoidal in shape, the parallel edges being

parallel to the principal propagation direction (the Z- direction as Y-cut lithium niobate was always used).

In spite of this precaution, however, the responses of the devices in this state were still very confused by spurious waves. Bulk waves were in general not a significant problem, more being a cause of interest if their effects were observed, and little was done to try to suppress them other than to roughen the backs of the substrates.

Surface waves, however, as has been mentioned before, are easily damped out by lossy materials on the surface of the substrate. In the work herein described the edges of the substrates, and any other places where it was wished that surface waves should not propagate, were coated with thin lines of 'Evostik' adhesive. The lines, about a millimetre or two wide and about half a millimetre thick, were easily produced by dragging a pintip loaded with the epoxy across the surface. This would provide about 20dB attenuation of the wave immeadiately, rising to over thirty once it had dried. This proved quite adequate to suppress most of the effects of spurious waves, and could easily be lifted off tne substrate, once dry, with another pin, leaving the substrate unmarked and with its propagation characteristics apparently identical to what they had been before the epoxy had been put down.

It is also well known that surface waves are heavily damped by water on the surface, and this was used where it was wished

to suppress the wave temporarily. Ethanol and butyl acetate, amongst other things, have also been suggested as being suitable, but they have a lower surface tension than water, and will actually wet the lithium niobate substrates used, spreading all over them and suppressing surface waves on all the substrate. Water, however, does not wet the substrate, but stays in drops, or in thin lines and will only suppress the waves in selected regions, which was generally found to be more useful.

It was found that the water could be most controllably put onto the substrate by dispensing it from an eye dropper onto the end of which had been fixed a hypodermic needle[37]. With such a device it was possible to draw relatively long, thin, lines of water, although such shapes have much higher surface energy than approximately circular 'blobs'. The device could also be used in reverse to draw most of any water on the substrate back up into the dropper, which allowed that left to evaporate much faster when it was wished to remove it again.

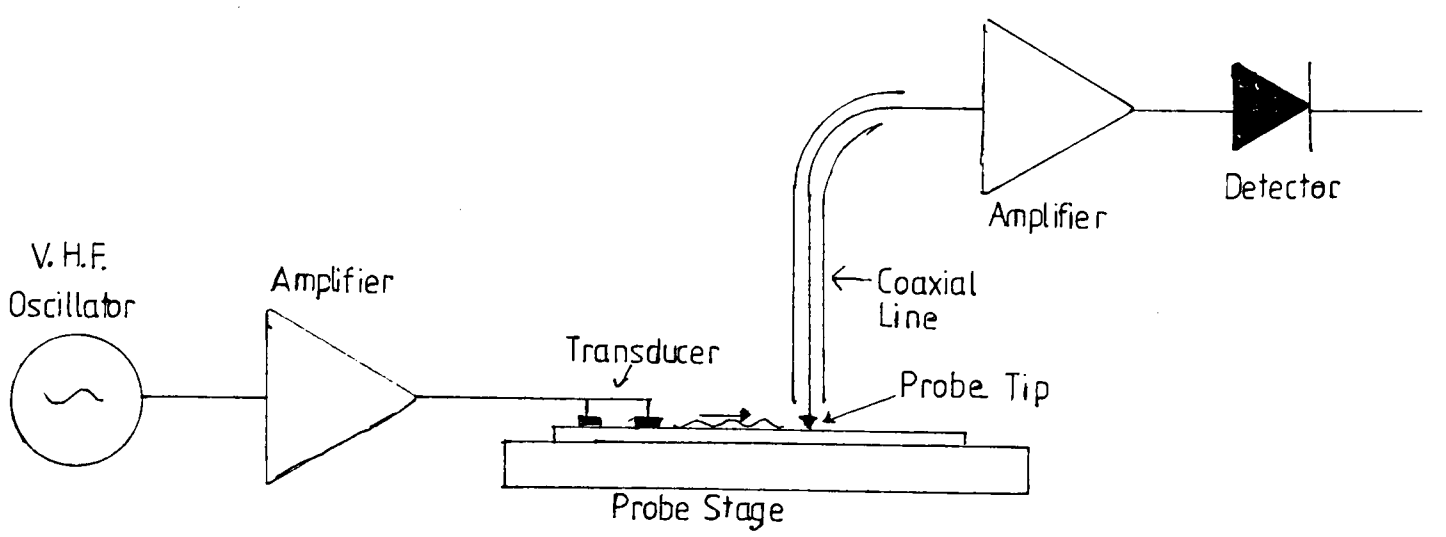

Figure 3.1 : A Potential Probe System In Outline

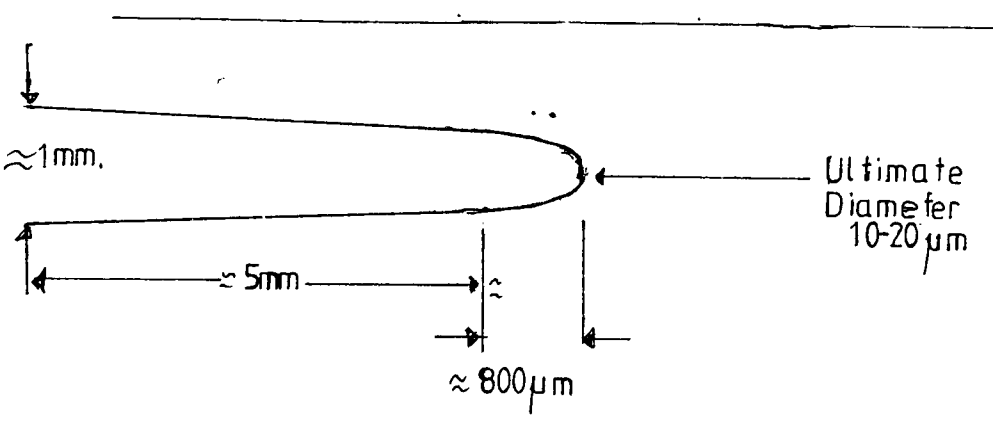

Figure 3.2: A typical Probe Tip

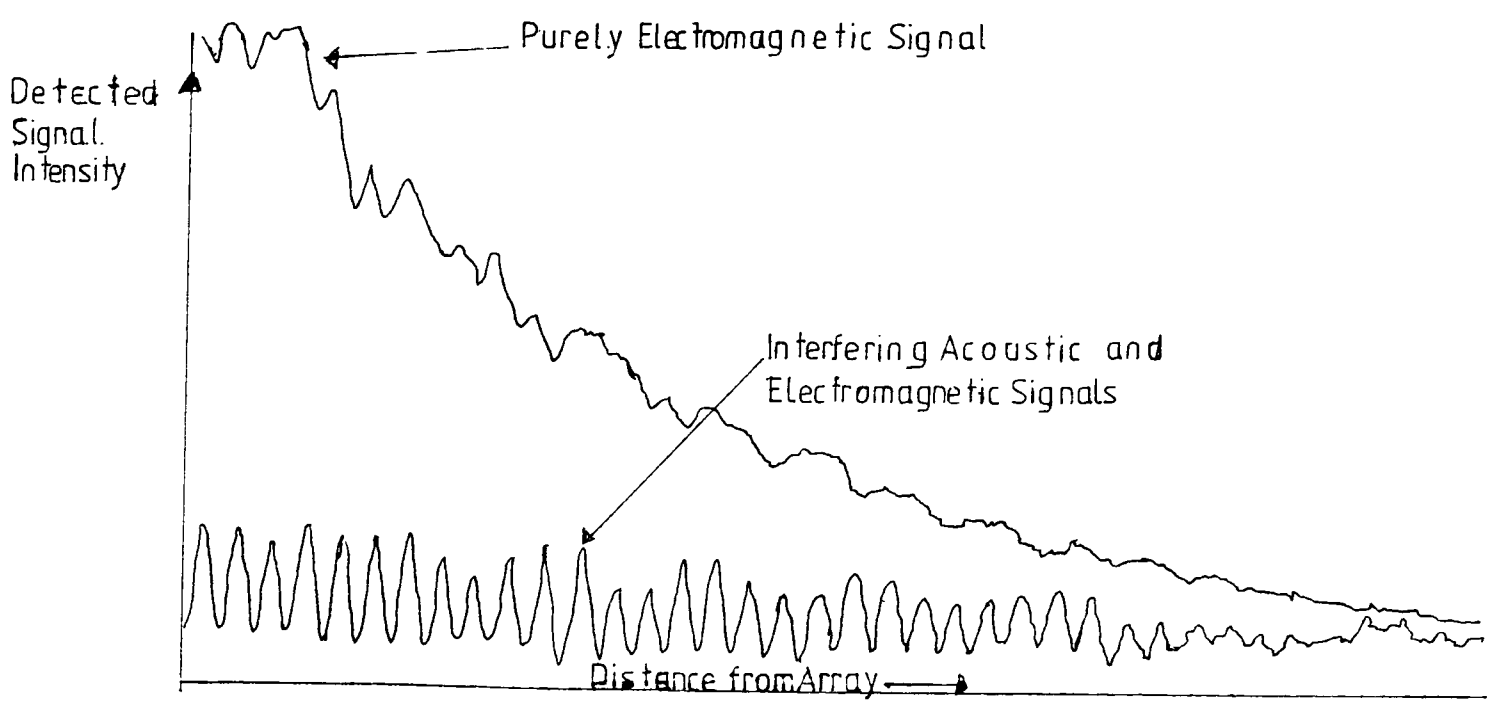

Figure 3.3: Showing Electromagnetic Signal Picked-Up by Probe from a Dot Array

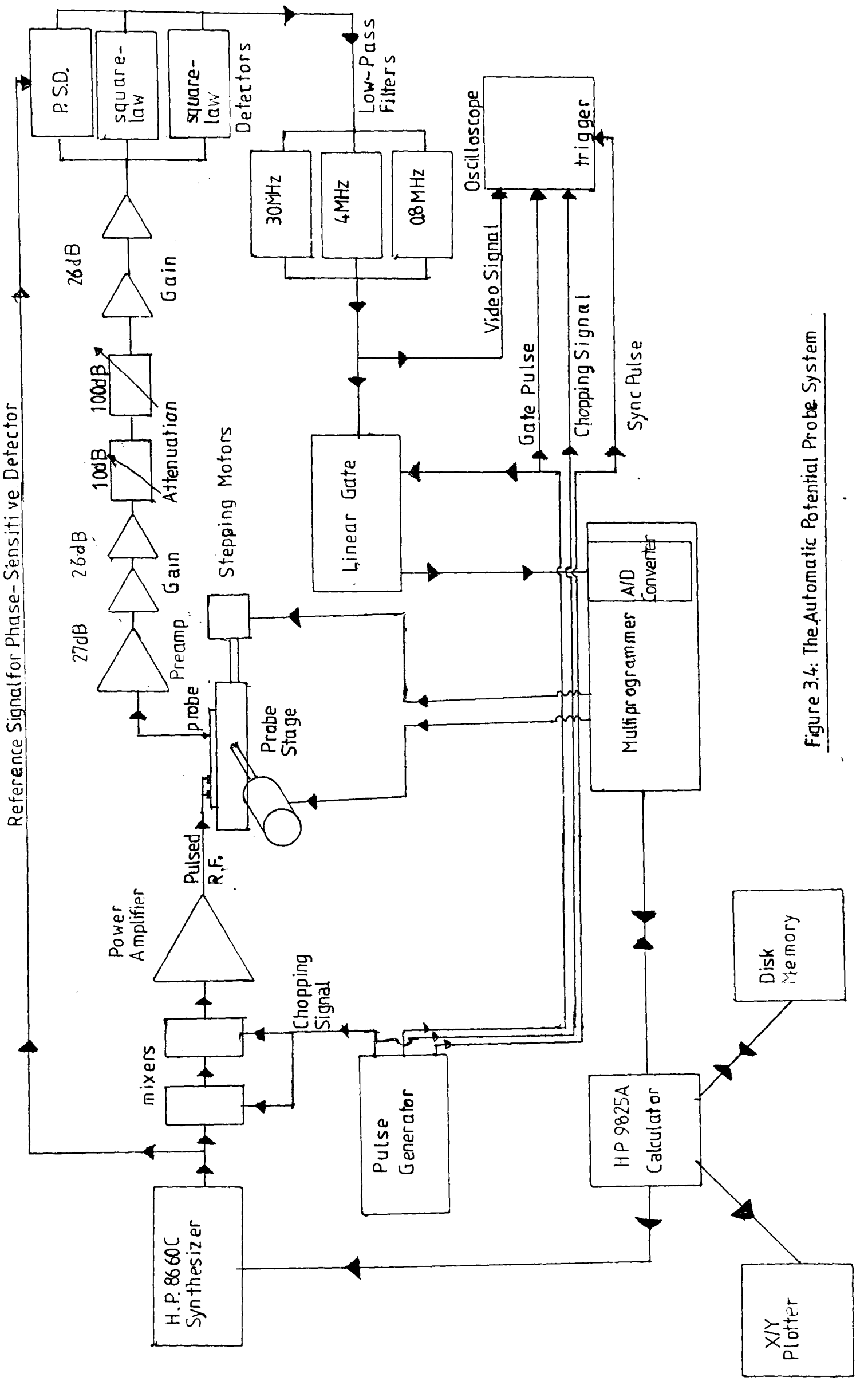

Figure 3.4: The Automatic Potential Probe System

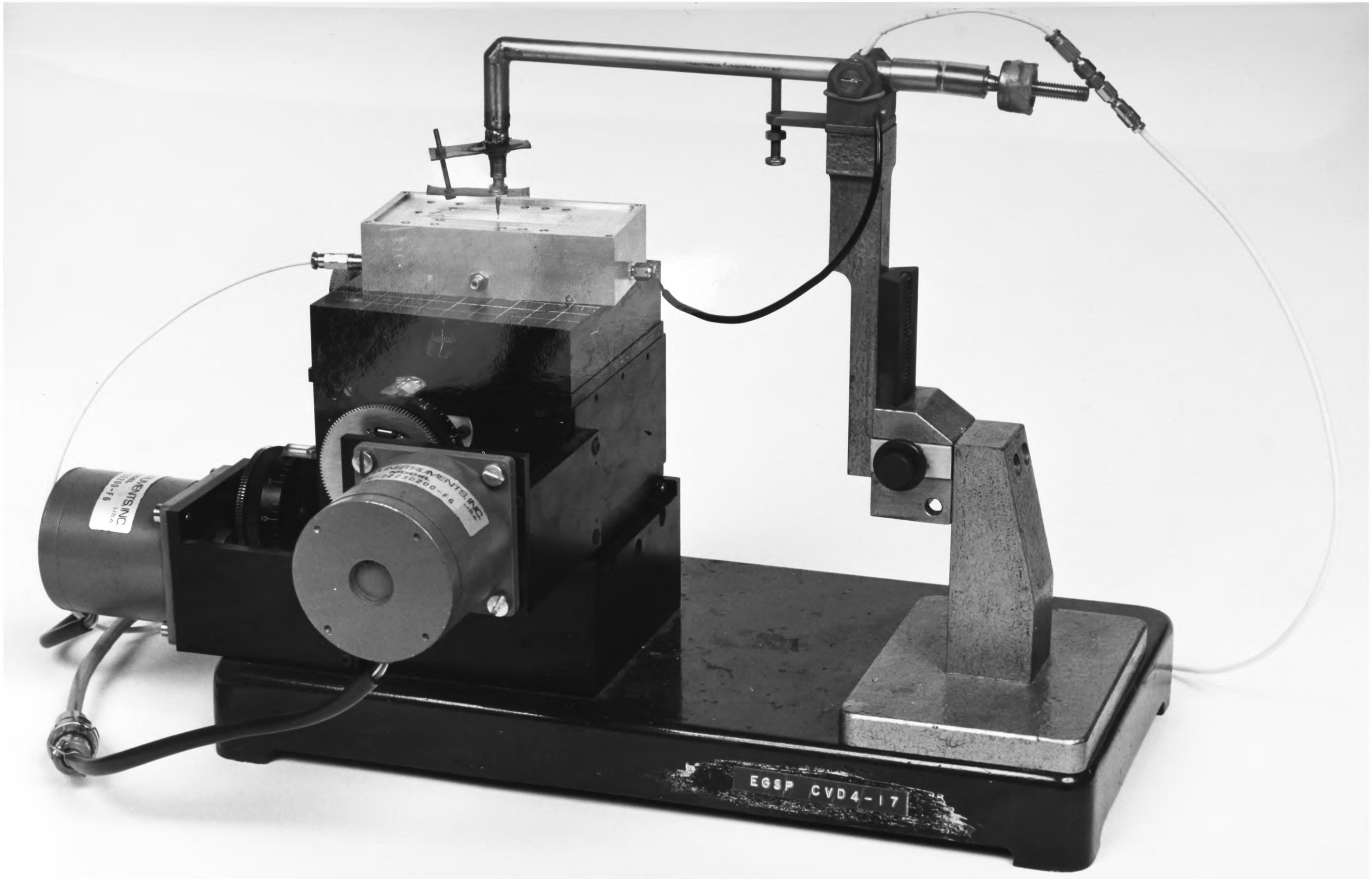
EGSP CVD4-17

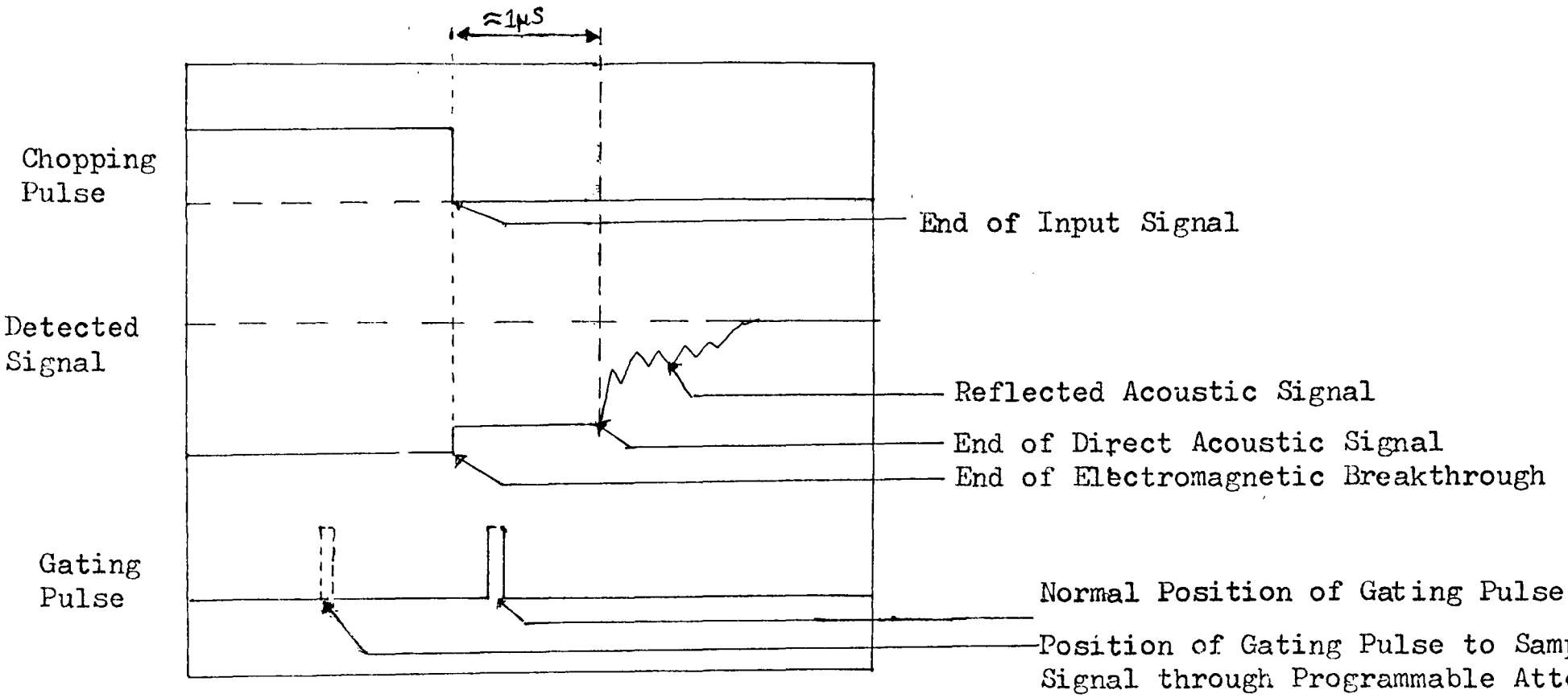

Figure 3.6: Timing Diagram for Pulsed Measurement Systems.

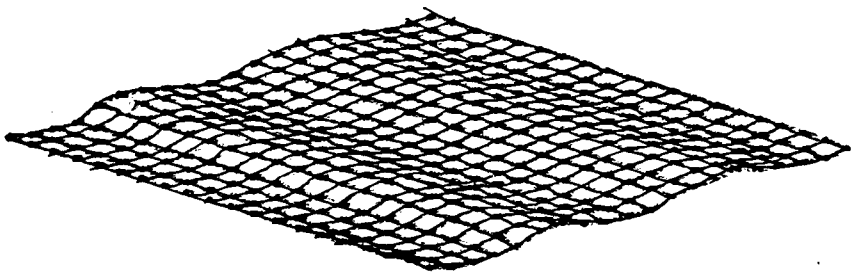

a) Isometric Plot

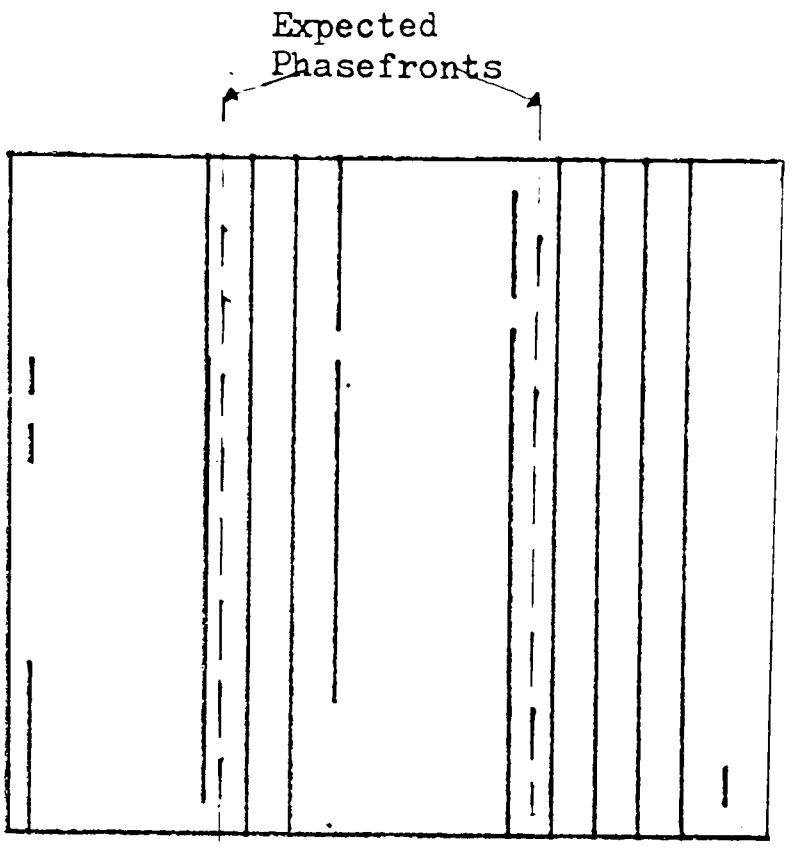

b) Zero-Crossings Plot

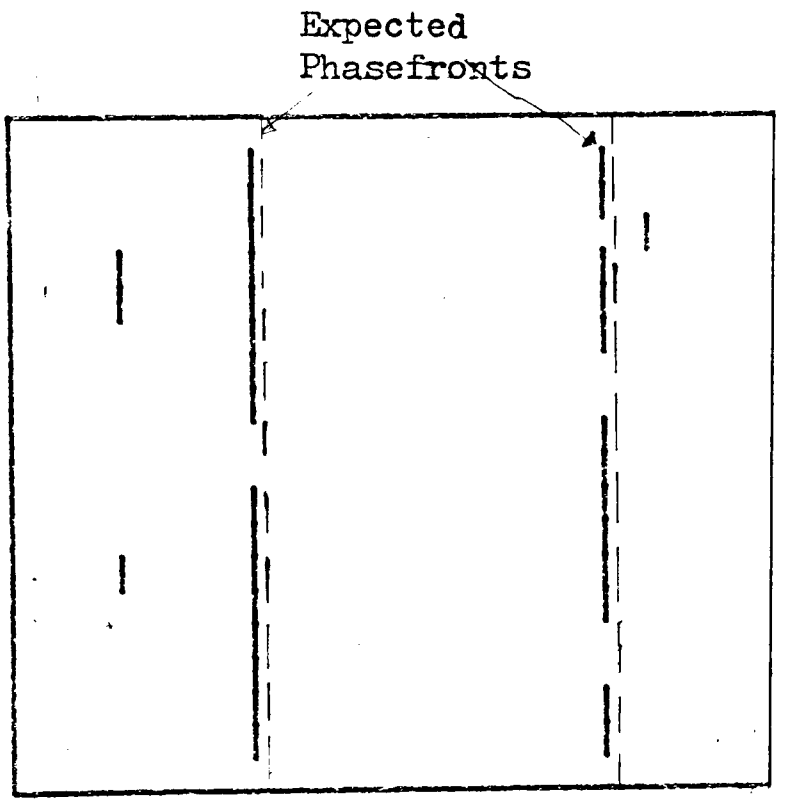

c) Plot of Peaks

Figure 3.7: Ways of Plotting Data from Potential Probe

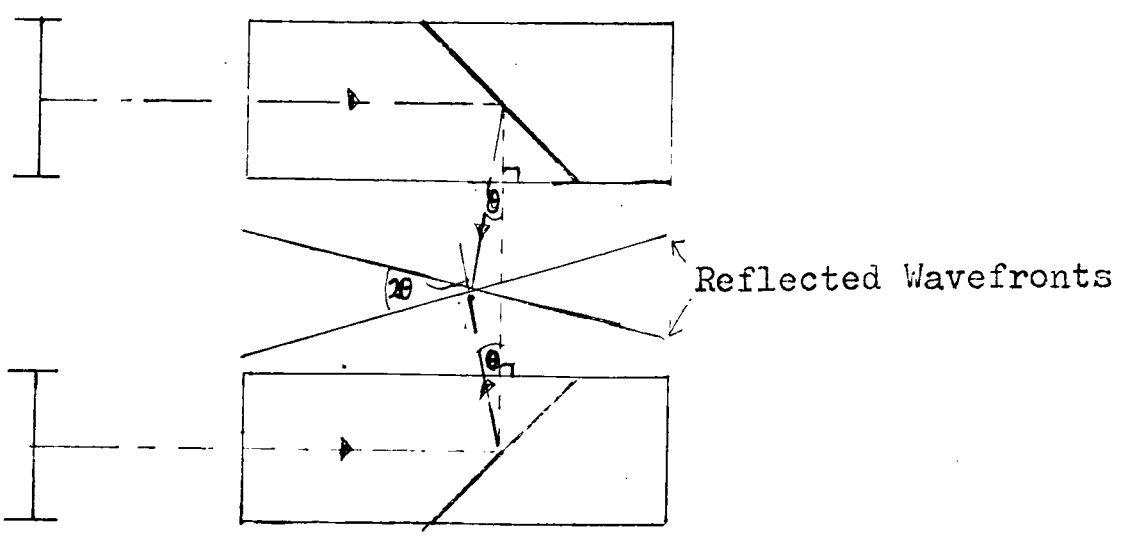

Figure 3.8: Illustrating Determination of Reflection Angle

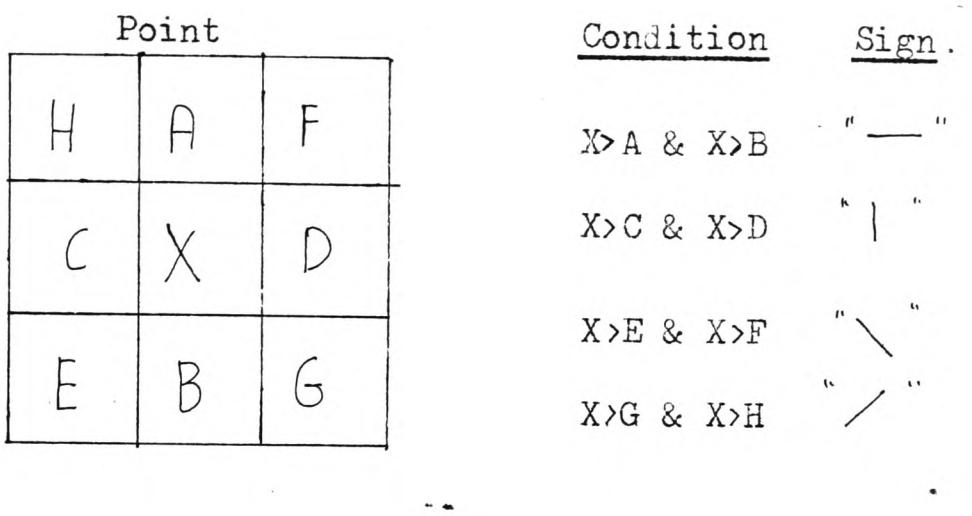

Figure 3.9: Illustrating Operation of Plot of Peaks

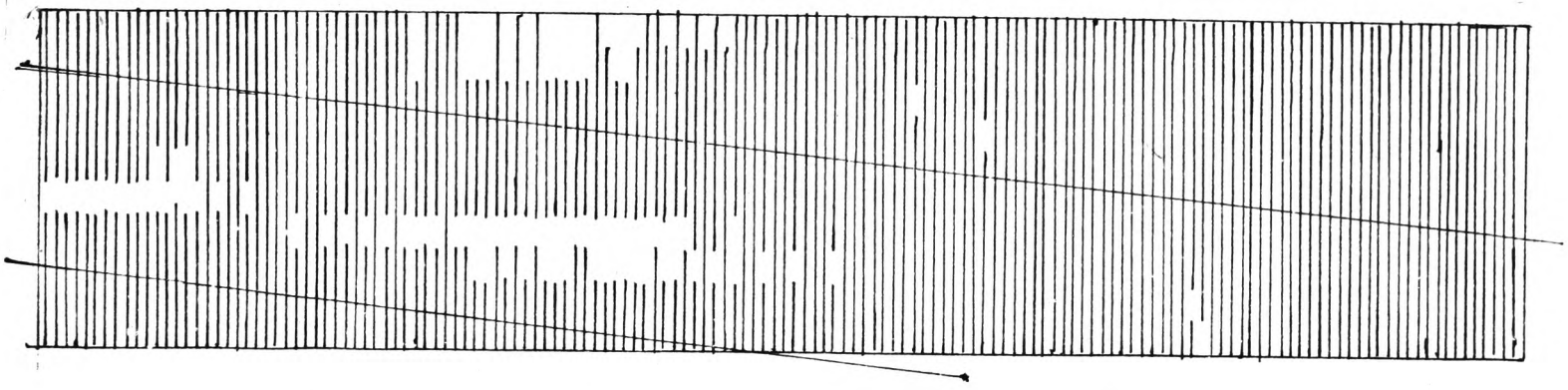

a) Zero-Crossing Plot

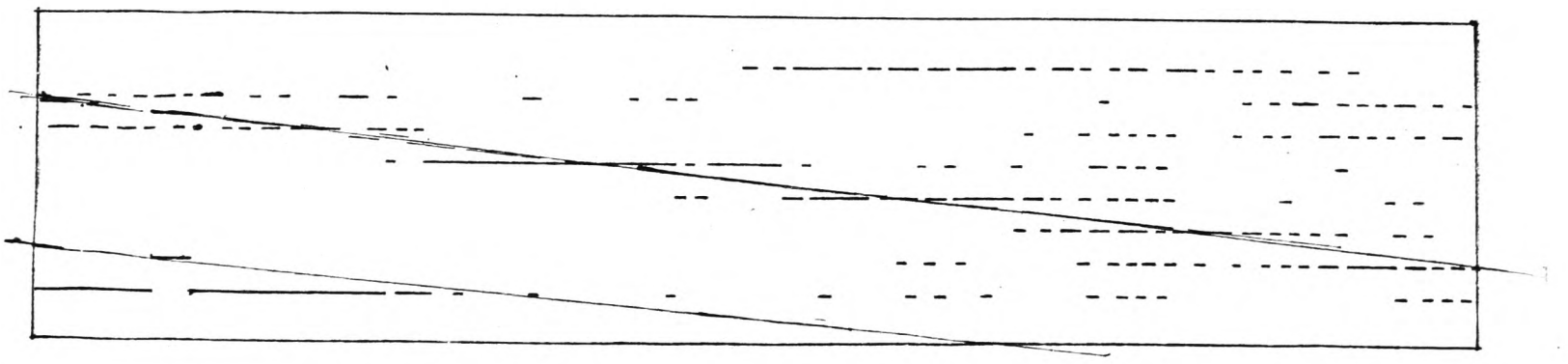

b) Plot of Peaks

(estimated positions of the phasefronts have been added onto) the plots.

Figure 3.10: Showing Advantage of Plot of Peaks

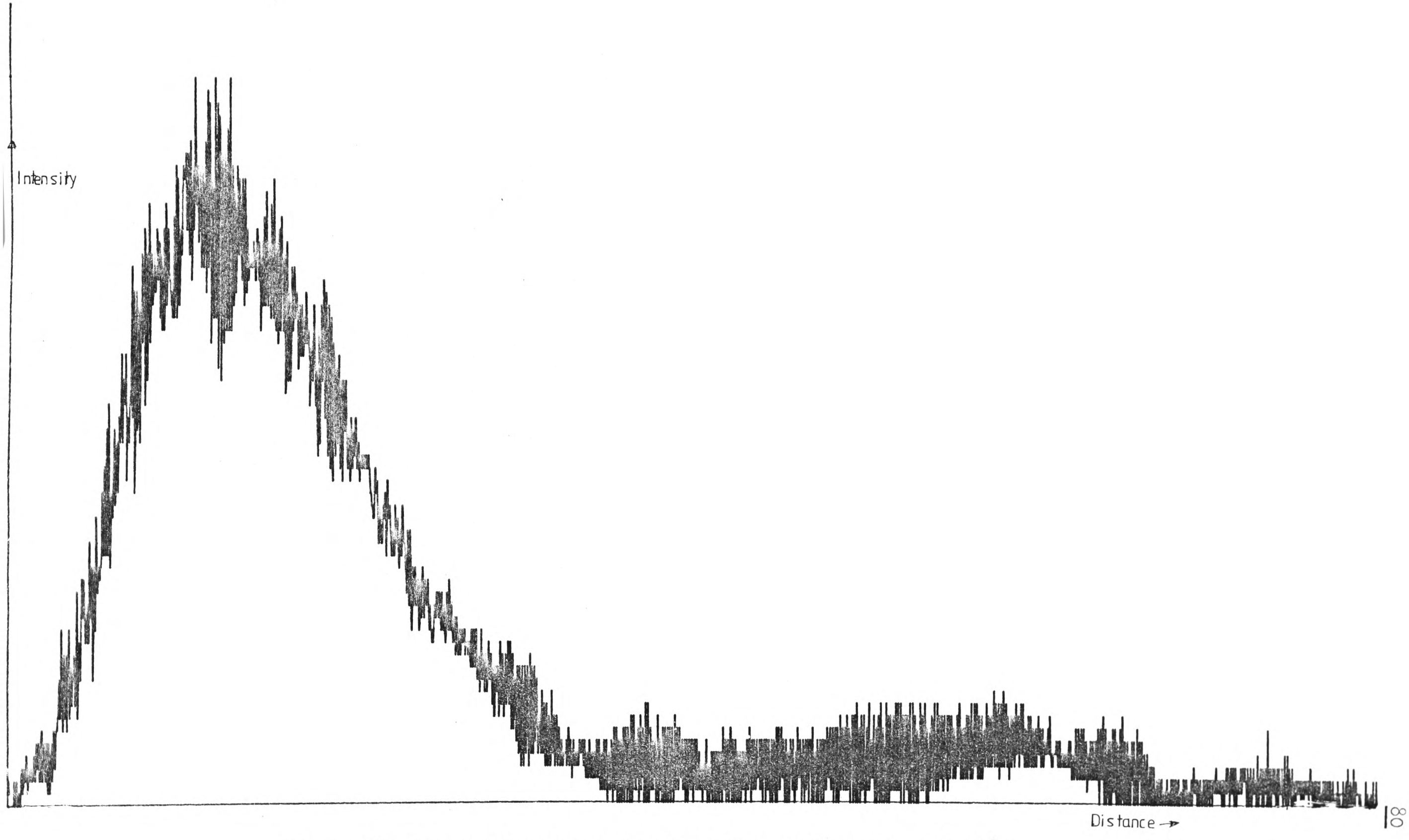

Figure 3.11: Potential probe results for a beam reflected through 90°

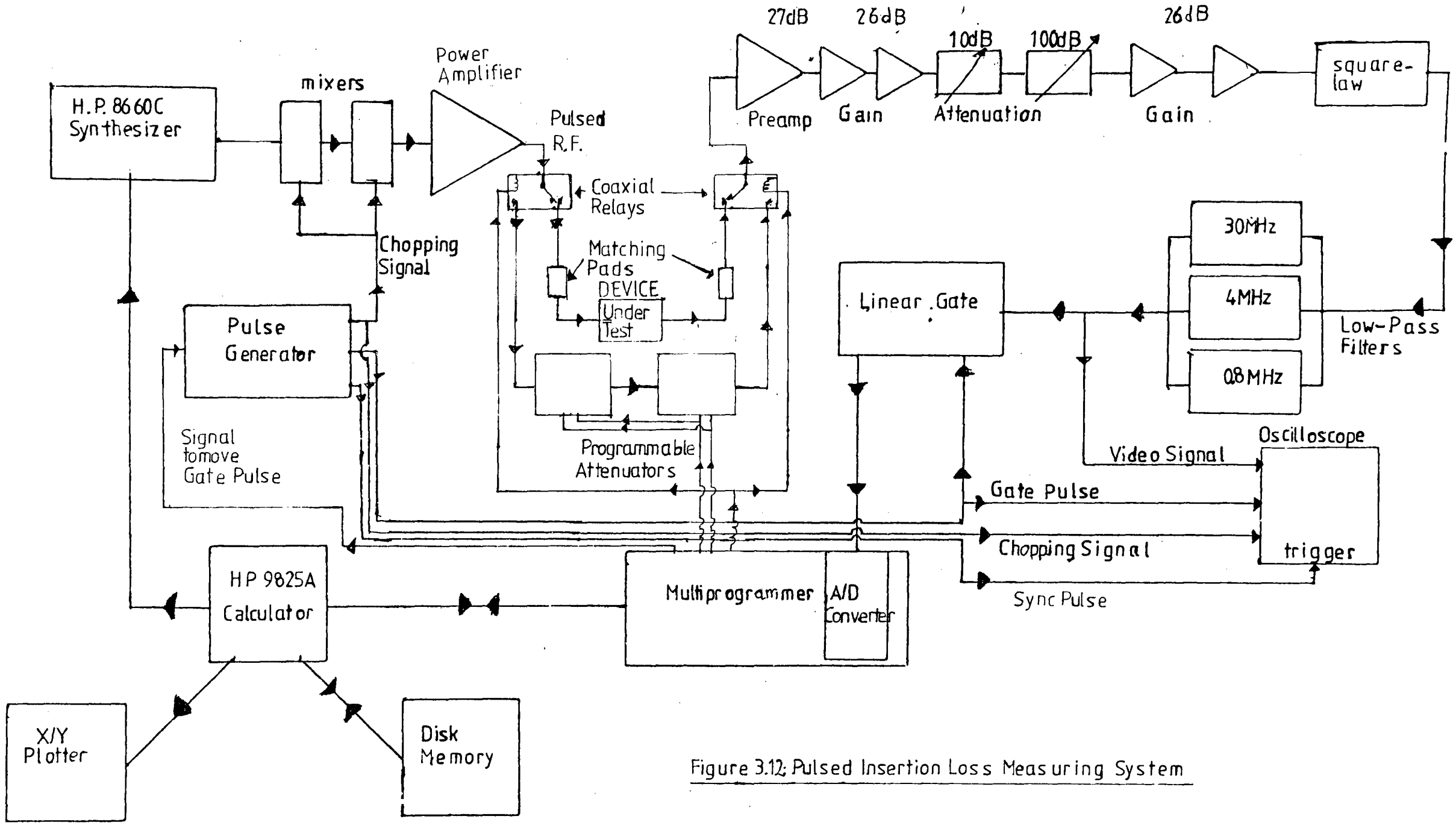

Figure 3.12: Pulsed Insertion Loss Measuring System

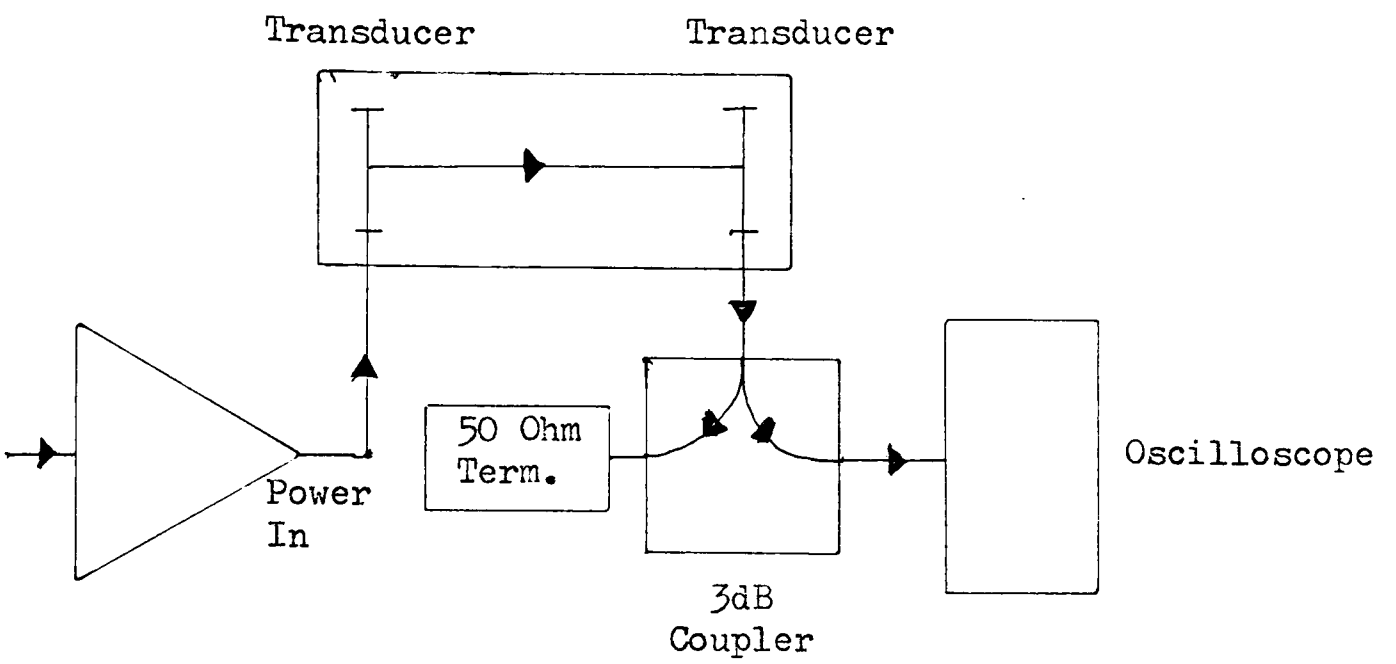

a) Calibration

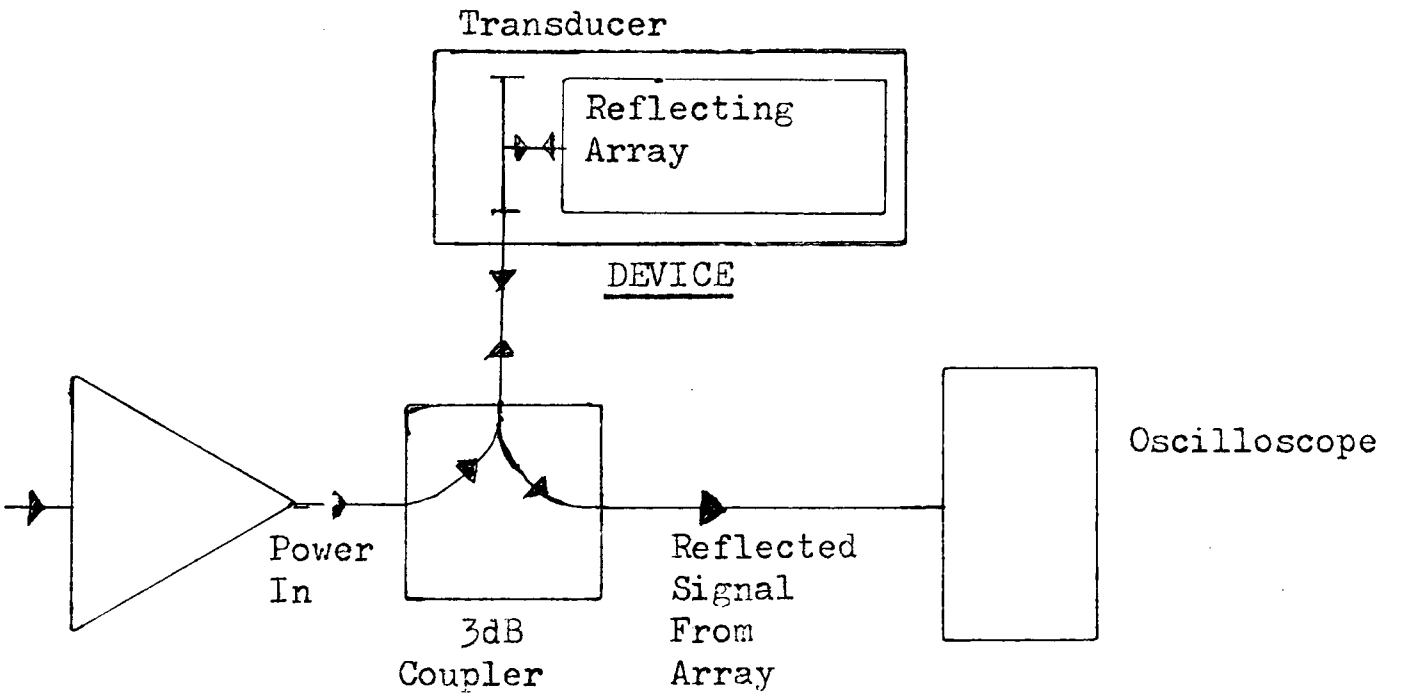

b) Measurement

Figure 3.13: Reflection Measurements Using 3dB Coupler

CHAPTER 4

DOT ARRAYS

4.1: Introduction

This chapter will describe the investigations undertaken into the combination of metal dots into reflective arrays. In principle this action must follow rather than precede the investigation of the reflective properties of the individual dots so combined, but as the reflection coefficent of the single dots is only of the order of 1% to 0.1% of amplitude, they are best investigated by observing their behaviour in arrays and attempting to deduce the behaviour of a single dot from the results obtained. This is what has been done, and in order to understand the limitations on the results obtained, and on the models derived therefrom, it is necessary first to report the investigations undertaken into the behaviour of the arrays.

There are three principal aspects of the behaviour of dot arrays in which interest could be expressed.

The first of these, on the anisotropic substrates upon which the surface wave dot arrays must be made, is the actual angle at through which the dot array scatters ,and how that angle varies as the frequency of the incident wave varies. This is a matter of critical importance to the design of arrays which will reflect through exactly ninety degrees.

The second problem is that of the reflection coefficent of the whole array. If this is very low, much less than unity, then the modelling of the arrays is a simple matter, but when the reflection coefficent approaches unity multiple scattering of the reflected

wave will complicate the problem. The work reported here provides information on the extent to which these simple, low reflection coefficent, models could be used. This factor also affects the manner of the variation of the reflection angle with frequency, for which a weak reflection model gives a simple prediction. The reflection coefficent of the array is, of course, a function of the reflection coefficent of each dot as well as of the effective number of dots in an array.

Akçakaya and Farnell[38] have suggested that for a weakly reflective array this function will be simply a product, but this assumes that the dots act independently of one another, and this is also an assumption which should be tested.

The third significant question which was investigated was that of the actual patterns of dots which should be used in the arrays, and of whether different patterns would offer any advantages over one another.

The basis behind this part of the work was the consideration of the array as behaving like a crystal lattice which will scatter the incident surface waves when they intercept suitable reflecting planes in the array. These planes are analogous to the Bragg planes in a crystal lattice which scatters x-rays or electrons or similar. Any reflective dot array must contain at least one of these planes, the one from which it is desired to reflect the incident wave in order to make the device work, but it can also however contain many other planes which would scatter waves within the passband of the device. Such spurious planes can produce two effects. The more unusual of these, but the more obvious, is the reflection of the

waves through the correct angle, but at some other frequency than that at which it was intended that that part of the array should operate. The more easily occuring case, however, is of spurious planes which will scatter energy which will not be reflected back into the output transducer of the device, but which will nevertheless be lost, and which may be a source of significant losses in the device

The importance of this effect is in part determined by the reflectivity of the array in the undesired mode, which will, in turn, be affected by the anisotropy of the reflection coefficent of the dots. Such modes can, however, wreck havoc upon the response of a badly-designed device. Results will be shown for one such device, which acts as a bandpass filter but suffers, amongst other faults, from a notch in the centre of its passband due to one such mode which had a significantly higher reflection coefficent than the intended mode, and which was co-incident in frequency with it (see figure 4.3).

In order to investigate the effects of these factors on the workings of dot arrays devices a series of periodic devices were made as described at the end of chapter 2 and their behaviour examined to provide information about the points mentioned above.

4.2: Dot Patterns.

Those investigations into the behaviour of dot arrays which gave information about the merits and demerits of different types of dot patterns will be described first. This is because faults in this aspect of the design can lead to troubles in the device which can be so drastic as to make any other results difficult to obtain. It is also necessary to explain some of the other patterns used to some extent in order to explain some of the other results obtained. This aspect of the work is also in some ways the easiest to investigate, because the dot patterns used in the devices are themselves easily and explicitly known, being built into the arrays when the masks for the devices are fabricated. The different dot designs used are shown in figure 4.1. and the patterns of devices in which they were used are shown in figure 4.2. All the dot patterns are shown with the unit cell shown dashed and with rays drawn to a dot and its nearest neighbour to illustrate their behaviour in reflecting waves through ninety degrees upwards and downwards and also back through one hundred and eighty degrees. All the patterns are shown as they would be made in order to reflect a wave incident from the left upwards through ninety degrees. The array angle, θ , is also shown.

The first devices made used either one or other of the two symmetric patterns S1 or S2. Pattern S1 was designed to be totally symmetrical with respect to reflections to either side and straight back. It will be seen that for reflections to either side,(ray paths A-B-C and A'-B'-C' and A-B-D and A'-B'-D',) the path difference for the two rays is one wavelength, so that the reflections from the

different dots add up in phase in both directions for waves incident at the device design wavelength. The same is also true for reflections straight back from the array, along paths A-B-A and A'-B'-A'.

In the type S2 array the unit cell contains only one dot and, again, the reflections from the dots will add up in phase for all three reflection directions at the device centre frequency. The ninety degree paths (A-B-C, A-B'-C' and A-B-D, A-B'-D',) differ in length by one wavelength and the back-reflection paths,(A-B-A, A-B'-A,) by two. This design differs from the type S1, however, in that it was hoped that if the dot itself behaved as a simple scatterer of energy from its edges it would reflect energy preferentially into the desired reflection direction. In fact this did not occur to any significant extent, probably for reasons connected with the nature of the electrical shorting reflection mechanism. The type S1 array also failed to be symmetrical in its reflection, because the dots had a much higher reflection coefficent backwards than they did sideways.

These dot patterns were used in unweighted rectangular arrays, used in devices of the type shown in figure 4.2a. These are like those shown in figure 2.5 except for the addition of the extra transducers 5,6,7 and 8 which were placed between the main transducers and the arrays. The main transducers and the arrays were designed to operate at 60MHz and the other transducers were designed to operate at 78MHz, and were added speculatively in case it was desired to observe the operation of the arrays at higher frequencies. The transducers all had seven pairs of fingers, giving

the main transducer a bandwidth of about 10MHz. The fingers were split[39] to try to suppress acoustic reflections from them.

The higher frequency transducers were little used, because little work was done on the operation of the arrayss at harmonics of their design frequency, and it proved possible to carry out such investigations using the main transducers operating off their design frequency for what work was done thus. The extra tranducers did, however, prove useful in monitoring the reflection back of the input wave by the arrays.

The inclination of the arrays to the incident wave (the array angle, θ, in figure 4.1) was made 46.95 degrees, that being the best estimate then available for the correct angle[15]. The U-path responses (figure 2.4b) were confused by errors in the array angles and by the 180 degree reflections in the array. These devices were, however, designed so as to be able also to operate in a Z-path mode (figure 2.4c). The Z-path insertion loss of the type S1 array, measured as described in section 2 of chapter 3, is shown in figure 4.3 as a function of frequency. It is free from confusion due to mistakes in the array angle, because the Z-path is insensitive to such errors,but shows well that there is a sharp notch in the centre of the passband, which could also be observed in the U-path response.

The whole response is not symmetrical about 60MHz because the period of the array for operation at that frequency was calculated using the free-surface value of the wave velocity, whereas it would be slowed somwehat on passing through the metallized array, it being on of the purposes of this work to determine by how much.

The width of the Z-path response of the S1 array is about 2MHz,

or 3% fractional bandwidth, which is what would be expected, given that the array is fifty wavelengths wide and that the Z-path should show no effects due to changes in reflection angle with frequency.

The notch in the centre of the response is about 1% wide and is attributed to reflection of the incident wave back through 180 degrees by the array (path A-B-A' in figure 4.1), so that little energy remains to be reflected through 90 degrees. This notch is wider than would be expected for reflections back from an array 500 periods long, which implies that the straight back reflection is operating in the highly reflective régime. The fact that the straight back reflection produces a notch in the Z-path response would suggest that energy is reflected back by this mode in preference to the ninety-degree reflection mode. This is a consequence of the anisotropy of the reflection coefficents of the dots themselves, which is an effect which was not considered when the arrays were designed, and which could not have been designed for, as there was then no data available upon which any modification of the design could have been based.

The effect of this reflection of energy back through 180 degrees can be seen more clearly in the straight-through response of the device. The signal path is that shown as 'straight through' in figure 2.5, and its insertion loss plot is shown in figure 4.4. The overall shape of the curve is due to the transducers and the narrow notch to reflections back by the array. The ripple on the response on the high-frequency side of the notch is probably due to the array coupling the input energy into various bulk waves. The sides of the notch are very steep, much steeper than those obtained from arrays where the reflection coefficents of the individual reflectors are much higher, such as metal strip arrays, in

which all the power is reflected within a relatively short distance, reducing the effective length of the array. The reflectivity of the Bragg planes in this device is about 1% amplitude, compared with 3% for full metal strips. The response of this device differs from the predictions of Otto[31], because those results were for the effect on the transmission response of the scattering of energy out of the sides of the array rather than back along its length. The effect here is different because the ninety-degree reflection coefficent is only a quarter or less of that back through 180 degrees, even before account is taken of the fact that the array is ten times as long as it is wide, allowing much greater scope for multiple reflections in that direction.

The use of surface wave devices to produces notch filters such as this has not been reported before and although its occurance was unexpected and, from the view of designing bandpass filters, undesirable, it would appear that it may have uses in the design of special bandstop filters.

These results apply to the type S1 array. Those for the type S2 array were similar, except that the shape of the notches was somewhat different, because the different dots had rather more symmetrical scattering patterns, so that the passband notch was rather more like those reported for strip devices by Otto than was the case for the type S1 array. This device thus added little to the knowledge of the behaviour of arrays of dots, although its different-shaped dots did give some new information about the scattering charactersitics of the dots themselves.

The S1 array similarly gave information about the behaviour of the individual dots, and in particular about the anisotropy of the responses of physically isotropic dots. It also gave

some dramatic evidence of the problems which could be caused by unfortunate array design. Despite the shortcomings of the insertion loss responses of these devices, however, they were able to give useful evidence of the variations of the reflection angle with frequency across the passband, which will be described in the next section.

The results of these first devices showed that in order to be able properly to synthesize dot array devices, it would be necessary to take precautions to design the dot arrays without spurious reflecting planes, to the extent that such a thing is possible. It cannot be done perfectly over an aribtrarily wide bandwidth, but the density of such planes can be reduced, and it is possible to ensure that they do not operate at the same frequency as does the desired reflection mode.

To this end the asymmetric dot patterns, A1 and A2 were designed, shown in figure 4.1. The first of these uses the same type and density of dots as does the type S1 array, but rearranged somewhat. The path difference between two rays reflected upwards off two adjacent dots in a unit cell,(A-B-C and A'-B'-C',) is now $\frac{1}{4}\lambda + \frac{3}{4}\lambda$, or one wavelength. For the backwards reflection it is $2 \times \frac{3}{4}\lambda$, or $1\frac{1}{2}$ wavelengths, so that the reflections interfere destructively.

If the device were strongly reflecting then the reflection downwards through ninety degrees would introduce a potential loss of 3dB into the array's operation as a reflector upwards through ninety degrees, and this design also suppresses that reflection,

the path differeance for this mode (A-B-D and A'-B'-D',) being $\frac{3}{4}\lambda - \frac{1}{4}\lambda$, or $\frac{1}{2}$ wavelength.

The type A2 array has the same properties as the type A1, but is designed using smaller dots than the latter. Here the upwards reflection path difference between the two dots is zero, whilst the backwards and downwards path differences are each half a wavelength at the designed operating frequency. These two array patterns each have different potential advantages and disadvantages. The type A1, with its larger dots, places less demands on the photolithography used to make the devices. Its larger dots also have a higher reflection coefficent than those used in the type A2. The result of this is that in spite of the greater density of dots in the type A2(four per square wavelength as opposed to two), the type A1 still has a higher reflection coefficent per unit area, which could be significant if space is limited and a low insertion loss is wanted.

The type A1 suffers potentially however from having its next nearest Bragg planes only about 20% in frequency away from the operating frequency, whilst those of the type A2 are an octave away.

Another array type which was designed at the same time as the types A1 and A2 was that designated S3. Its form was similar to the type S2, but with slightly smaller dots. This type was made, however, to see whether it would the dot shape itself would suppress the undesired reflection modes.

The type S3 dot can be considered two S1 or A1 dots placed touching each other. If this were a valid representation of the dot, and its reflection effects were calculated in the manner used bore of drawing rays reflected from the centre of the dots, then the diagram for the two S1 dots making up the one S3 dot would be the same as that of the A2 dots, so that the dot itself would suppress reflections backwards and downwards.

This idea would only work if the reflections were caused by purely local mechanisms, such as changes in material impedance at the edges of the dots. In view of the behaviour of the type S1 and S2 dots this would seem most unlikely, and not surprisingly the type S3 array did not work as intended to suppress backwards and downwards reflections. It did, however, work relatively well as a reflecting array and provided more useful information about the behaviour of different-shaped dots. The failure of the dot shape to suppress downwards and backwards reflections was itself, of course, a useful negative result.

In an attempt to improve the performance of the arrays, their overall shape was changed as well, to that shown in figure 4.2b.

The higher frequency transducers were dispensed with, those remaining being still of seven finger-pairs each, with split transducers.

More significantly, the array shape was changed to 100 wavelengths square. It had been suggested that a strongly reflecting array could be made most efficent if it were square rather than rectangular, and our arrays were made square because we did not know whether they would be strongly reflecting or not. It had been known that the type S1

and type S2 arrays had been strongly reflecting backwards, but it was not known how strongly reflecting the arrays could be expected to be once this undesirable side-effect had been removed.

Nash has suggested [15], that unwanted reflection modes could be suppressed by randomizing the positions of the dots along the desired Bragg plane, in order to prevent the formation of any other coherent reflecting planes.

The effect of this would be that instead of there being specific spurious reflection planes, energy would tend to be randomly scattered from the array in all directions and at all frequencies. There is at present little information about how this solution would compare with that of careful array design, but it is difficult to see that it would be able to offer much to compensate for the general scattering of spurious energy. There are two disadvantages with this approach. One is that for a heavily-weighted array, which will only have comparatively few dots, one would have to know how 'random' it could in fact be. Randomization also has to pay a high price at the present, when the pattern generators upon which surface wave device masks are made are designed to operate with repetitive structures. Dispersive dot arrays are difficult to make, requiring large amounts of input information, but one of the advantages of regular bandpass arrays is that they are suited to fabrication on devices which prefer repetitive arrays to random ones.

The array angle in the A1,A2 and S3 devices was changed, for the worse as it turned out, to 47.10 degrees. This mistake arose because at the time the devices were designed no satisfactory

models existed whereby the data obtained from the earlier devices could be correctly interpreted.

Figures 4.5 and 4.6 show the U-path response of the devices made using the type A1 and A2 arrays respectively. It can be seen that the responses are much cleaner than those of the type S1 device. The asymmetries in the frequency responses can be sucessfully attributed to the consequences of errors in the array angle. The dotted lines accompanying the insertion loss curves correspond to the predictions of a simple model of the array which will be described in the next section of this chapter. These curves show that the arrays are weakly reflecting, as indicated by the ease with which a simple model could be fitted to them. That model has also enabled the errors in the array angle and the reflection coefficent of the individual dots to be found from the values of the parameters required to fit the model to the actual insertion losses. The transducers contribute about 15dB to the measured insertion losses, the rest being attributable to the reflective arrays.

The straight-through path for these devices showed no notches comparable to that given by the type S1 array (figure 4.4), which confirmed that the arrays were weakly reflecting. That and other measurements also confirmed that, as intended, the type A1 and A2 arrays suppressed the straight back and downwards reflections.

It can therefore be stated that dot patterns could be sucessfully synthesized to suppress unwanted reflection modes, provided that they did not try to rely on the behaviour of the single dots

for their effect. Besides being necessary in itself in order to synthesize dot arrays with predictable characteristics, the design of suitable dot patterns proved to be a necessary prerequisite to the contruction of arrays which were sufficently well behaved for their behaviour to be sufficently understood for it to be improved upon.

As was mentioned when its design was being described, the type S3 array did not behave as it had been thought it might. Instead it behaved as a simple cubic array, which reflected both upwards, downwards, and backwards. The relatively large dots also had a much higher reflection coefficent than would have been the case had they behaved simply as two S1 dots side by side, with the result that the whole array was strongly reflective. Figure 4.7 shows the U-path insertion loss of the device. It can be seen that there is a narrow notch which may be due to straight back reflections at about 59.0MHz, but its much less dramatic appearance than that of the corresponding feature of the type S1 array means that the dot itself, despite its shape, is behaving in a more nearly isotropic manner. The relatively low insertion loss and the very distorted shape of the response are evidence of the strongly reflective nature of the array.

Figure 4.8 shows the Z-path insertion loss of the type S3 array device. It shows obviously that the dot shape has failed to supress the unwanted ninety degree reflections, without which the Z-path cannot operate. the insertion loss through this path is in fact even lower than that through the U-path. Its shape

has also been distorted by multiple reflections through the device. The device also showed a notch in its straight through response, and reflection measurements made with the 3dB coupler technique described in section 3 of chapter 3, also showed that the backwards reflection was strong.

It was this array pattern and the type S2 pattern, both of which contained only one dot per square wavelength, which radiated electromagnetic energy from the array, as detected by the potential probe as described in chapter 3 section 1. This is because in these two arrays all the dots are excited in the same phase by the incident radiation, as can be seen from figure 4.1.

The failure of the type S3 array to suppress the Z-path and the straight back reflections was not unexpected, and whilst it added no further knowledge about the placing of dots in arrays, it did provide more information about the behaviour of the dots themselves, which will be detailed in the next chapter.

The experiments with different dot arrays have shown that it is both possible, over a limited bandwidth, and sometimes necessary to design dot arrays in order to suppress unwanted reflecting planes. The type A1 and A2 arrays have been shown to fulfil this requirement.

4.3: Measurement of Reflection Angle and Models of Dot Arrays

It has been said repeatedly before that it is vital to the sucess of reflective dot array devices using 90 degree reflections that the reflection angle is correct. In order to analyze the observable effects of errors in the reflection angle in order to correct them, it is necessary to have a suitable model for the array's behaviour. It has been suggested, in the discussion of the results of the experiments into different array patterns, that arrays have been made which can be analyzed using a simple model, and that such a model was available.

The model for the array which will be used can be set up as shown in figure 4.9a. A U-path device will be considered, where each array has an aperture of A wavelengths and a length of B wavelengths at the design frequency of the device. The arrays will be assumed to be uniformly weighted, and to consist of a square array of point reflectors spaced a wavelength apart. The actual array could be modelled by replacing the point reflectors by a model for the actual reflectors found in the array. The arrays will be assumed to be weakly reflecting. A happy consequence of the assumption of weak reflection is that the response of a real array can be found from that of the hypothetical array of point scatterers by multiplying its response by that of a square wavelength of the real array. The design frequency of the array will be called f_0 and the corresponding x-direction wavelength λ_0.

The model ignores the effects of diffraction and of beam-steering upon the behaviour of the array, as they were expected to be of minor significance.

Figure 4.9b shows how the variation of reflection angle with frequency can be deduced from the model chosen. It is assumed that the array is perfect, i.e. that it reflects the wave through ninety degrees at its design frequency. At a frequency $f_0-\delta f$, below the design frequency, the corresponding input wavelength, $\lambda_0+\delta\lambda$, will be greater than the period of the array, λ_0. Hence the lengths of the two ray paths A-B-C and A-B'-C' will differ by an amount $\delta\lambda(v_y/v_x)$, where v_y/v_x is the ratio of the y- and x-direction wave velocities, in addition to the expected one wavelength path difference. If the phase front for the output wave is now drawn, it will slope at an angle, $\delta\theta$, to that for the ninety-degree reflected wave, where

$$\delta\theta = \tan^{-1}[(v_y/v_x)(\delta\lambda/\lambda_0)] \ .$$

For small $\delta\theta$ and small $\delta\lambda$, this approximates to

$$\delta\theta = (v_y/v_x)(\delta f/f_0) \ ,$$

if δf is now defined as the frequency deviation above f_0 rather than below it as before.

In the devices which were made, f_0 was nominally 60MHz, the x and y directions were the Z and X crystal axes of Y-cut lithium niobate , and the velocties v_y and v_x were the corresponding surface wave velocities.

For a free surface $v_x = 3488\ ms^{-1}$ and $v_y = 3724\ ms^{-1}$, so that the expected value of $d\theta/df$ is about 1.02 degree per megahertz.

If the array itself were misaligned by an angle ϕ, then the reflected wave would be mis-directed by an angle 2ϕ, so that the

modified equation for the wave angle would become

$$\delta\theta = (v_y/v_x)(\delta f/f_0) + 2\phi \,. \qquad (4.1$$

There are two consequences of this. One, which can be seen simply from figure 4.9b is that if the unit cell is such as to allow reflections back through 180 degrees, then that reflection will occur at the same frequency as that at which the array reflects through ninety degrees. At that frequency the path difference between backwards reflections from the two dots will be two wavelengths and that for upwards reflections one wavelength.

The second consequence is that for any array there will always be some frequency at which the wave is reflected through ninety degrees. This is not to say, however, that the problem of array angle is insignificant, because if the array is mis-angled then the reflections from different planes will not add up in phase at the frequency at which the wave is reflected through exactly ninety degrees.

Figure 4.9c shows the diagram with the help of which this latter effect can be quantified.

If the dot at the centre of the array is taken as the reference then, at the ninety degree reflection frequency, all the upwards reflections due to the other dots to the left and right of it will be in phase. If the wavelength is not correct for matching the wavelength in the y-direction with the vertical period of the lattice however, then the waves reflected upwards will not add up in phase. If the y-direction wavelength is $\delta\lambda$ greater than the array period, λ_{y0}, then the wave from the i'th dot above the centre one will suffer a phase lag of

$2\pi i\delta\lambda/\lambda_0$ with respect to it. If the array is 'A' wavelengths wide, then the amplitude of the total emergant wave will be

$$r \sum_{i=-A/2}^{i=A/2} \exp(-j2\pi i\delta\lambda/\lambda_0) ,$$

where j is the square root of minus one and i is the counting variable, and r is the reflection coefficent of each dot.

This is a geometric series which sums to

$$r \frac{(\exp(-j\pi A\delta\lambda/\lambda_0) - \exp(j\pi A\delta\lambda/\lambda_0))}{(\exp(-j\pi\delta\lambda/\lambda_0) - \exp(j\pi\delta\lambda/\lambda_0))} .$$

Using the identity $e^{jx} - e^{-jx} = 2/j \sin(x)$, this reduces to

$$r \times \frac{\sin(\pi A\delta\lambda/\lambda_0)}{\sin(\pi\delta\lambda/\lambda_0)} ,$$

If the total reflection coefficent of the column, rA, is taken out of the expression, and the approximation made that $\delta\lambda/\lambda_0 \approx -\delta f/f_0$, then the reflection coefficent for the row becomes:

$$rA \frac{\sin(\pi A\delta f/f_0)}{A \sin(\pi\delta f/f_0)} . \qquad (4.2$$

The above expression gives the effect on the amplitude of the reflected signal in changing the input frequency of the wave. For an infinitely large array (A tends to infinity), the response will reduce to that predicted by Bragg, that is a response at f_0 and its multiples only.

It will be seen that the observed response from a finite sized reflecting array will be influenced by two effects. The

first is that of the fall-off in the amplitude of the reflected wave, and the second is the variation in the direction of travel of that wave as its frequency is varied. The effect of misangling the array, it will be seen, is to create the situation where the frequency at which most energy is reflected by the array and that at which the energy which is reflected is reflected through exactly ninety degrees no longer coincide. It is this failure of coincidence which gave rise to the asymmetry in the frequency responses of the type A1 and type A2 array devices as first fabricated (figures 4.5 and 4.6).

The actual effect of the variations of angle of the wave upon the frequency response of the device is a function of the aperture of the receiving transducers, which will, of course, normally be the same as the width of the arrays.

The effect of the misalignment is for the wave detected by some parts of the transducer to be out-of-phase with that detected by other parts, as shown in figure 4.9d. Figure 4.9a shows that if the wave reflected from one array is misaligned by a small angle $\delta\theta$, then that reflected from 2 arrays in a U-path will be misaligned by an angle $2\delta\theta$. The effect of this upon the process of detection by the output transducer is that a portion of the wave detected at a distance y ~~above~~ the centre of the transducer will be out of phase with that detected at the centre by an amount $\exp(2jky\delta\theta)$, where $k = 2\kappa/\lambda_0$. If the transducer aperture extends from $y = -A\lambda/2$ to $y = +A\lambda/2$, where λ is the y-direction

wavelength corresponding to λ_0 in the x-direction, and the detected signal is q_0 per unit length of transducer, then the total detected signal is

$$q_0 \int_{-A\lambda/2}^{A\lambda/2} \exp(2jky\delta\theta)\, dy$$

$$= q_0 \frac{\sin(kA\lambda\delta\theta)}{k\delta\theta} .$$

The maximum signal which could be detected, when $\delta\theta = 0$, is $A\lambda q_0$. The reduction in possible detected signal due to misalignment of the output beam is thus

$$\frac{\sin(kA\lambda\delta\theta)}{kA\lambda\delta\theta} . \qquad (4.3$$

If the expression 4.1, $\delta\theta = (v_y/v_x)(\delta f/f_0) + 2\phi$, is substituted into the above, the overall expression for the effect on the received signal of the misalignment of the arrays and of the variations in reflection angle with frequency is obtained:

$$\text{reduction} = \frac{\sin(2\pi A(\delta f/f_0 + 2\phi))}{2\pi A(\delta f/f_0 + 2\phi)} . \qquad (4.4$$

This ignores a multiplier of (v_x/v_y) on the 2ϕ term, but this is normally nearly unity.

The overall response of an array device will be the product of three terms. There will be one term for the fall-off in efficency of each array as the input frequency varies from

the design frequency, and the third term due to the variation in reflection angle with frequency and with misalignment of the arrays.

The overall response will be:

$$A(\delta f) = ABr^2 \frac{\sin(\pi A\delta f/f_0)}{A\sin(\pi\delta f/f_0)} \frac{\sin(\pi B\delta f/f_0)}{B\sin(\pi\delta f/f_0)} \frac{\sin(2\pi A(\delta f/f_0 + 2\phi)}{2\pi A(\delta f/f_0 + 2\phi)}, \quad (4.5$$

where A is the aperture of the system, B is the length of the arrays, δf is the frequency variation above the nominal operating frequency f_0, and ϕ is the error in the array angle.

A similar expression was obtained by Otto[31], for an array of weakly reflecting strips, by considering the scattering of each cell of one array into the second array, and then the scattering of that signal by each unit of the second array into the output transducer. As this is an entirely discrete model it gives a term of the form sin(Ax)/Asin(x) for the variation of signal as the reflection angle changes, rather than the expression above of sin(Ax)/Ax. Where x is small, i.e. near the design frequency of the device, there is little difference between these models, but the form with the sine on the denominator allows for the operation of the device at harmonics of the design frequency, as would be expected from a model where the reflectors were treated as isotropic point radiators. The calculation of the signal detected by the output transducer, however, assumed that the output wave was continuous, and would thus have no harmonic responses. If the point scattering array had been replaced by

one with a continous, sinsoidally-varying reflection coefficent, such that it should not have any harmonic responses, the sin(Ax)/Asin(x) responses for the arrays would have been replaced by the more commonly-found sin(Ax)/Ax form. The hybrid form of the expression quoted above is due to the inconsistancy of taking the output wavefronts from a discontinuous scattering array to be continuous, but the differences will only show up far off the operating frequency of the device, where the model will not be used anyway, as the responses of the arrays were only measured near their design frequencies to obtain the required parameters for their operation.

The model chosen ignores many second-order effects, such as the loss of efficency due to the mis-aligned output beam entirely missing the second array or output transducer, as well as such effects as diffraction. Over the range of frequency within which the model is to be compared with actual measurements these effects were reckoned to contribute less than a decibel or so to the overall response, and the quality of fit obtained is good for such a simple model.

One of the advantages of the model as formulated is that it allows a clear distinction between the effects of reduction in efficency due to changes in reflection angle with frequency and those due to the lack of synchronicity between the waves and the Bragg planes of the array, a distinction which is useful in interpreting the results in terms of the parameters used to design the arrays, which is something which is not so readily apparent in the formulation used by Otto.

Otto's model of the weakly reflecting array was itself not designed specifically to model weak arrays, but to produce a model

for a weakly-reflecting sub-unit which could be used as a cell in a model for a strongly reflecting array, such that multiple reflections between the cells would need to be taken into account whereas those within the cells could be ignored. This model was intended for use in predicting the behaviour of metal strip arrays, which are of necessity strongly reflecting because of the high reflection coefficent of the individual strips. The full Otto model was set up on a computer, and some predictions from it compared with the results obtained from a reflective array made using plane strips instead of dots, in a device of the form outlined in figure 4.2b, as a comparision with the dot arrays.

The first prediction of equation 4.5 to be tested was that that the angle of the reflected wave from a device designed to operate at about 60MHz should vary at a rate of about 1 degree per megahertz.

The directions of the reflected wavefronts for several devices were determined for a range of frequencies within the operating frequency range of the arrays, using the potential probe system described in the previous chapter, and the results are shown in figure 4.10.

The dot arrays examined were the types S1 and S2 and the type A1. The results of the variation of reflection angle with frequency for these three devices are shown in figure 4.10, together with best straight line fits for them and with a dotted line showing the predictions of equation 4.1. The standard deviations of the points from the best fit lines were calculated,

and some error bars are shown for ± 2 standard deviations divergance, which gives the 95% confidence limits for the data. The principal causes of error are believed to be inaccuaracies in the estimation of the directions of the wavefronts from the output plots from the potential probe, and in the assumption behind the operation that the wavefronts were in fact strictly plane.

It can be seen that within the experimental errors the curves obtain match the theoretical prediction. The intercepts of the lines on the frequency axis are indications of errors in the design of the device, that the array angle was wrong and that the array period was wrong for the intended operating frequency of 60MHz. The intercept of the theore-tical prediction is arbitrary, as it is only the slopes of the lines which are being compared

The fact that the results of the type A1 array should match the theory is not surprising in view of the ability of the simple theory to account for its overall insertion loss characteristics (figure 4.5), but the fact that those for the S1 and S2 array devices also match the theory is unexpected in view of the confused nature of their insertion losses. It must mean that although they behave as strongly reflecting devices as far as the straight-back reflections are concerned, as far as the ninety degree reflections are concerned they behave, at any rate to this extent, as weakly reflecting arrays.

The corresponding plot of reflection angle against frequency for the full strip array mentioned above is also shown in figure 4.10, together with the dotted line representing the predictions of Otto's strong-reflection theory designed to describe it. The situation is here less simple than in the other cases, in as much as there is no one 'reflection angle', because the wavefronts of the

reflected wave are not plane. There is, however, a distinct section of the wavefront which has a minimum deviation of reflection angle from ninety degrees, and it is the angle of this part of the wavefront which is plotted in figure 4.10. Again the theoretical predictions agree quite well with the practical results, where both exist, most dramatically to the extent of both showing a flattening of the rate of change with angle with frequency around the ninety-degree region. It would be expected that this should show itself up in a broadening of the frequency response of the device compared with one which was weakly reflective, as the effects on the response of the variations in reflection angle will be reduced. This effect is in fact observed in the U-path response of the device, which is shown in figure 4.11. It is also to some extent present in the results of the highly-reflective type S3 array devices , figure 4.7.

The results of this investigation showed that the reflected wave on the surface of the device was indeed behaving as predicted, and this result led to the use of the full model for the weak array to fit the observed frequency responses of the type A1 and type A2 devices. The model gives all the information needed to predict the response of the devices, except for the transducer characteristics which can be easily found from the many models existing, and from the overall shape of the straight through response for the device. Other than that the only parameters are the dimensions of the array, which are known, its operating frequency the reflection coefficent of the 1 square wavelength unit cell, and the array angle error, ϕ .

In order to fit the theory to a measured insertion loss

characteristic, such as that of the type A1 device, figure 4.5, the transducer loss is first accounted for, then the array angle error is found from the ratio of the main-lobe to side-lobe amplitudes, and then the array operating frequency is found from the position of the frequency response and the reflection coefficent from the level of the insertion loss.

The results of such a fit when applied to the type A1 array were of an array centre frequency of 59.3MHz and an array angle error of -0.20 degrees and a reflection coefficent of .25% amplitude per square wavelength (= 0.13% per dot). The errors in the design frequency and in the array angle were due to errors in the assumed values of the two perpendicular wave velocities. The theory also suggests that if the array angle is 0.2 degree too great then an increase in frequency of about 0.4MHz should make the output wavefronts parallel to the output transducer. This implies that the 90 degree reflection frequency should be 59.7MHz, which is what the graph figure 4.10 suggests. The apparent main lobe in the response is then centred on the correct reflection angle, whereas the side lobe is centred on the maximum reflection frequency of the array. The corresponding parameters for the type A2 array are a best array frequency of 59.4MHz and an array angle error of -.23 degrees and a reflection coefficent of .12% amplitude per square wavelength, (=.03% per dot). These figures would suggest that the frequency for ninety-degree reflection for this device was around 59.86MHz. The lower reflection coefficent of the type A2 array meant that there was insufficent reflected wave amplitude for the variation of reflection angle with frequency to be measured, so this prediction could not be checked in this case. These frequency values

would be expected to be higher than those for the type A1 array because the type A2 has a lower proportion of metal on its surface (12½% of the surface of the array area is metallized as opposed to 25% for the type A1), so that the waves would be expected to be subject to less slowing, and therefore to be intercepted at higher frequencies.

In order to confirm that the model would enable the correct array angle to be deduced, further devices were made using both type A1 and type A2 arrays, but with the array angle altered in the light of the experiance gained. The original array angle was 47.1 degrees. This was modified to 47.1 - 0.20 = 46.90 degrees for the type A1 array. The calculated angle for the type A2 array on this basis was 46.87 degrees, but it was suspected that the model might not be sufficently accurate, due, for instance, to the effects of diffraction and of beam-steering to justify this extra precision, so both new devices were designed using an array angle of 46.90 degrees. The arrays were specified to the computer programme which generated the data from which they were made by the pattern generator in the form of the spacing of the unit cells along the original propagation direction (x on the model, Z on the crystal) and the angle of the array planes to that direction. The spacing which had originally been used is that which corresponded to a wavelength at 60MHz on a free substrate. The theory said that this distance should correspond to the wavelength at which the wave was reflected through exactly ninety degrees, this being 59.7MHz for the type A1 array.

It was decided for simplicity to remake the arrays with the same defined spacing between the cells and to just change the array angle. This should have had the effect of leaving the

ninety degree reflection frequencies unchanged and pulling the peak scattering frequencies to coincide with them.

Figures 4.12 and 4.13 show the insertion loss characteristics of the resulting devices, which were again made to the pattern shown in figure 4.2b so as to be identical to the previous versions except for the changed array angle. Figure 4.12 shows the new type A1 array device. Its frequency response is now much more symmetrical, and centred, as was predicted, at about 59.7MHz. The insertion loss shows one sidelobe 20dB down on the main response, whereas the ideal device would have two symmetrical sidelobes each of which would be 26dB down on the main lobe. This fault is the result of a residual angle error of about 0.04 degrees. There has however been a great improvement from the earlier version with its sidelobes about four decibels down to this one with its sidelobes 20 dB down.

Figure 4.13 shows the response of the new type A2 device. Its centre frequency is near the predicted value of 59.86MHz, and its insertion loss is even cleaner than that of the type A1. The fitted curve implies that the the angle is right within about a hundredth of a degree. This shows that the suspicion that the previous data was inadequate to define the array angle too closely was correct, as this device was in fact made to an array angle which was expected to be up to about .05 of a degree off. The accuracy to which the array angle can be obtained is limited by the absence of observable sidelobes in the passband and by the limits to which the

model fits the data. It appears that to explain the anomolous lack of sidelobes a second-order model of the array would have to be developed, but this is of secondary importance, because the simple model has suceeded in explaining the main features of the response of the unweighted bandpass filters, and has enabled their performance to be improved and predicted. The actual parameters for the new arrays are:

	ARRAY TYPE		
	A1	A2	
Working Frequency	59.76MHz	59.87MHz	±≈0.02MHz
Array Angle Error	0.05°	0.0°	± 0.01°
Reflection Coefficent			
Per Square Wavelength	0.29%	0.19%	
Per Dot	0.15%	0.05%	

It is observed that the reflection coefficents measured here are slightly higher than those measured with the earlier devices. In view of the greater signal levels available with the later arrays, the values for those arrays would be expected to be the more reliable, especially as they are also higher per dot, whereas any contamination on the surface of the device would tend to increase the insertion loss and thus reduce the apparent reflection coefficents. The higher values would thus probably be more reliable. The differences are only of the order of one or two decibels, and therefore within the sort of range of error which might be expected.

It is noticable that, as was predicted at the outset, besides affecting the form of the insertion loss characteristics of the devices, errors in the array angles also greatly increase their

insertion losses. The insertion loss of the type A1 array was reduced by about 12dB and that of the type A2 by 20dB by improving the array angle error in the one case from 0.2 to 0.05 degrees and in the other by 0.23 to 0 degrees. The insertion loss of the type A1 array with the improved angle is now about 38dB, of which 15dB could be attributed to the untuned transducers, leaving a loss of about 12dB per array. This is relatively efficent, particularly in view of the fact that the array remains weakly reflecting, in as much as its response can be well described by models which take no account of multiple reflections within the array.

The models used have been effectively far-field models, which have treated the arrays, and the dots within them, as specular reflectors. This is of course not strictly true, but works in respect of the insertion loss because the transducer, because of its great sensitivity to the angle of approach of any wave it detects, behaves such that only waves which are travelling in the right direction are, to first order, detected by it, so that the overall response is as it would be if the various components of the devices were all strictly within each other's far fields. It is therefore incapable of explaining an effect observed with the type A1 array particularly, that there would appear to be a lot of standing-wave type effects in the waves travelling between the two arrays. Figure 4.14 shows the result of probing the intensity of the waves in a first-model type A1 array (with the angle wrong). The probe was taken along an approximate wavefront of the wave travelling between the arrays, and shows a lot of deep, fast, ripple in the energy distibution.

The ripple is as fast-varying at a given point as the frequency of the wave is changed as it is in space at a given frequency. The effect is present to a lesser degree in the type S3 array, which is a strongly-reflecting device, in which each reflector has a much higher reflection coefficent than do those of the type A1 array (about 1% amplitude as opposed to 0.15% amplitude). It is altogether absent from the full strip device, which has a higher reflection coefficent yet. The explanation for this is unknown, and it does not seem to have been predicted or observed before.

It would be useful to be able to predict, rather than to have to measure, the correct reflection angle for a metallic dot array when the percentage of metal on the surface is known. This angle is the arctangent of the ratio of the wave velocities in the two perpedicular directions between which the array is to reflect the wave. The wave velocities of the free and the completely metallized surfaces are known for both the Z and the X propogating surface wave on Y-cut lithium niobate. The metallized surface velocity is less than the free surface velocity by an amount proportional to the piezoelectric coupling to the surface wave in that direction, and also by an additional amount proportional to the thickness of the metal coating. This latter extra slowing is small for the amount of aluminium used in the devices described at the frequencies used. The aluminium was 4000Å thick, about 0.7% of a wavelength at 60MHz. The effect of this slowing is shown in figures 4.15 and 4.16 for the Z- and X- propagating waves respectively. The data for the free-surface and just-metallized velocities are from data obtained at University College, London[40], and the values used are accurate to about 1 metre per second. The data for the slowing

due to the mass of the aluminium was obtained from a computer programme at R.S.R.E. Malvern, and is proportionally much less accurate, but has probably a similar absolute accuracy for the thicknesses of metal used in this work.

The simplest prediction for the wave velocity under an array would be to assume that the wave velocity moves linearly between its free surface and its metallized value as the proportion of the surface of the array which has been metallized varies between zero and unity.

Figure 4.17 shows the expected reflection angle arising from this simple assumption. There are five experimental points for comparision. Firstly there are the trivial end-points for the free surface and for the fully metallized surface, and then there are the two points for the 12½% and 25% metallized surface corresponding to the type A2 and A1 arrays respectively, which have been deduced in this work. The error bars show the limits within which the reflection angle used in the simple model could be varied without significantly altering the quality of the fit between the model and the experimental results.

The point corresponding to the full strip array is also shown for comparision. By observing the variations in the total power scattered by the array with frequency, using the potential probe, it was found that this was a maximum at about the ninety degree reflection frequency. If the array had been weakly reflecting then, in accordance with the simple model, the array angle would have been correct at 47,1 degrees for this device. This estimation is less accurate than was the fitting of curves to the results for the weakly reflecting arrays. The result has thus been shown with correspondingly larger error bars, of the order of a tenth of a degree each way.

It will be seen from the graph that the accurate results for the simple reflecting structures definitely do not lie on the curve, which is almost, but not exactly, a straight line.

The 50% metallization point for the strip array might lie on the curve, but this is not known to the same accuracy.

From the few points available it would seem clear that the general trend predicted by the linear approximation to the intermediate velocities is almost, but not exactly, correct. The velocity for the Z- propogation direction can be obtained by the simple theory from the ninety degree reflection frequency, and is shown as a function of metallization percentage in figure 4.18. The values for the type A1, type A2 and strip arrays are 3468, 3480 and 3441 m/sec respectively. From these Z-velocities and the measured array angle errors the X-propagation velocity within a given array can be deduced. The values obtained are shown in figure 4.19, being 3712, 3719 and 3703 m/sec respectively for the A1, A2 and strip arrays.

The strip array point (50% metallization) is again inaccurate in Z-velocity, and the deduced X-velocity shows very large possible errors. The error bars on the points for the A1 and A2 arrays are at $\pm$1m/sec, and within these limits, which are also the limits on the accuracy of the theoretical values the points appear to lie on the line. The simple hypothesis that the velocity varies linearly with the proportion of metal in the array would thus appear to be vindicated within the accuracy of the values of the theoretical values of the velocity. The data presented in figure 4.17 would appear to imply, therefore, that the available values of the free-surface and metallized-surface velocities are not known to sufficent accuracy for them to be used in the accurate design of dot array devices. The available data would have given errors

in the type A1 and A2 array angles of about 0.05 degrees, which in those devices would have given sidelobes about 20dB below the main lobe, rather than the theoretical 26dB below. It is coincidental that the linear theory's prediction and the chosen value for the type A1 array angle were each 0.05 of a degree out on opposite sides of the correct angle.

The angle which would now be predicted as being right for the type A1 array, 46.90 + 0.05 = 46.95 degrees, is the same as that found by Nash [15]. This work has improved on his result, however, in that it has shown that that angle would have been wrong for an array with a different amount of metal on its surface. Simple models have been developed for both the dot array itself and for the variations in the wave velocity within the array, and both have been found to be sucessful, within the limits of experimental error, in explaining the effects observed.

One result of this work which is encouraging to the attempt to make weighted dot array devices is that, below a certain percentage metallization, the reflection angle should be independent of the amount of metallization, at 46.90 degrees, to within an accuracy of $\pm$ 0.02 degrees, which is sufficently accurate for most RDA devices. This can be said because when the proportion of metal on the surface of the array is reduced from the type A2 value of 12½% to zero, the array angle must vary between 46.90 degrees and the free surface value of 46.88 degrees. This latter value is accurately known to within about 0.01 degrees from that U.C.L. velocity data.

Results have been obtained to confirm the above hypothesis

from some comparision devices to the type A1 and type A2 array devices which were made using the same patterns of dots as the former, but with only one third of the number of dots present. The responses of the type A1 and type A2 versions of these devices are shown in figure 4.20 and 4.21 respectively. As can be seen the array angles for these devices were correct. They were made with the same array angle of 46.90 degrees which was used for the later A1 and A2 devices, so that their correct array angles can be said to be the same as for the latter device, at 46.90± 0.01 degrees. The proportions of metallization in the thinned type A1 and type A2 devices are 8.3% and 4.2% respecively, so that they would come between the type A2 array and zero on the metallization/angle curve, confirming the prediction made above. The data from them was not, however, drawn onto the curve because it adds nothing qualitatively different from the points already plotted, but merely strengthens the implications of those results. The calculated reflection coefficents per dot for the thinned arrays were found to be 0.12% and 0.03% respectively. These correspond to the figures for the full arrays of 0.15% and 0.05% respectively. The source of these anomolies has not been ascertained, but if they are really caused within the arrays, as seems likely by the effect's appearing with both array types, they are probably due to some sort of interactions between the effects of the separate dots.

4.4: Effects of Metal Thickness.

Another effect which was investigated was that of possible variations in the reflection coefficent of the dots and in the operating frequency and reflection angle of the arrays which would be caused by varying the thickness of the metal used to make the arrays, which would alter proportionately any effects due to the effects on the wave of the mass of the dot, but would not affect any phenomena due to its electrical properties, The thinnest practicable aluminium thickness, around 1000Å, still leaves a film which behaves practically as a perfect conductor, hence the metal thickness should have no effect on any electrical phenomena present.

The type A1, A2, and S3 arrays described previously had used 4000Å thickness of aluminium. The type S2 array had used 1200Å. The type S1 array had been made with both 1200 and 4400Å of aluminium, but the complexity of the response of that device meant that no information could be gleaned about the effect of the different metal thicknesses. In order to obtain unambigous information about the effects of changing the metal thickness another type A1 array, with the corrected array angle, was made using 1000Å of aluminium metallization.

The insertion loss response of the device is shown in figure 4.22, together with the best-fit curve for the simple model. The much higher insertion loss of this device makes its observed response much more susceptible to the effects of spurious acoustic signals than that of any of the other devices reported, hence the rough nature of the curve. The accuracy of the fit of the model is also thereby reduced, and the measured fitting paramters have wider error bounds than for the thicker aluminium devices.

Table 4.2 below compares the values of the fitting parameters used for the thin aluminium array with those for the thicker device reported earlier. Except for the thickness of aluminium used both devices were identical.

Table 4.2: Effect of Metal Thickness on Behaviour of Type A1 Dot Array

	Aluminium thickness	
	1200A	4000A
Working Frequency	59.82MHz ± 0.02MHz	59.76 MHz ± 0.02MHz
Array Angle Error	$0.07^{\circ} \pm 0.02^{\circ}$	$0.05^{\circ} \pm 0.01^{\circ}$
Reflection Coefficent		
Per Square Wavelength	0.10% ± 0.02%	0.29% ± 0.03%
Per Dot	0.05% ± 0.01%	0.15% ± 0.02%

The most noticable, in fact the only unambiguous, effect of reducing the metal thickness is to reduce the reflection coefficent of the dots. This shows that the reflection mechanism of the dots is predominantly due to mass loading, although the fact that a four-fold reduction in dot thickness produces only a three-fold reduction in the reflection coefficent shows that there must be some electrical shorting present, although its effect is only about as much as that of the mass-loading effect of about 500 to 1000 angstroms of aluminium. This dominance of the reflection coefficent by mass-loading effects has been reported by Solie[13] for smaller dots than those in the type A1 array, and the fact that it should still occur in dots half a wavelength long on the diagonal is prehaps a surprising result.

Within the limits of experimental error the operating frequencies and correct array angles of the devices appear unaffected by variations in metal thickness of the order of those described above. This implies that the variation in metal thickness from 1000 to 4000 angstroms at 60MHz should alter the wave velocity be amounts of about 1 m/sec or less. This is in agreement with the simple linear model for the wave velocities within the arrays, which would predict an increase in both Z- and X- velocities of about 1 m/sec for such a variation in metal thickness in a 25% metallized array.

This experiment has shown that the variation of metal thickness within reasonable limits has only a secondary effect upon the wave velocities, such as would be expected from a simple assumption about the wave velocities in the array. It has shown however that varying the metal thickness in a type A1 array varies the reflection coefficent of the dots by almost the same proportion. This proportionality would be expected to be more exact for the type A2 dots, which, being smaller, would be expected, prehaps, to have a less-strong electrical effect than the type A1. The proportionality should not, however, hold for the type S3 and larger dots the anomolous reflection behaviour of which, compared with simple theory, strongly suggest that electrical shorting is an important reflection mechanism in them.

4.5: Weighting of Dot Arrays

The problem of the weighting of dot arrays is that of designing an array to have a given, predetermined, reflection coefficent by a suitable choice of type and density of dots. It is involved with the problem of trying to give the array the lowest possible overall insertion loss without becoming involved, it is hoped, in the problems caused by an over-strongly reflecting array. The aim is to use the highest possible reflection coefficent whilst still being able to analyse the array using simple models such as that developed for the uniform array in the previous section of this chapter. In the general case there is also a need to vary the weighting within different parts of s single array. This latter is probably a more difficult problem, because, in such systems as compressive receivers the relative weighting within the array is more critical to the overall performance of the system than is the absolute insertion loss of the compressors and expanders.

The results produced by the U-path responses of the later type A1 array and the type S3 array show that the minimum insertion loss which can be obtained whilst allowing the simple model to be used, for a uniform array, is somewhere between the 12dB per array of the type A1 and the 5dB of the type S3. The lower limit of insertion loss will tend to be higher for a weighted than for a uniform array, because the minimum insertion loss which will allow the reflection to be simply analysed is determined by the reflection strength at the most strongly reflecting part of the array, whereas in a weighted array most of the array will be less efficient as a reflector than that.

A simple estimate of the point at which an array will cease to behave in a simple manner is when a significant portion of the reflected wave will itself be re-reflected before leaving the array. If the amplitude reflection coefficent is 'r', then the energy reflection coefficent is r^2. If the total number of dots is then AB, as defined in section three of this chapter (figure 4.9a), then the total reflection coefficent of the array will approach unity when $ABr^2 = 1$.

This is the point where almost all the energy in the reflected wave will be re-reflected again by the array, so that the simple model of the reflection behaviour of the array is then, obviously, inapplicable, and some more sophisticated, but usually less general, analysis such as the coupled-mode theory[41] must be employed.

For the type A1 array using 4000Å of aluminium $ABr^2 \approx 0.02$, whereas for the type S3 array $ABr^2 \approx 0.6$, so that the failure of the simple theory in the latter case is as would be expected from the criterion mentioned above. This would seem to limit the minimum attainable insertion loss for a dot array device to about 10dB, giving a minimum insertion loss for a dot array device of around 26dB, 10dB for each array and 3dB bi-directionality loss for each transducer. This figure is consistant with the best reported results for dot arrays.

In a dispersive array the factor 'B' in the formula used above, the number of rows of dots across the path of the incident wave, is replaced by $B/\sqrt{T}$, where T is the time-bandwidth product of the

disperser. This factor corresponds to the approximate numner of reflective planes in a dispersive RAC which act coherently.

The design procedure for a dot array device should thus include a determination of the length of a uniform array, as the reciprocal of the desired bandwidth, or the factor $B/\sqrt{T}$ for a dispersive array. It should then be possible to determine the reflection coefficent which is required for the dots from the criterion of the highest possible reflection coefficent compatible with simple behaviour.

The desired type of dot could then be chosen from those available, or an attempt could be made to design a new type of dot from the model developed in the next chapter. The discussion of what information is available about the reflection coefficents of the individual dots is the subject of the next chapter of this thesis, but it will be mentioned here that dot types have been found which exhibit ninety-degree reflection coefficents which vary from nearly 1% amplitude per dot per wavelength of incident wavefront down to less than 0.05%. For the arrays which were made in this work the type A1 dot appears to give the best results by the criterion outlined above, but for shorter arrays (with greater bandwidths or higher dispersivity) the dots with the higher reflection coefficents (S2 or S3) would be more suitable, and, conversely, for arrays where more dots act together the type A2 dot could be more suitable.

Once the dot type has been chosen the array could be weighted by thinning out the dots within the array, as this will probably be easier than changing the dot type along the array.

The results for the thinned-down versions of the type A1 and A2 arrays show, however, that the procedure of thinning down the arrays can itself present problems. The reflection coefficents of the individual dots would appear to vary as the density of their packing is changed, an effect which can be put down to the mutual capacity between the dots. This phenomenon is discussed again in the next chapter, but no model for it has been proposed. It would appear that for each dot type which it is intended to use a test piece device should be constructed, so that a calibration curve of dot density against relative weighting of the array insertion loss could be made, so that the subesquent design could be carried out by taking account of the non-linearities in the curve produced. As the number of dot types which would be needed in the construction of a variety of devices would be fairly few this should not cause too much of a problem.

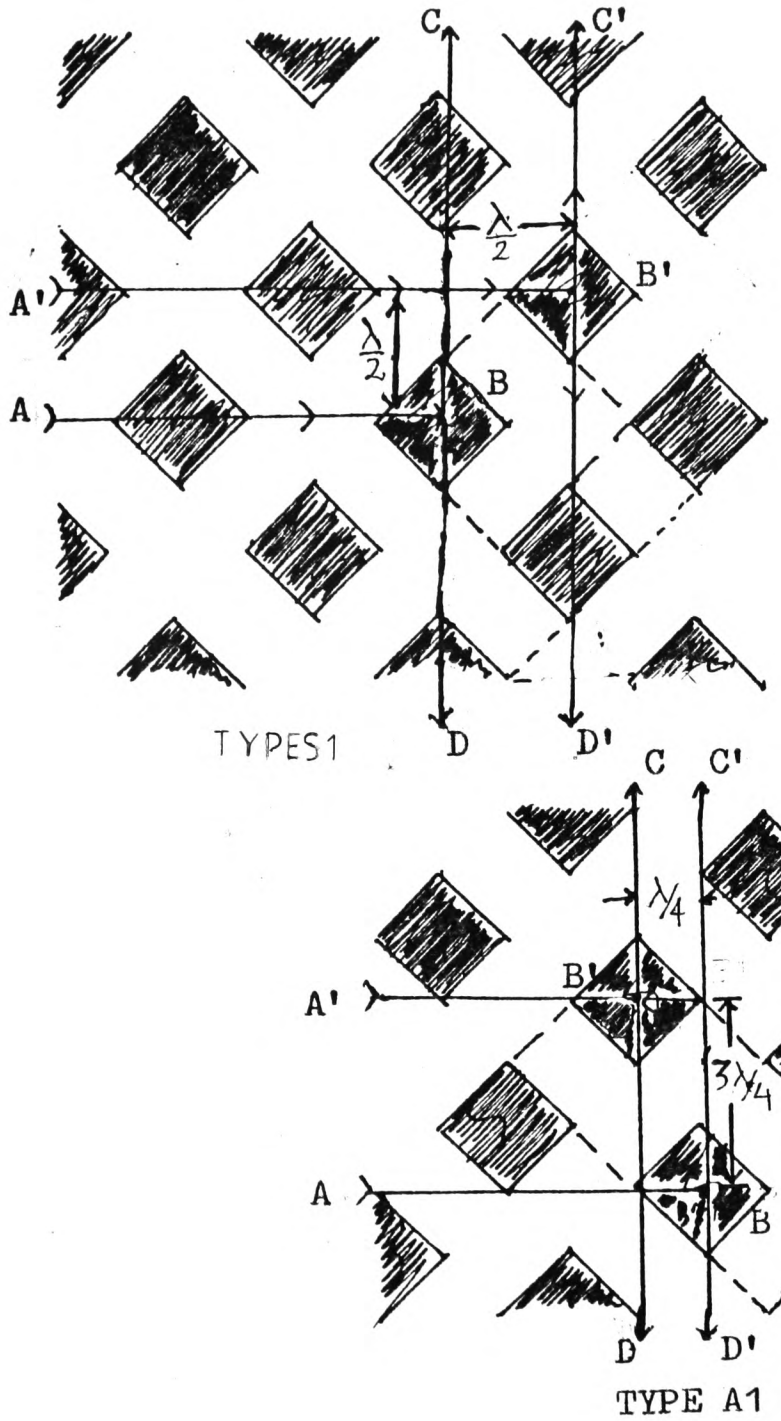

TYPES1

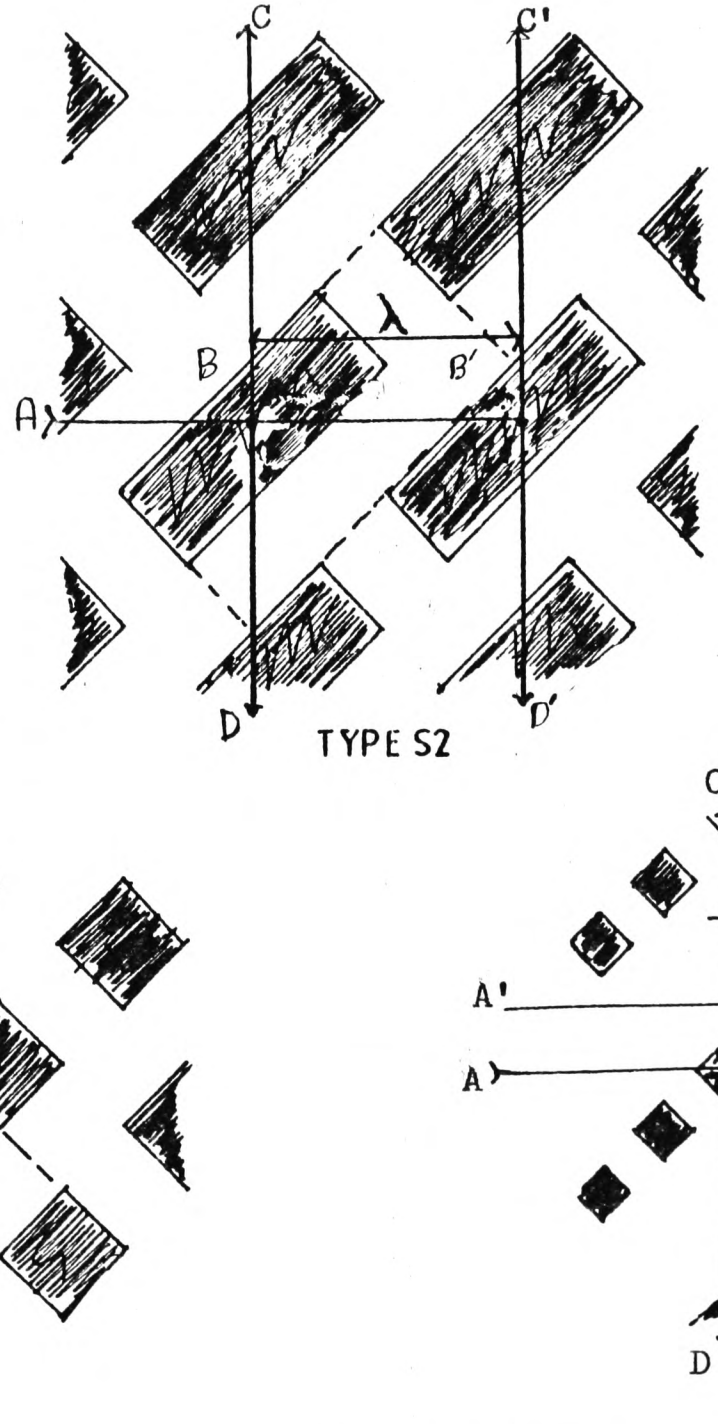

TYPE S2

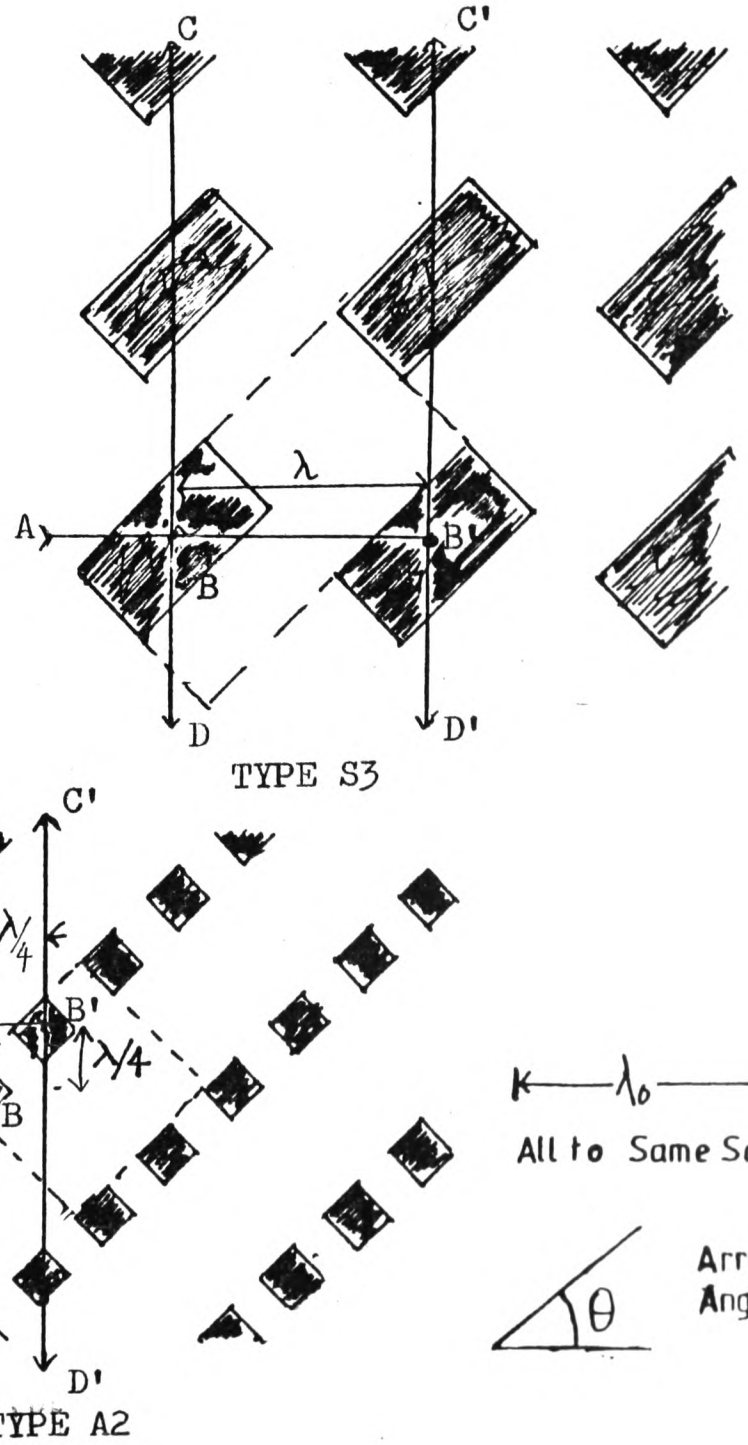

TYPE S3

TYPE A1

TYPE A2

Figure 4.1: DOTARRAY PATTERNS

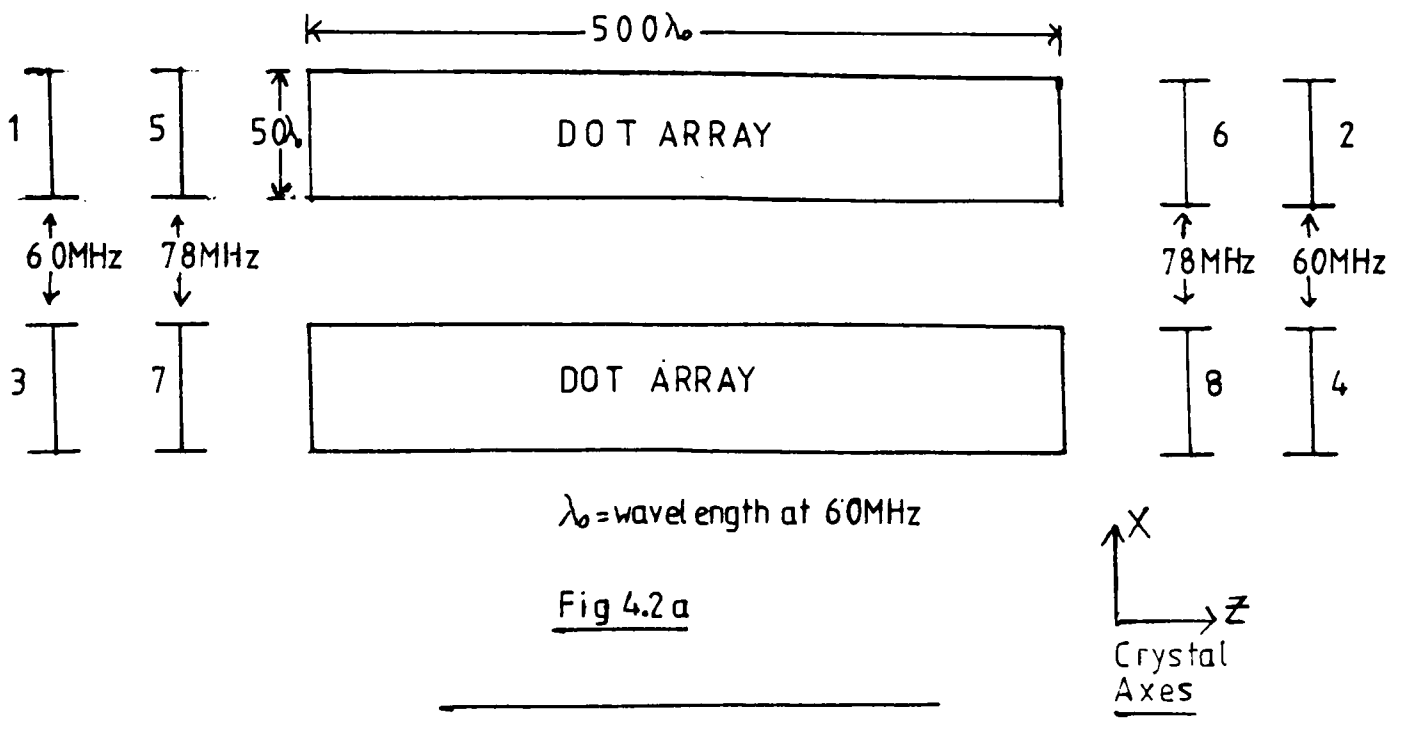

λ_0 = wavelength at 60MHz

Fig 4.2a

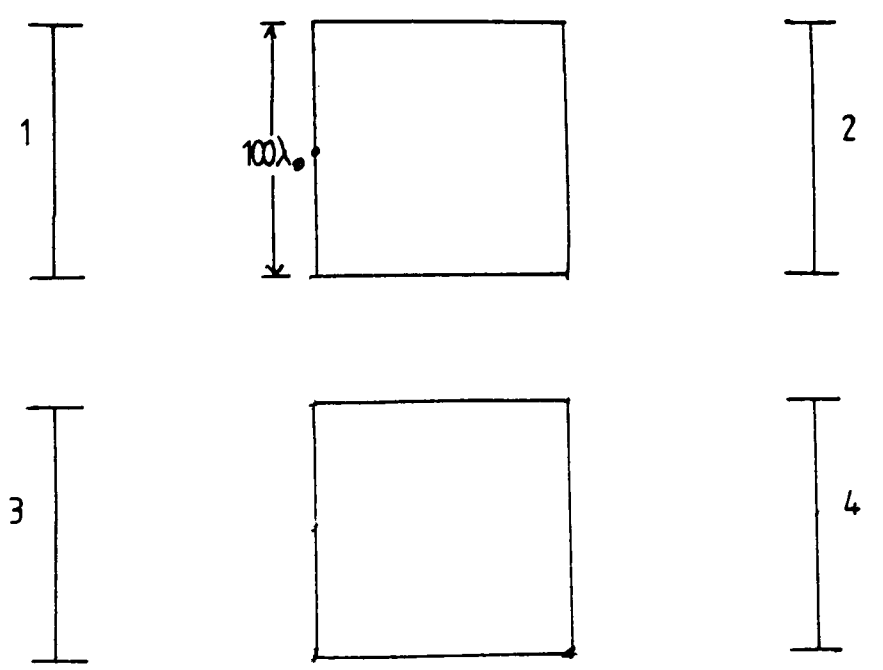

Design Frequency = 60MHz

Fig 4.2b

Figure 4.2: OVERALL DEVICE DESIGNS

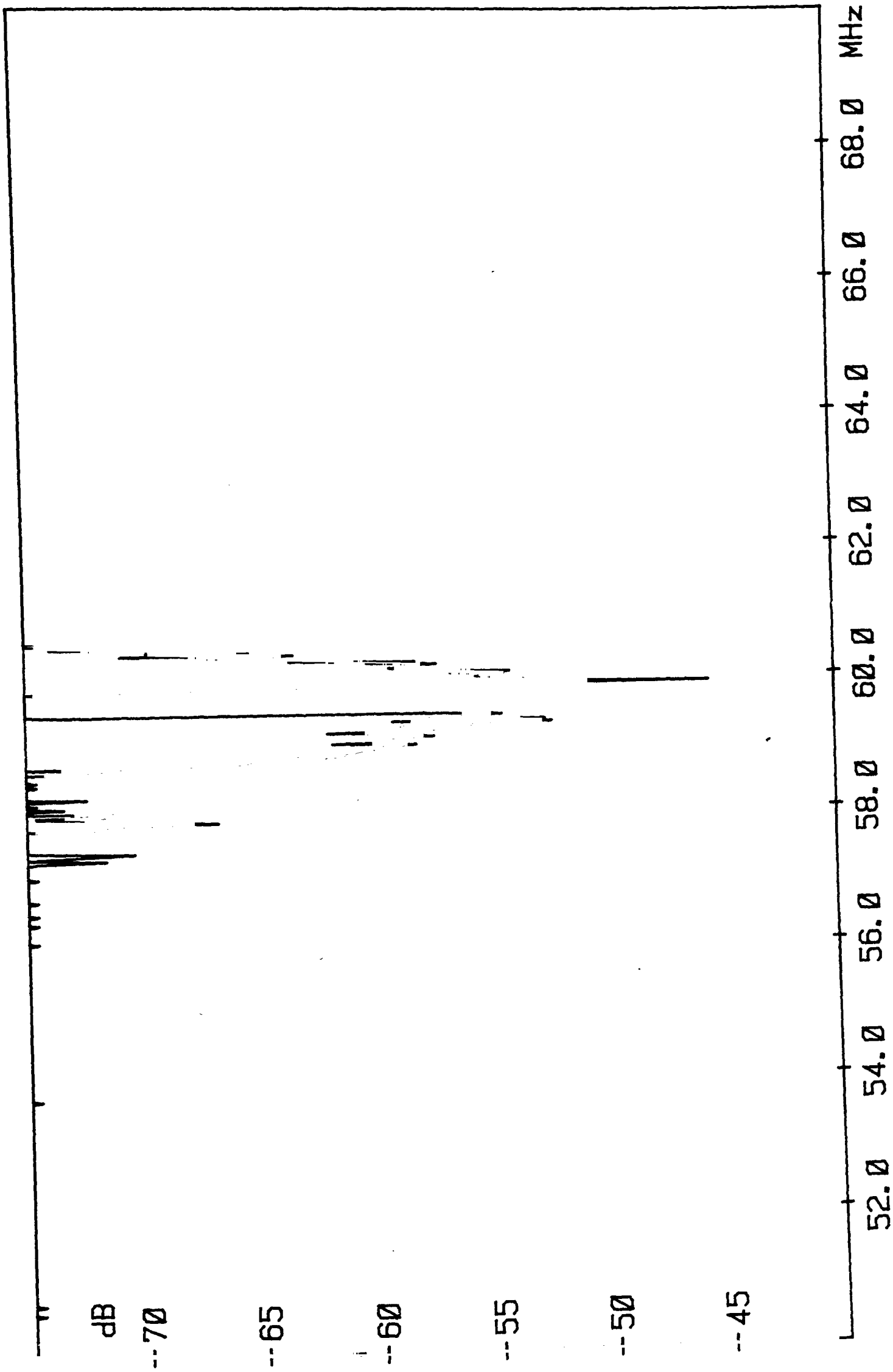

Figure 4.3: Type S1 Array, Z-path Response

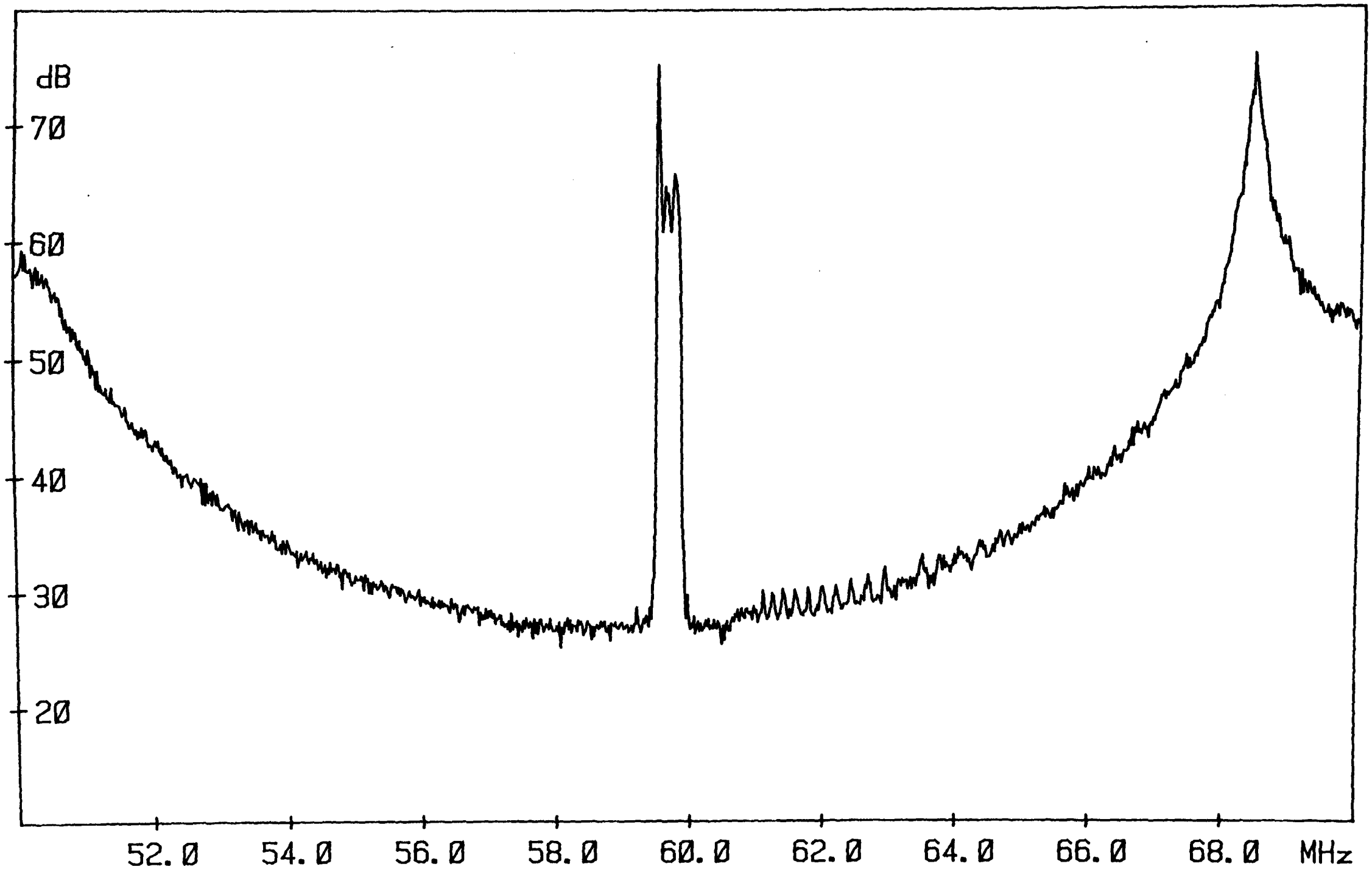

Figure 4.4: Type S1 Array, Straight Through Response

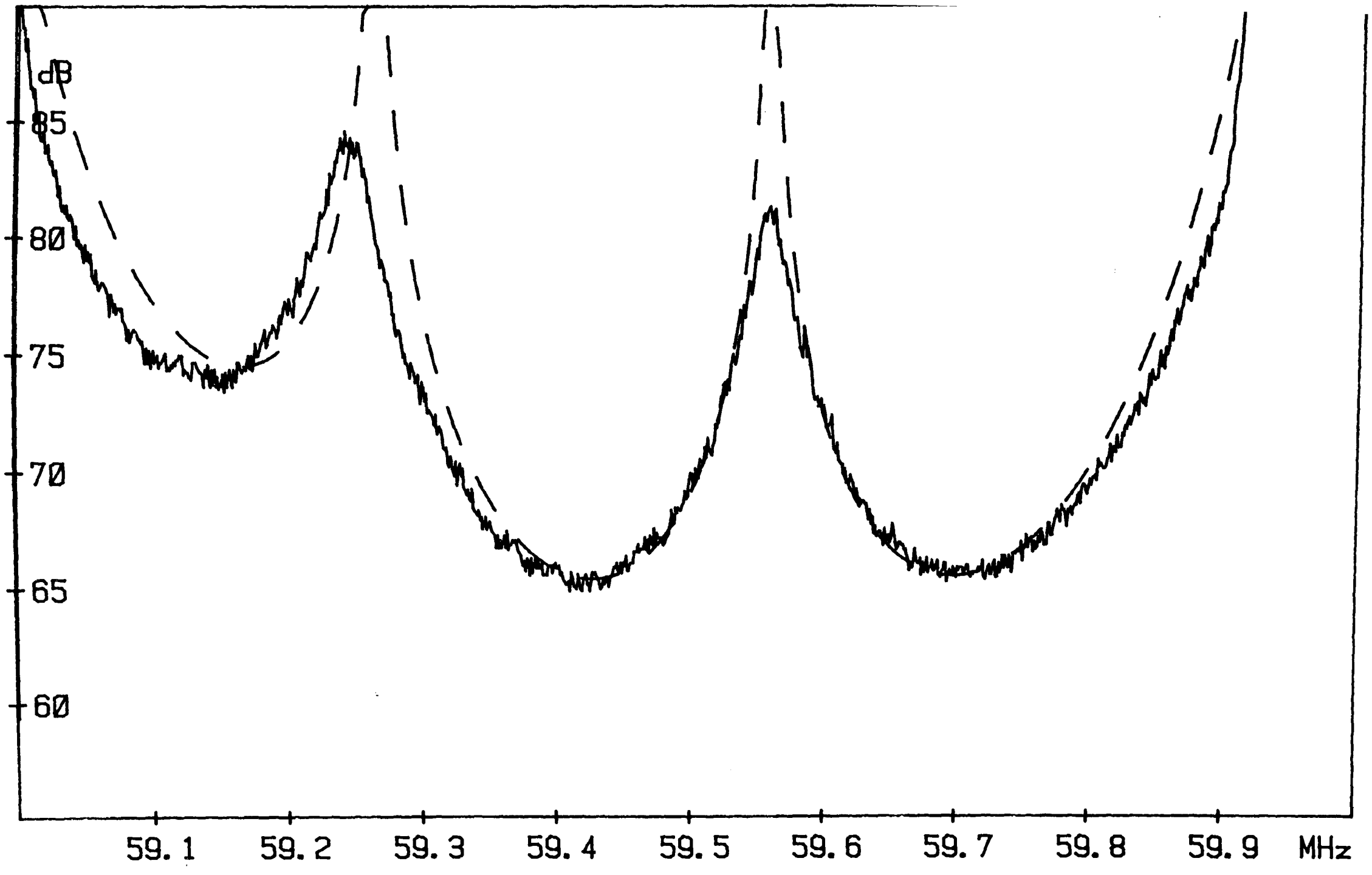

Figure 4.6: Type A2 Array, U-path Response, Showing Effect of Incorrect Array Angle

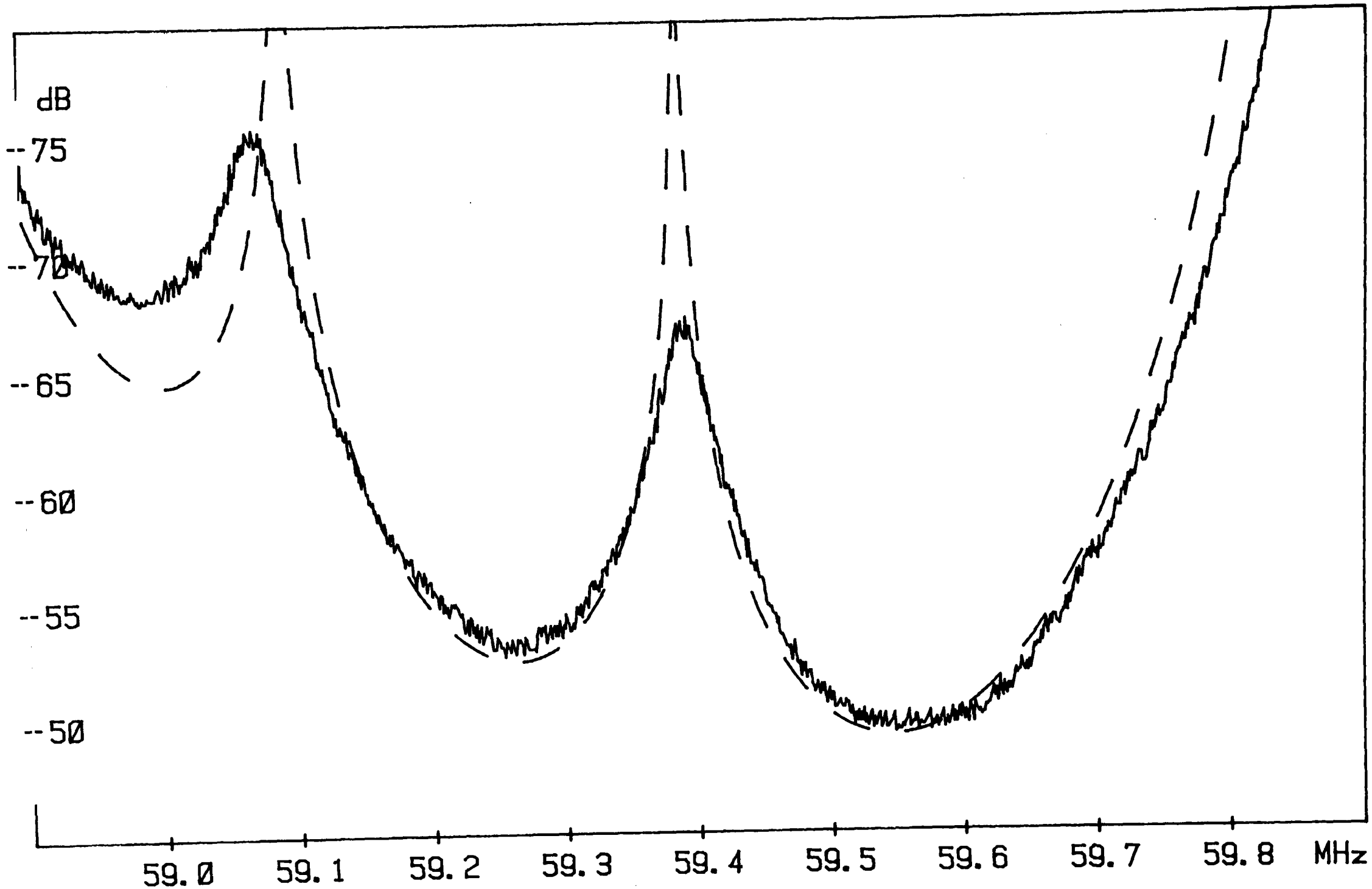

Figure 4.5: Type A1 Array, U-path Response Showing Effect of Incorrect Array Angle

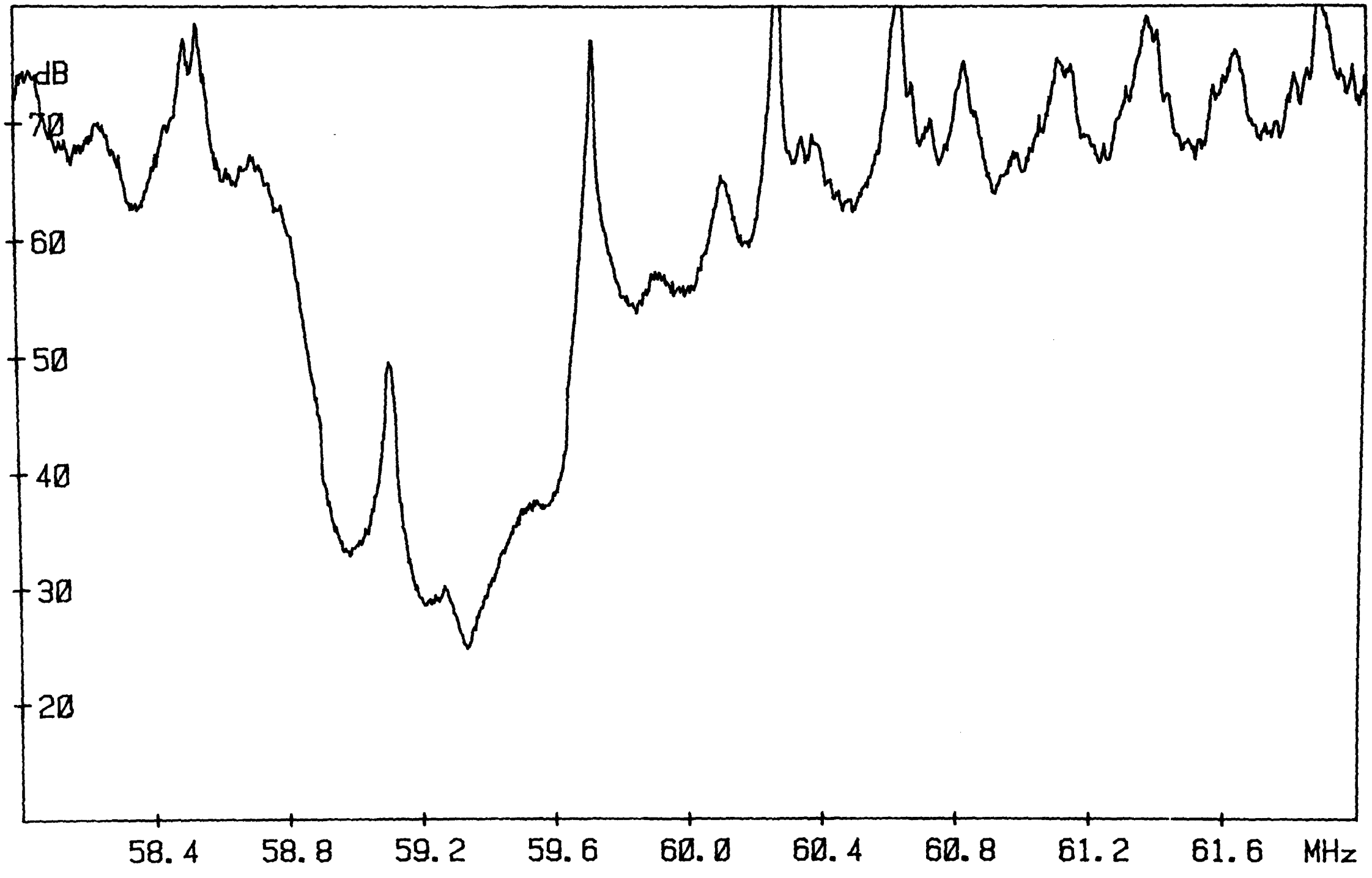

Figure 4.7: Type S3 array, U-path Response

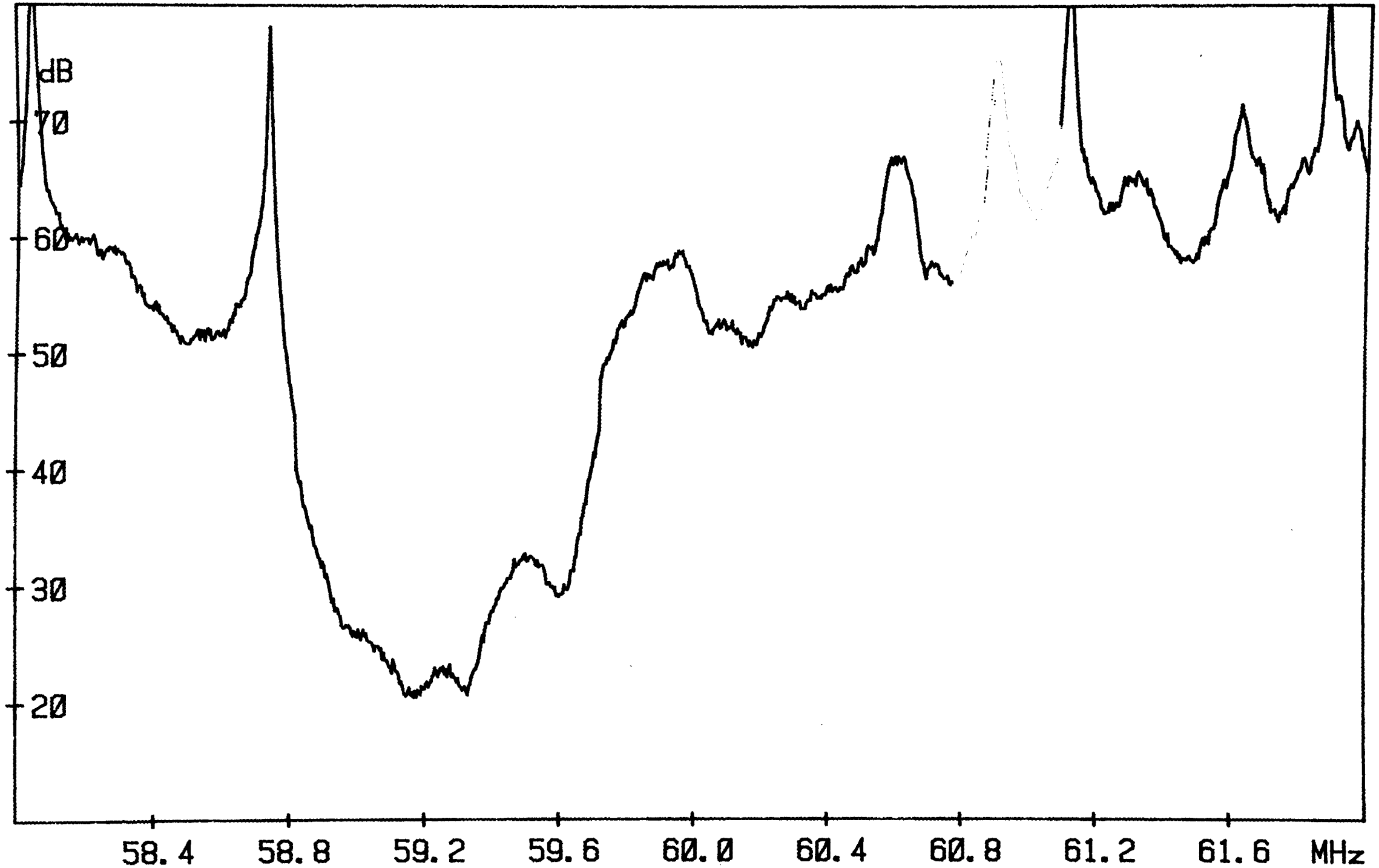

Figure 4.8: Type S3 Array, Z-path Response

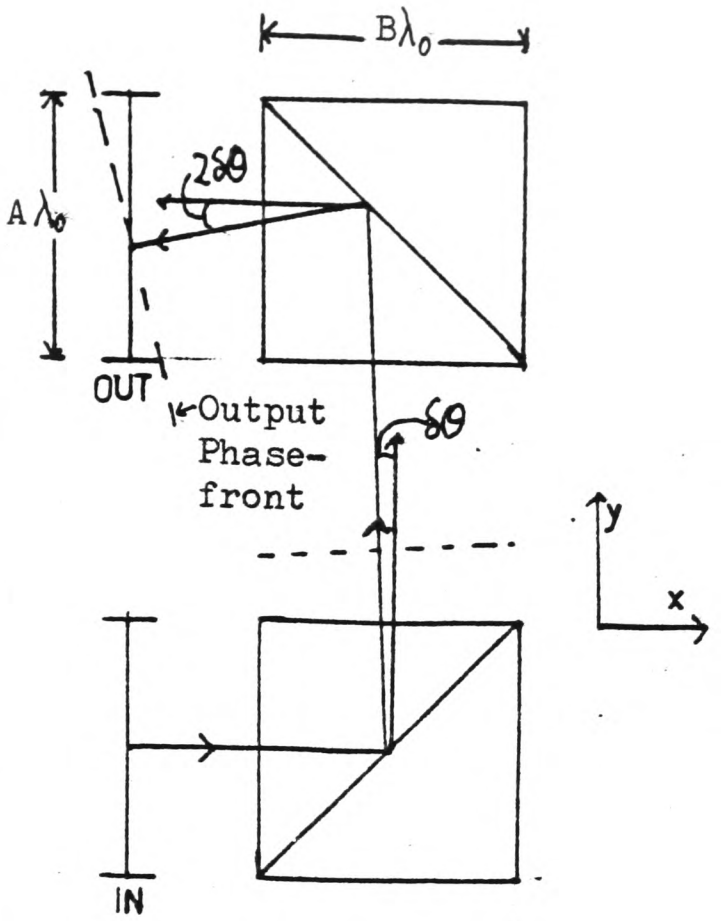

4.9a: General Arrangement

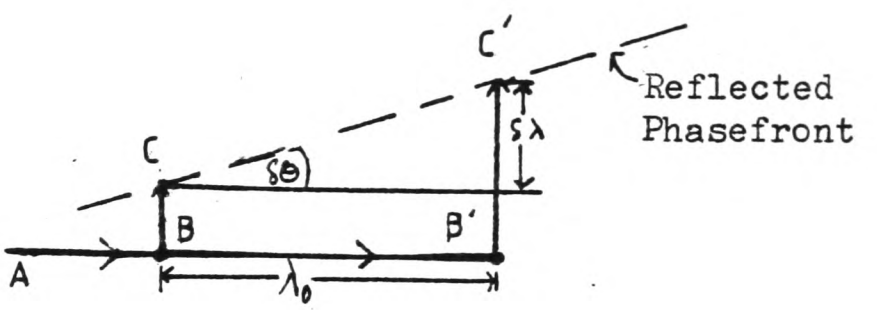

4.9b: Variation of Reflection Angle with Frequency

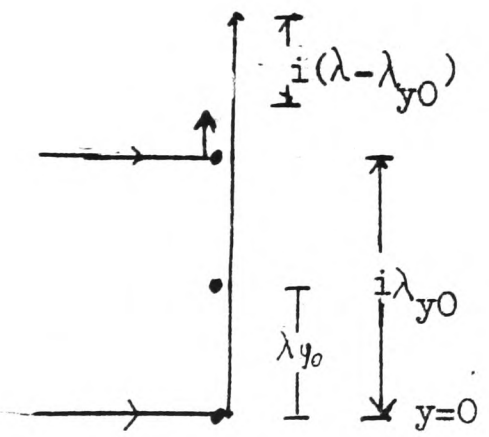

4.9c: Effects of Non-Constructive Interference

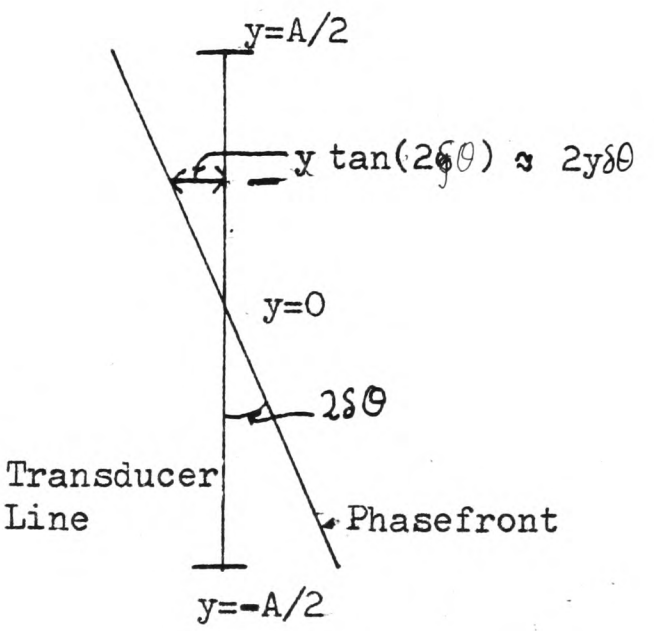

4.9d: Misalignment of Output Wave

Figure 4.9: Derivation of Simple Theory for Dot arrays

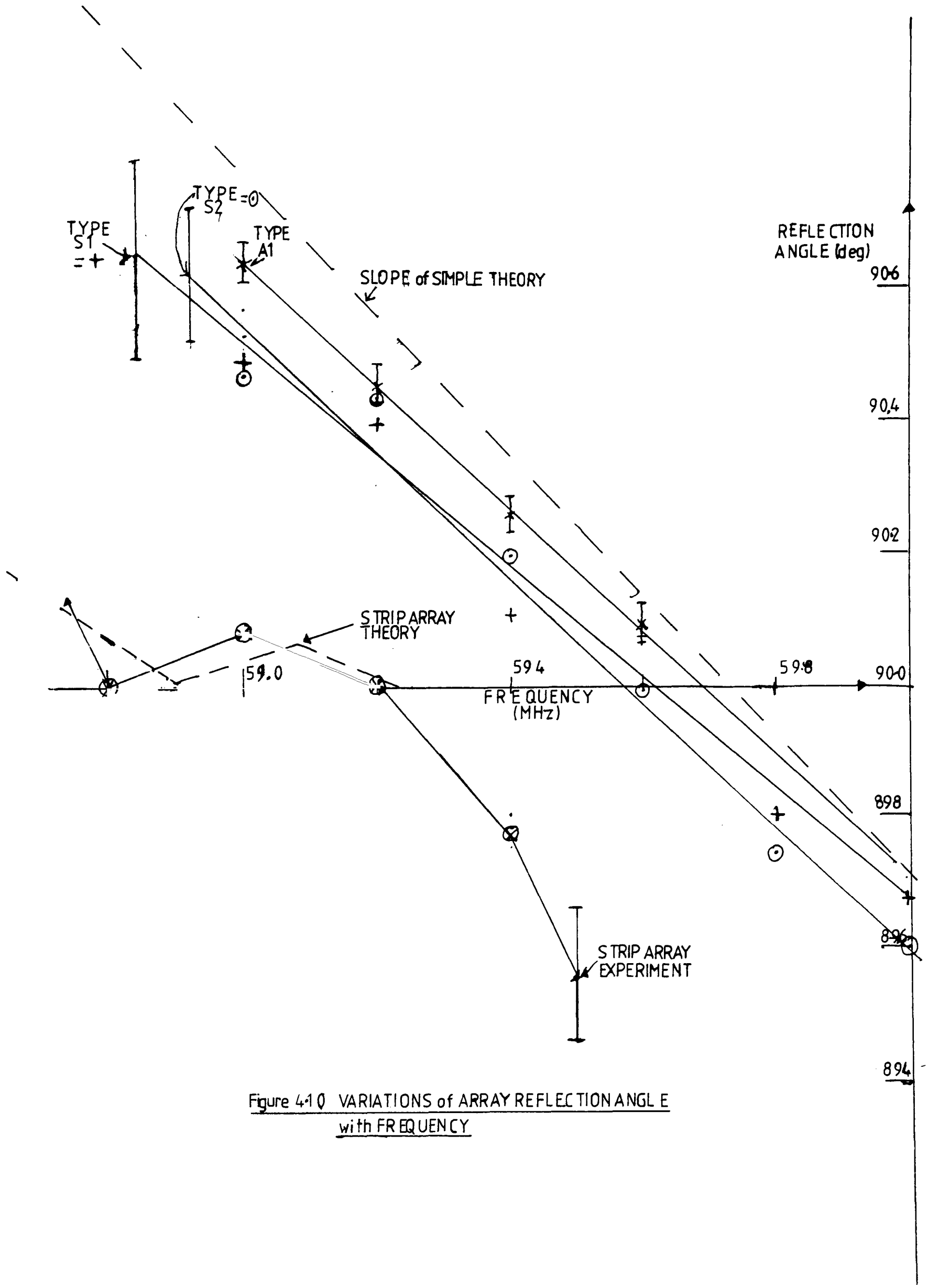

Figure 4·10 VARIATIONS of ARRAY REFLECTION ANGLE with FREQUENCY

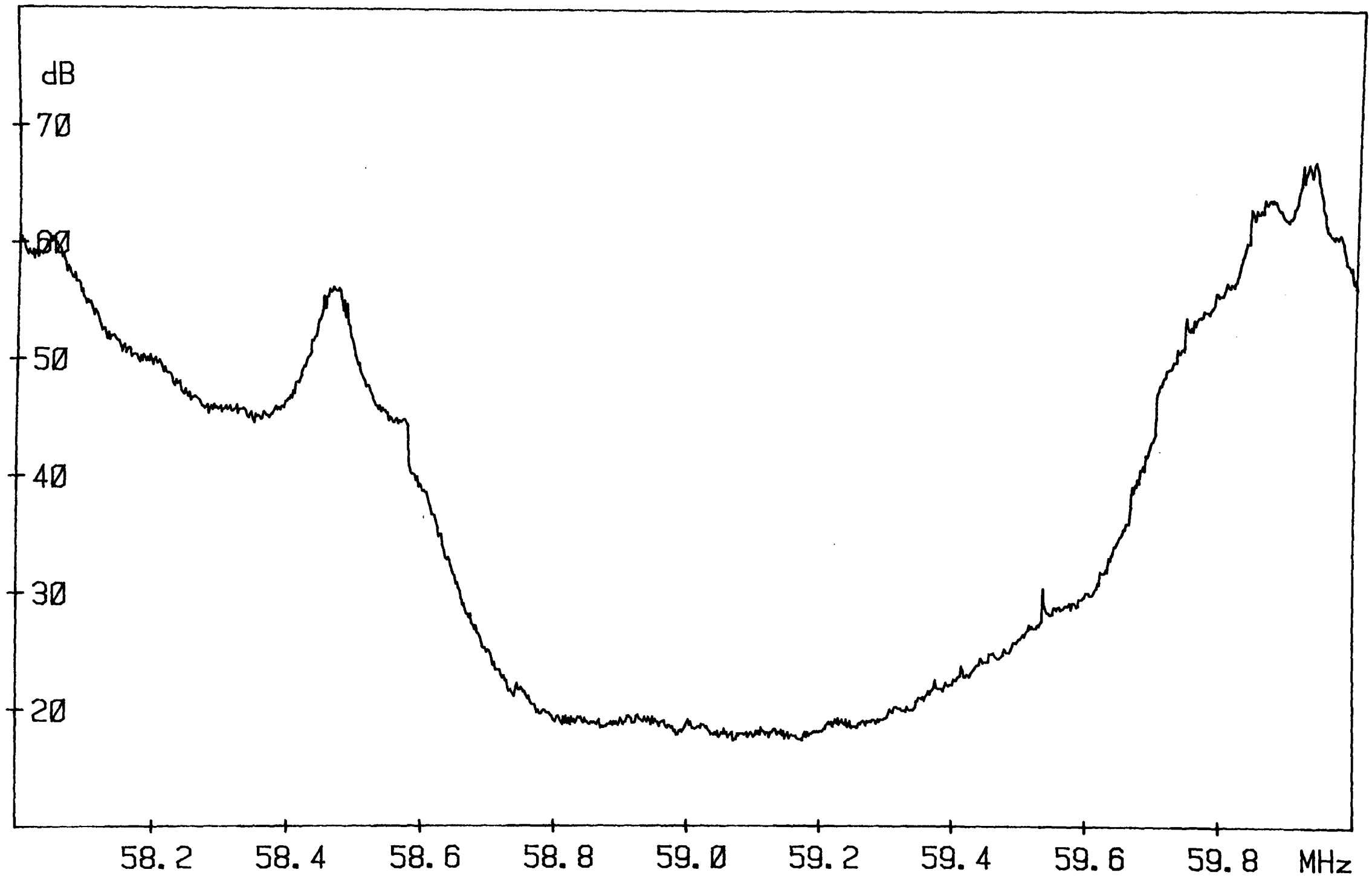

Figure 4.11: Strip Array, U-path Response

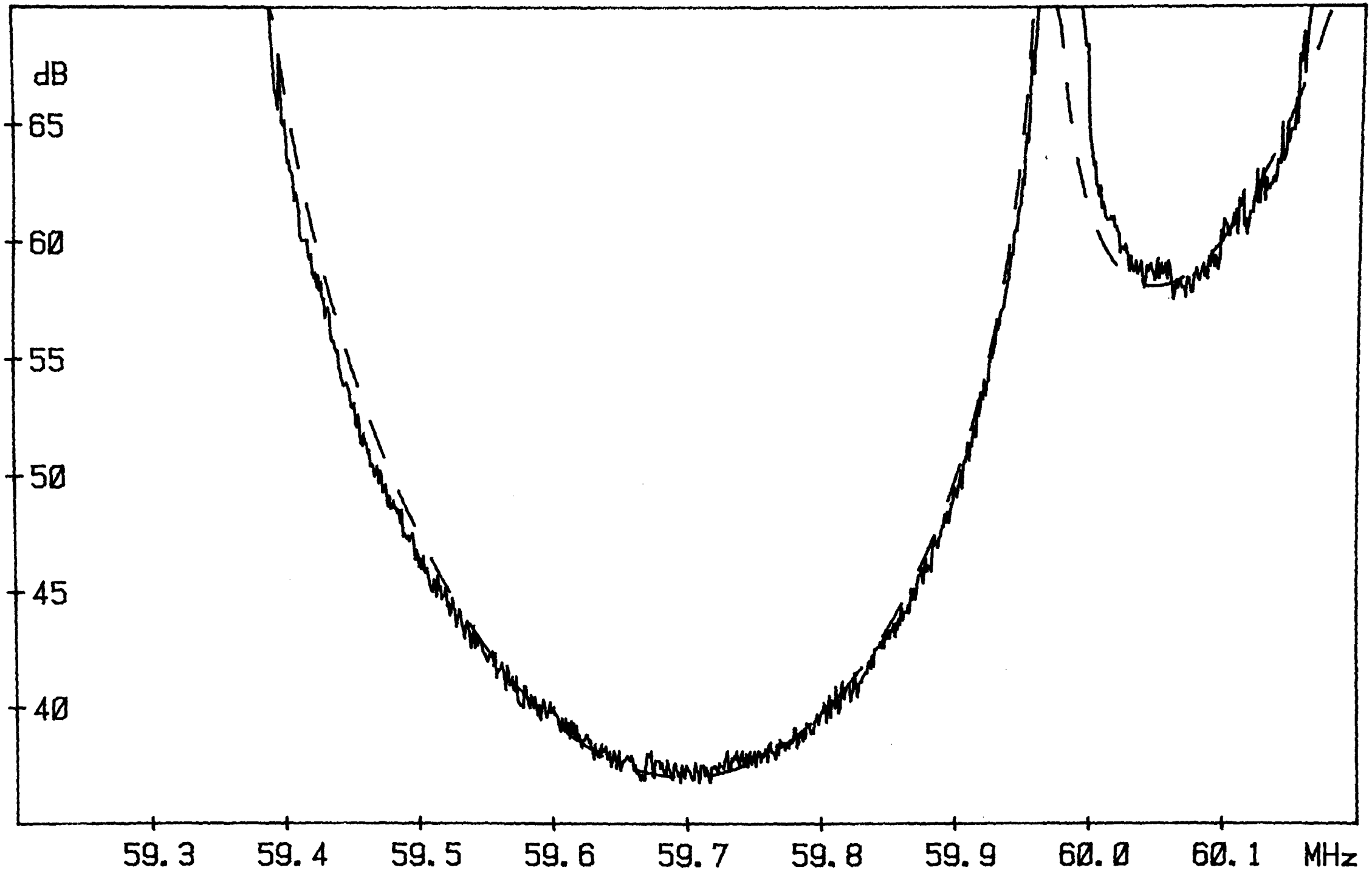

Figure 4.12: Type A1 Array with Improved Array Angle,

U-path Response

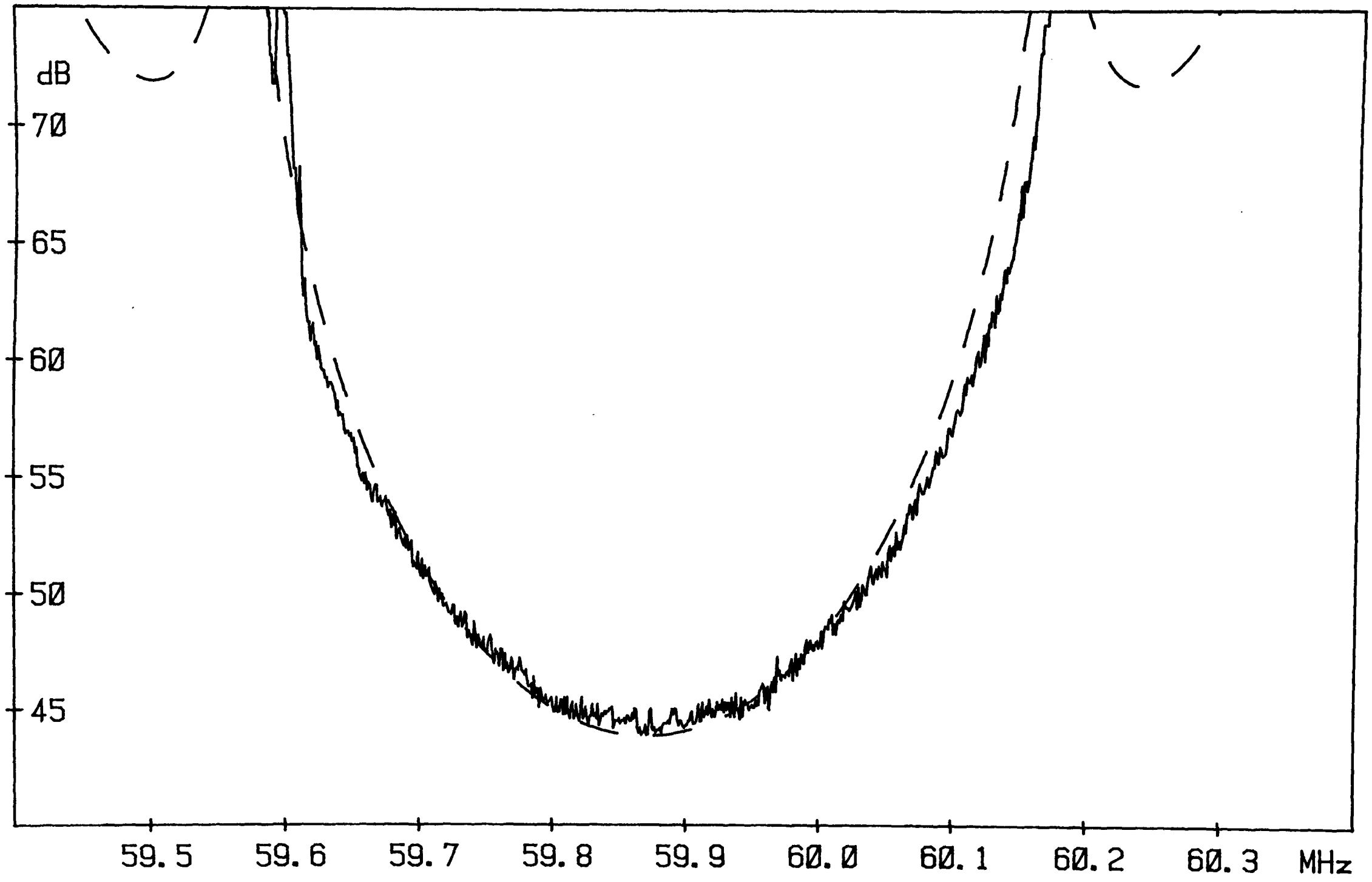

Figure 4.13: Type A2 Array with Corrected Array Angle, U-path Response

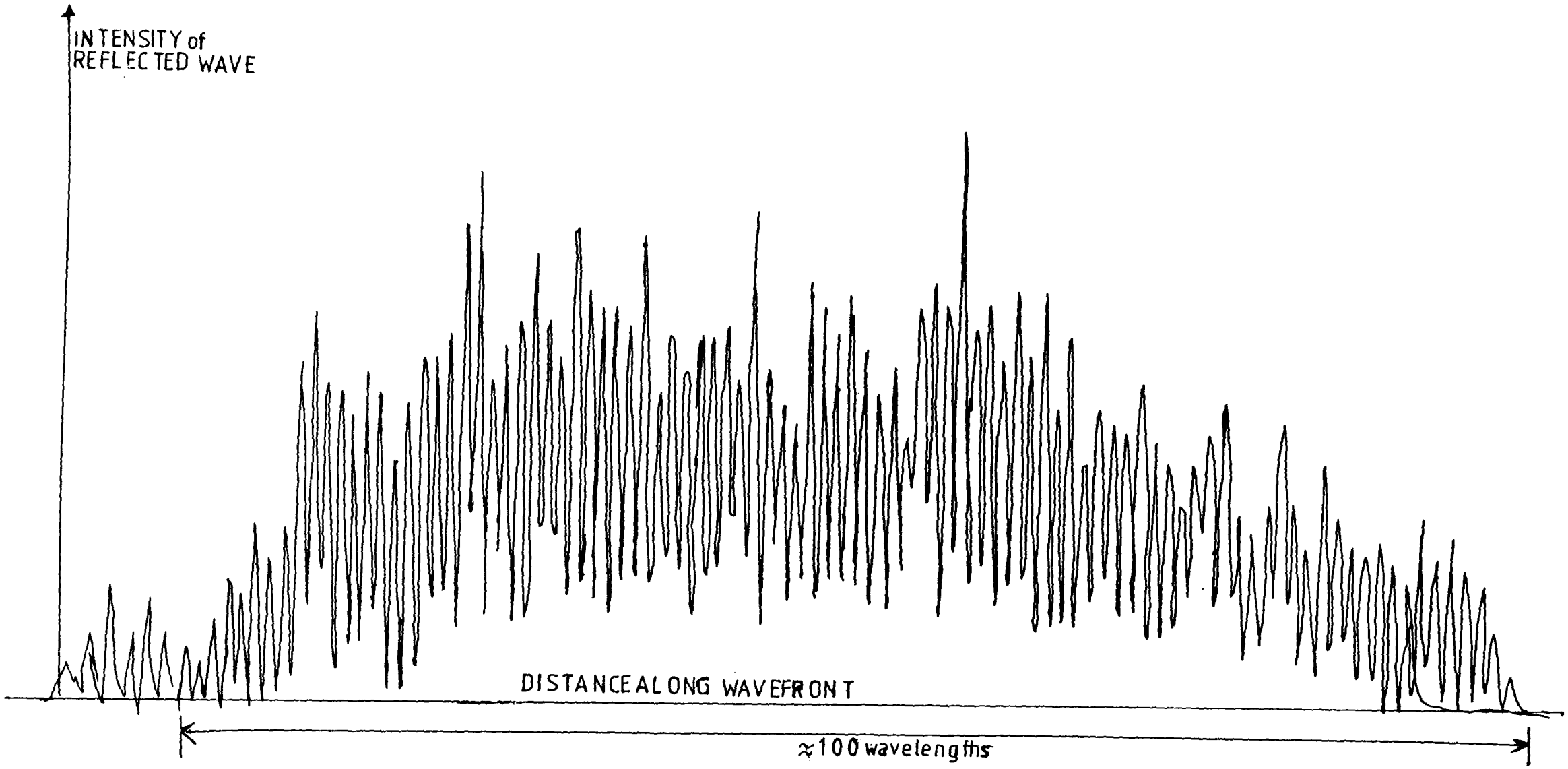

Figure 414 : NEAR-FIELD ENERGY DISTRIBUTION
REFLECTED from a TYPE A1 ARRAY

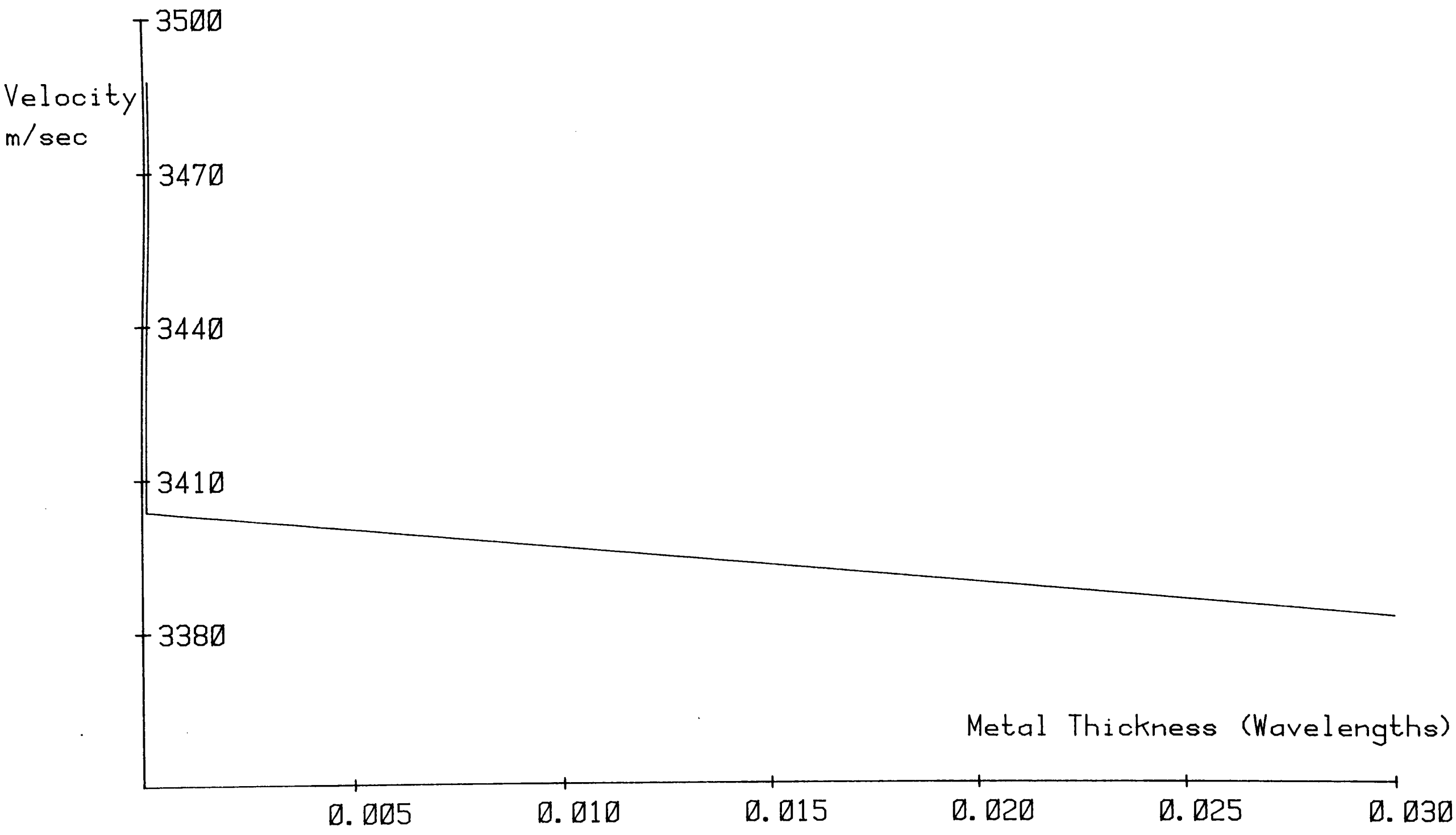

Figure 4.15: Reduction of Velocity of Z-propogating Surface Wave On Y-Cut Lithium Niobate Under a Layer of Aluminium

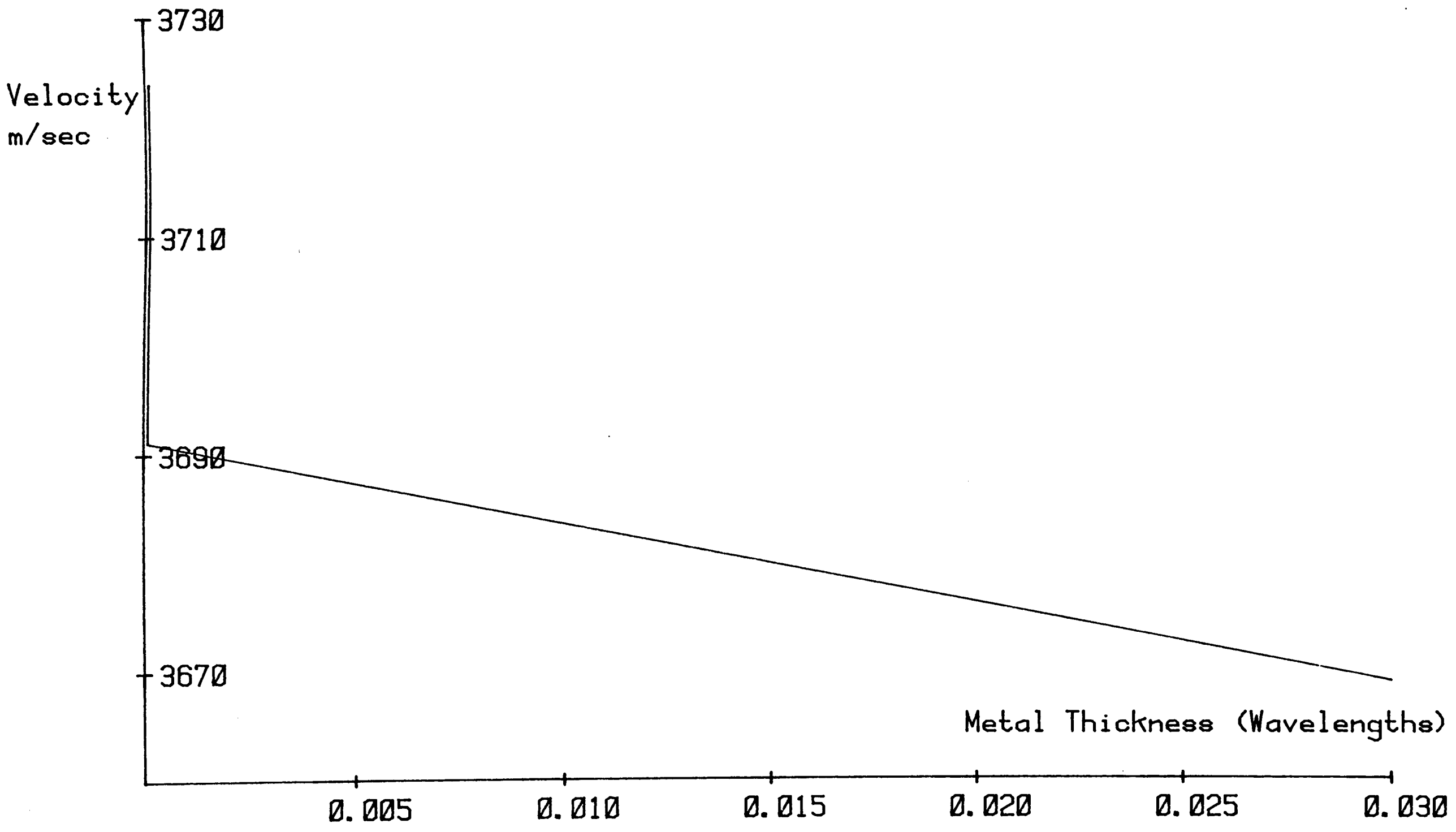

Figure 4.16: Reduction of Velocity of X-propogating Surface Wave On Y-cut Lithium Niobate Under a Layer of Aluminium

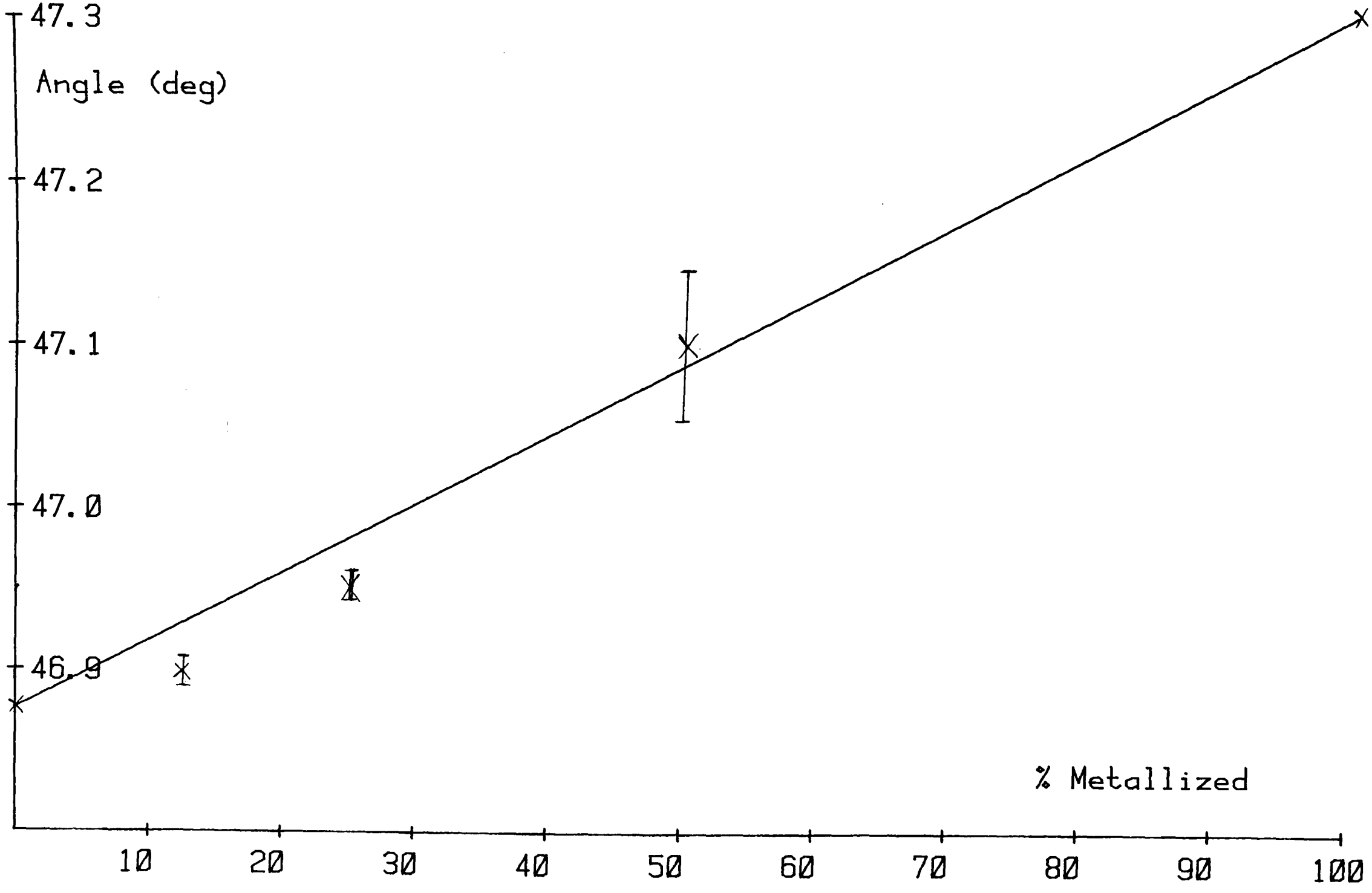

Figure 4.17: Experimental Variation of Array Angle with Metallization

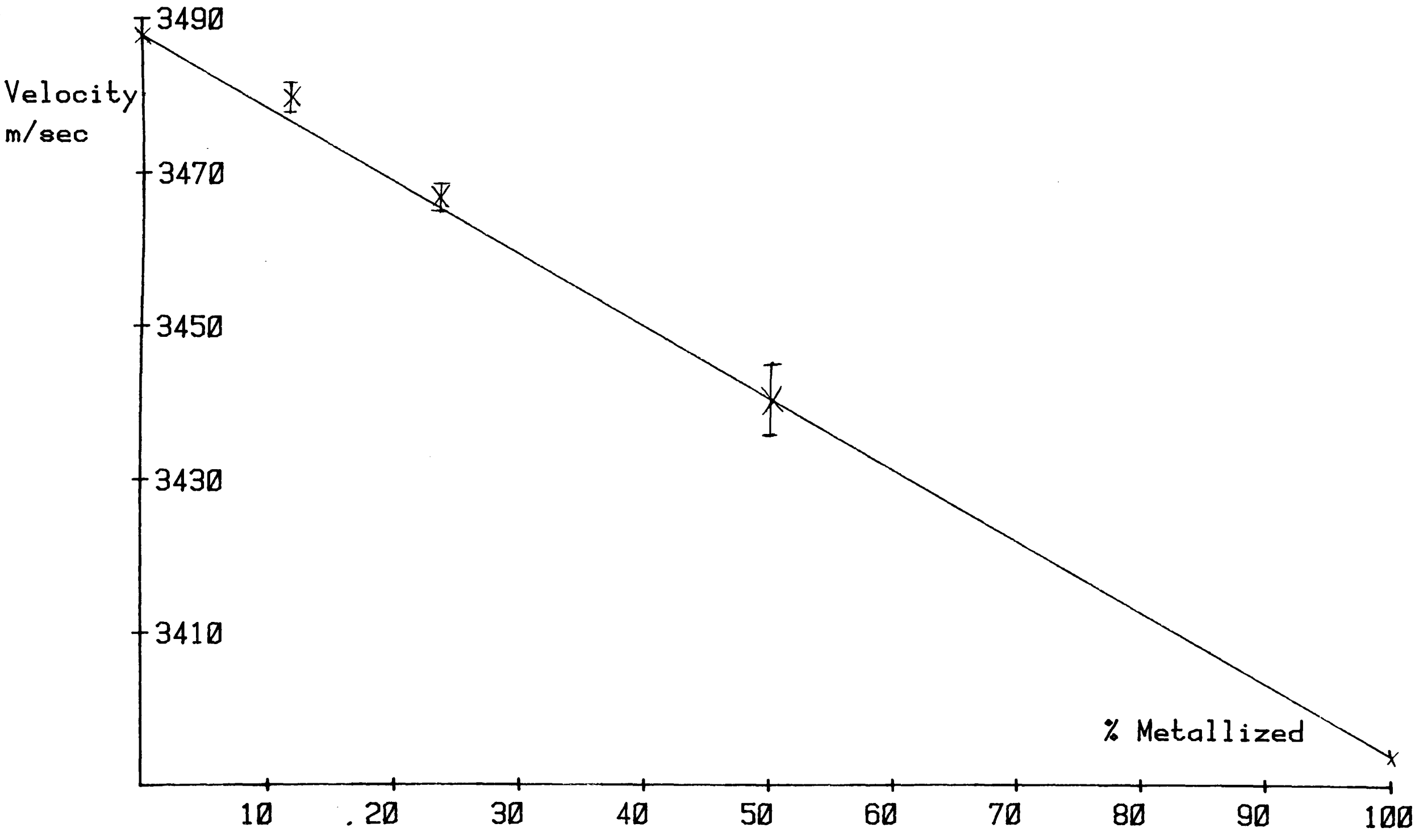

Figure 4.18: Variation of Z-Velocity in Array with Metallization

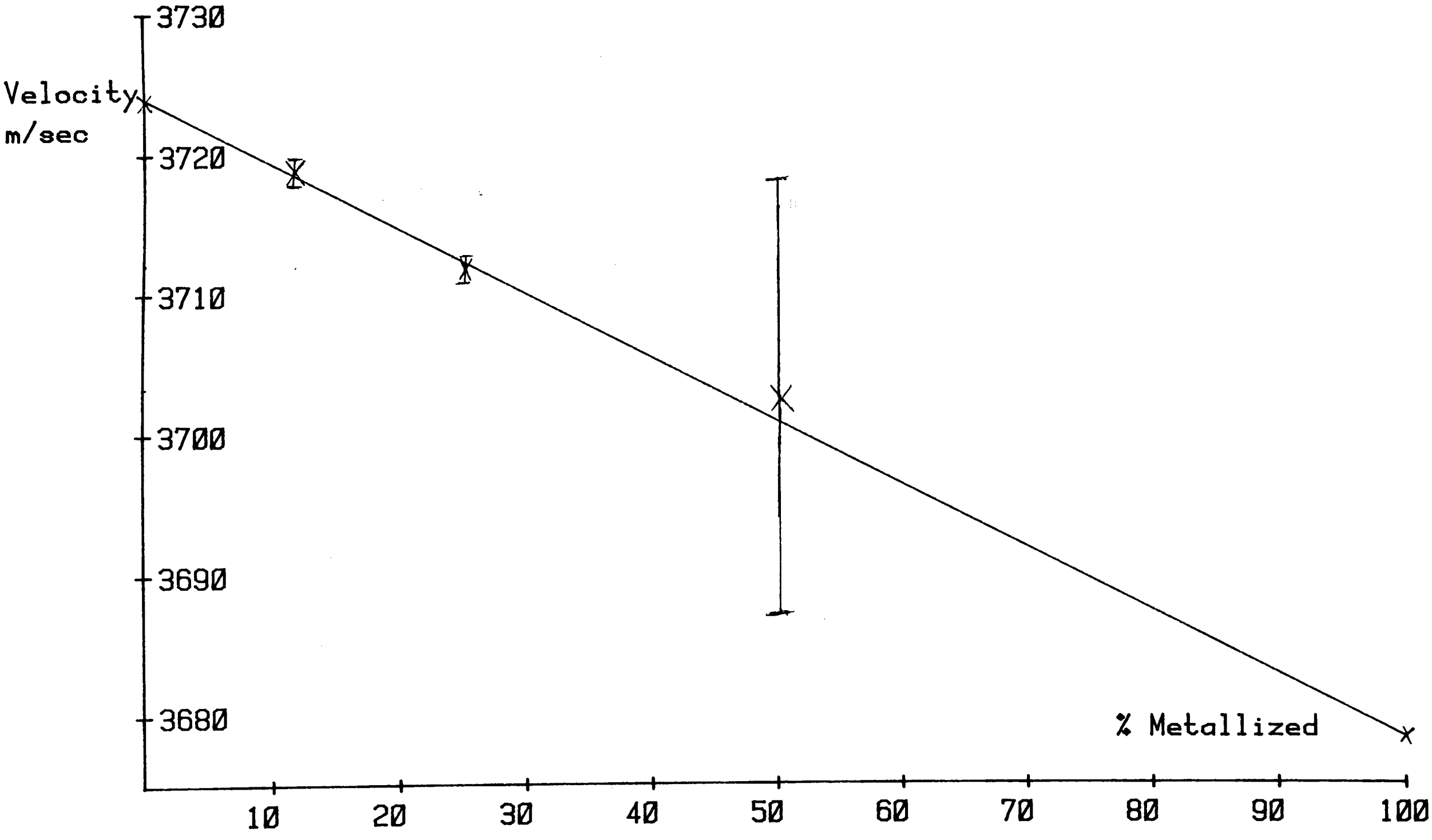

Figure 4.19: Variation of X-Velocity in Array with Metallization

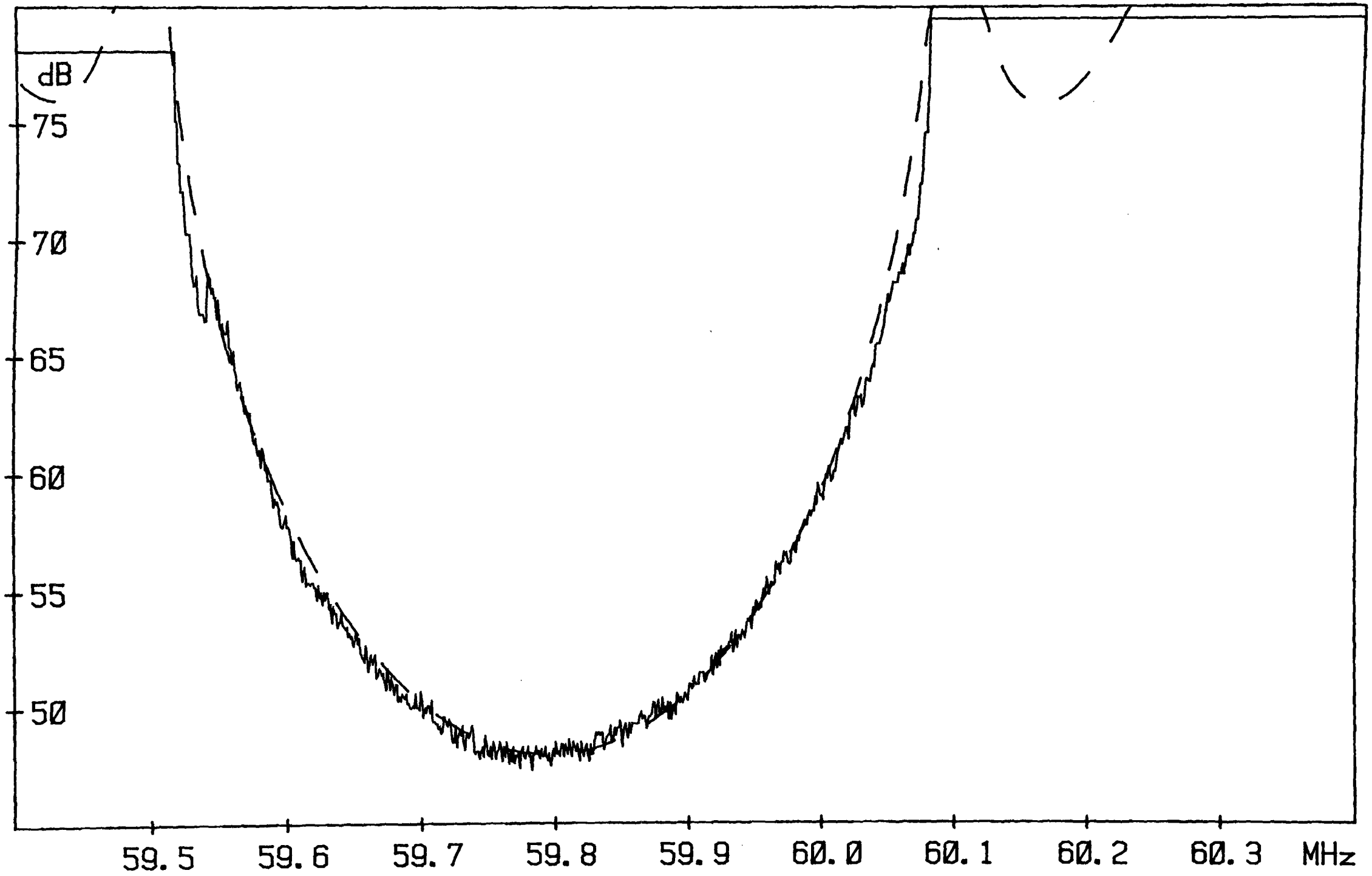

Figure 4.20: Thinned Type A1 Array, U-path Response

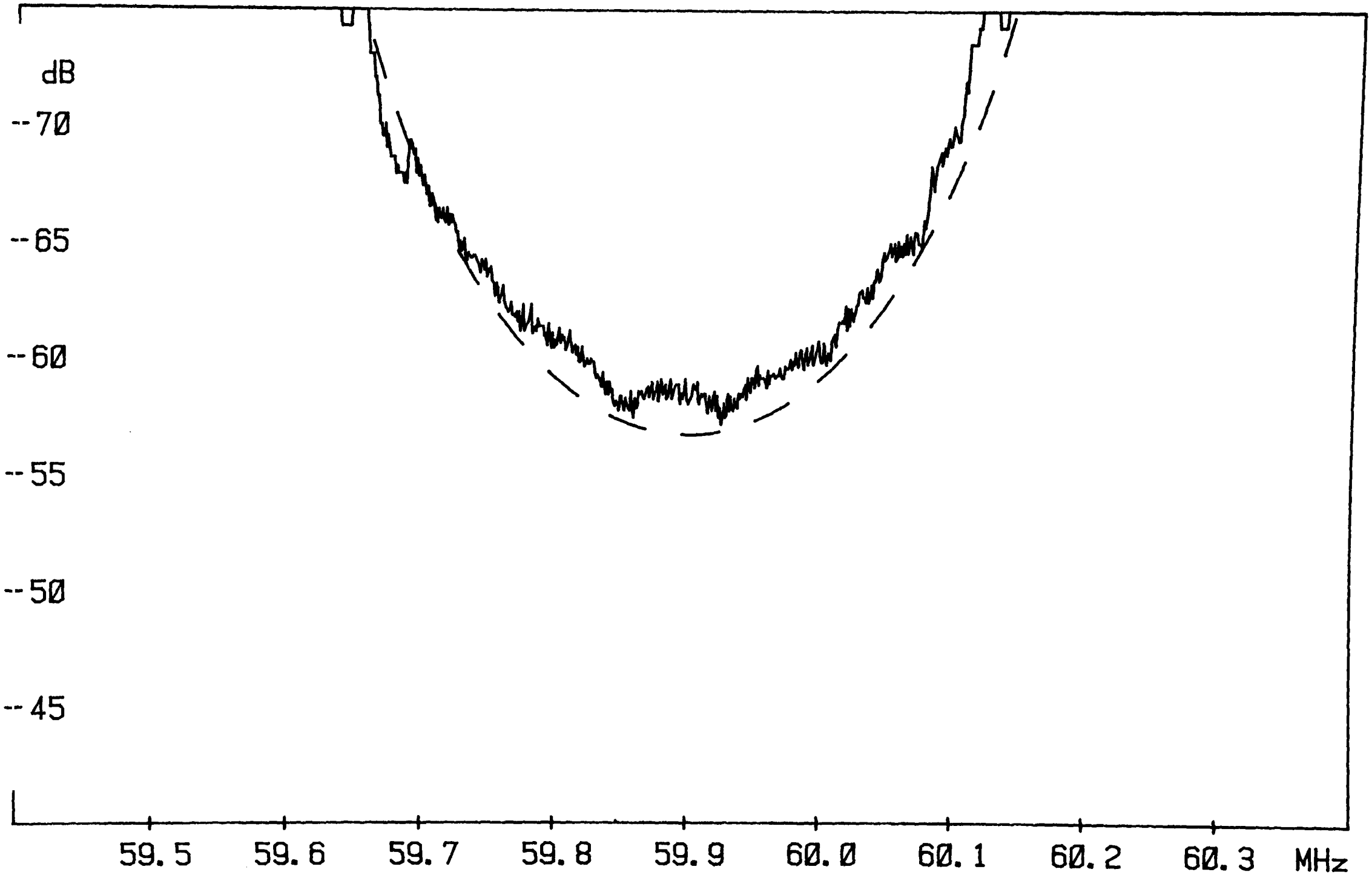

Figure 4.21: Thinned Type A2 Array, U-path Response

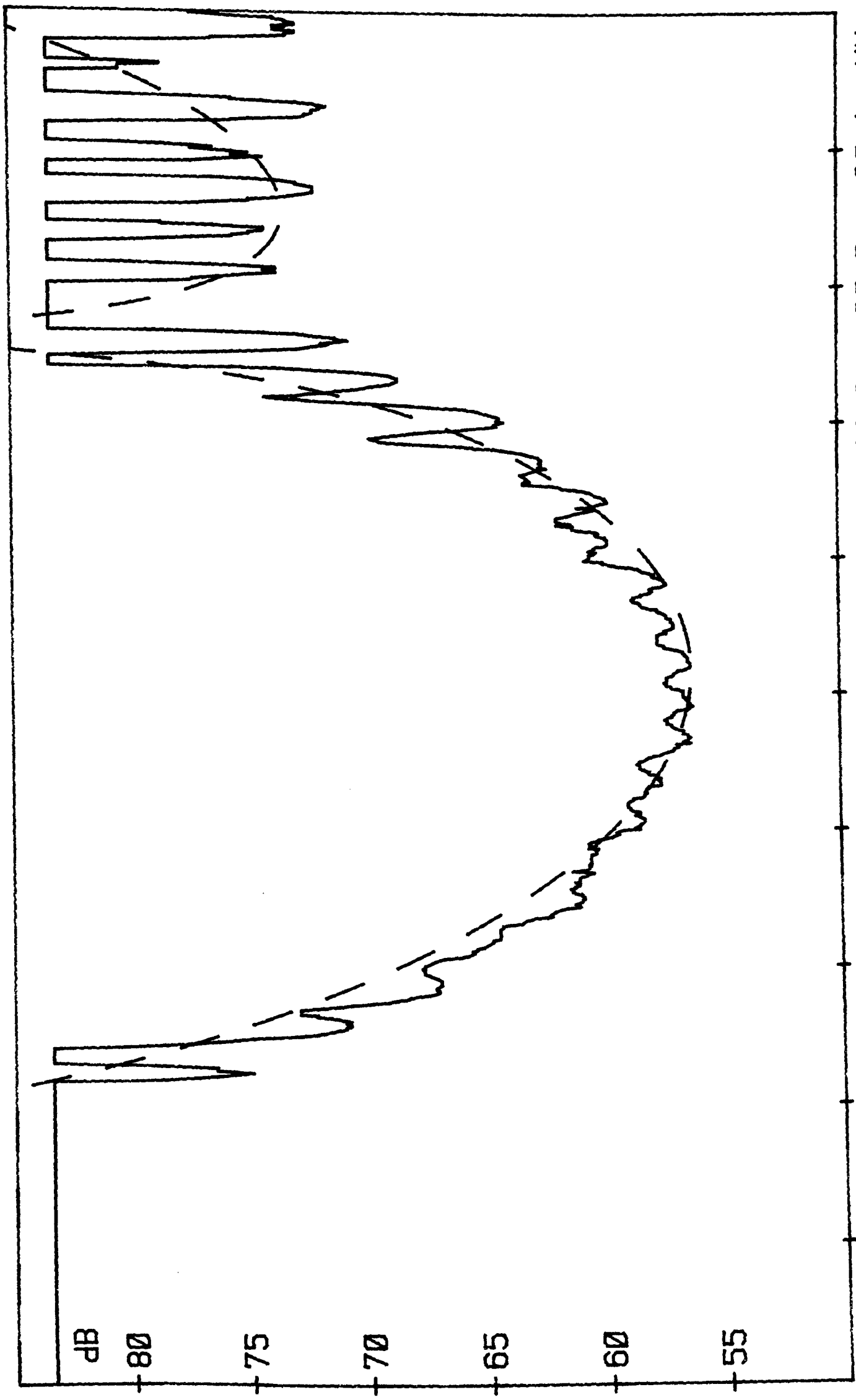

Figure 4.22: Light Aluminium Type A1 Array, U-path Response

CHAPTER 5

DOT AND STRIP REFLECTIONS

5.1: Introduction

In the previous chapter it was said that an understanding of the behaviour of reflective dots is basic to the manufacture of reflective dot array devices, no less than the behaviour of the arrays themselves. The behaviour of the arrays was then discussed, and some properties of the individual dots deduced from their behaviour in arrays. The effect of weighting the arrays be changing the density of the dots was also discussed there, and some anomolous effects have been observed.

In this chapter the behaviour of the individual reflectors will be discussed. The simplified problem of reflections back through 180 degrees by metal strips will also be discussed, so that some theoretical and practical results can be compared, and the practical results so far obtained on the reflection properties of dots will be collated.

The reason for studying the reflection characteristics of metal strips first is that theoretical solutions exist for this one dimensional problem[23,24]. These theoretical results are the product of very complicated models, which would become even more complicated if they were to be used to solve the problem of scattering from dots, which is a two-dimensional problem.

This part of the work has been sucessful, in that the models have been shown to be accurate in their predictions, and has produced useful results. The extension of the modelling to try to explain the experimental reflection coefficent results for dots would be the next step for this work. Due to its complexity this has not been done, but the experimental results have been gathered together, and in themselves constitute useful information for the design of dot array devices.

5.2:Reflections from Metal Strips

The problem of the scattering of surface waves by metal dots on the surface of the substrate across which they are propagating is, as has been said, a complicated problem. The simpler one-dimensional analogy is that of a plane surface wave being reflected straight back from an infinitly long strip of metal normal to its path. The only spatial dimension left in the problem is that along the propagation direction, if the decay of the wave into the bulk can be taken as implicit.

Cambiaggio and Cuozzo produced their theoretical results[33] by a finite-difference solution of the electrical and strain equations for the travelling wave under the metal plate, using a computer programme apparently developed for the purpose. Milsom[34] modified a programme which was designed to calculate the significant parameters of the behaviour of surface wave transducers, which has been described in detail

elsewhere[7]. In essence it first calculated the amplitudes of the various waves which would be launched in the given direction on the given substrate by an impulse of charge. It then calculated the actual charge distribution present and obtained the overall response by convolving these two factors. The model was intended to give information about the reflection of surface waves from a transducer. It considered the reflecting strip as two transducer fingers at the same potential and touching. Rather than modelling the actual single strip it in fact modelled two half strips with zero seperation between them. The charge distribution was found for each seperatly. This should, of course correspond to that for one strip in the limit where the two half-strips were touching, although the procedure would increase the possibility of slight errors due to the numerical techniques used to calculate the charge distribution. Any such errors, if actually present, seem not to have had any significant effect on the model's predictions. This approach was used, rather than the modelling of a single finger, because that was how the programme had been set up, in order to model transducers with many fingers, and the programme was unaltered, treating the strip as a rather strange form of transducer, because the predictions were made by Milsom as a favour to this work. These predictions were valued because the programme which was used to generate them is generally agreed to embody one of the most accurate models in existance of the behaviour of surface waves in the presence of free charges.

The predictions of these two models were tested against

some experimental results obtained from devices which were made specifically in order to obtain such results. The design of these devices was mentioned at the end of chapter two and illustrated in general in figure 2.6 .

The detailed design of the first device made is shown in figure 5.1. It consists fundamentally of a series of reflective test strips and input and output transducers as shown in figure 2.6 . One such input transducer is that labelled 'f_0 test', which is designed to launch a surface wave towards the reflectors at a given frequency. It consists of five fingers, giving a bandwidth of about forty percent around the design frequency. This enabled the changes in reflection coefficent of a strip to be seen over a wide variation in the period of the incident wave. Such relatively poor frequency selectivity also rendered the transducers susceptible to the launching of bulk waves, so the output beam is diverted through a multistrip coupler[26]. Such a device has been described in chapter two as a power divider in an inline RDA. Here it is made twice as long as in that application, and is used to transfer all the surface wave power from the beam of the input transducer to a beam which will intercept the output transducer, shown schematically after it. The bulk waves will not be intercepted by the coupler and will pass straight through it and miss the reflectors. The multistrip coupler thus 'cleans-up' the device and ensures that the signals seen at the output transducer are due to surface waves rather than to spurious bulk waves.

The signal which has passed under the output transducer is then reflected by the test strips, and the reflections again seen by the output transducer, as described in chapters two and three in the brief description of the device and in the discussion of the measurement techniques employed. The strips were designed to be one eighth, one quarter, three eighths or one half a wavelength wide at the design frequency of the transducers. Each of the four blocks shown consisted of ten strips of one width, seperated by a design-frequency wavelength. This was done in order that if the device was fed with long pulses of r.f. power at its design frequency, the reflections from each of the ten strips would add up in phase, increasing the amplitude of the reflected signal to enable it to be more accurately examined. The maximum length of the input pulse was limited by the need to keep the incident pulse and the various reflected pulses distinct at the output transducer, and there was no point in making it longer than twice the length of the groups of strips (i.e. about twenty wavelengths long), at which length of pulse the constructive interferance from the strips reaches a plateau. The widths of the strips and the aperture of the output transducer were made narrower than the aperture of the input transducer to try to guard against the effects of diffraction at the edges of the beam. The one-eighth wavelength wide strips were nearest the output transducers, and the wider strips grouped progressively further away.

In addition to this arrangement, a similar set of transducers and multistrip coupler was designed to launch waves to the test reflectors from the opposite side of the opposite side of the array and at twice the original design frequency of the device. This arrangement allowed further effective strip widths of one quarter, one half, three quarters and one wavelength to be investigated. The spacing of the strips within the groups now corresponded, of course, to two wavelengths at this doubled frequency.

The quarter and half wavelength measurements made with the shorter strips at the doubled frequency could be compared with the equivalent results for the longer strips at the lower frequency. The longer strips at the higher frequency extended the overall range of strip widths for which the reflection coefficent could be measured to one eighth to one wavelength.

There were two respects in which this device would not lead to an experiment with exactly the same conditions as those from which the theoretical predictions were made. The first is that the predictions were made from an infinitely thin, i.e. massless, electrical reflector, which is obviously unattainable in practice. The second is that the predictions were obtained for strictly isolated strips, whereas in this device the strips were arranged in banks, as has been described, so that any intercapacity effects between the strips or similar effects would alter the response from that predicted, besides the fall-off in overall response if the wavelength of the input wave no longer corresponded with the periodicity of the strips within the group.

The effects of the finite mass of the strips can be minimised by making them as thin as is practicable consistant with a reliable uniformity of metallization and by ensuring that the metallization

was of aluminium rather than gold, it being assumed that the finite conductivity of the strip would not be a significant factor altering the response from that predicted. The device was designed to operate with a wavelength of 64 microns, corresponding to a fundamental frequency, f_0, of around 54MHz. Using aluminium metallization 1000Å thick the metal would be 1/600 wavelengths thick, in which case it was predicted that the effects of mass loading would be insignificant compared with those predicted for the electrical reflection, of the order of 0.1% from the formula given in section 2 of chapter 2.

Figure 5.2 shows the results obtained for the amplitude reflection coefficent of thin metal strips as a function of their length in wavelengths up to a length of one wavelength.

The predictions of Cambiaggio and Cuozzo and of Milsom are shown on the same graph for comparision. It can be seen that most of the points agree qualitatively with the theories, but that the quantitative agreement could be better. The results would appear, however, to support Milsom's generally lower predictions for the reflection coefficent against Cambiaggio and Cuozzo's higher values.

The most startling disparity between theory and experiment occurs where the strip length is three quarters of a wavelength, where the experiment which was performed shows no indication of the null in the response which is predicted by the theories. It was possible to vary the frequency of the input wave pulse so as to vary the effective strip widths around the value of three quarters of a wavelength over a sufficent range to be certain that the null was not just slightly displaced from the theoretical values. It was confirmed, rather, that it was indeed not present at all.

The measured values of the reflection coefficents of the quarter- and half-wavelength wide strips at the two available operating frequencies (upper curve is at lower frequency) are also inconsistent.

The probable cause of these discrepancies is the mutual intercapacity of the strips. This could not be modelled, either to enable it to be shown to be the explanation, or to be dicounted, but in view of the thoroughness and rigour particularly of Milsom's treatment of the problem, it was thought that this was the most probable source for the observed discrepancies. The experiment had shown, however, that the reflection coefficents of the individual strips were sufficently high for them to be measured without the reinforcement of using a bank of them.

In the light of this information another experiment was performed on a device of the form shown in figure 5.1 wherein nine of the ten strips in a bank were carefully removed by scraping a pin over the surface of the substrate, allowing the behaviour of an isolated strip to be observed. This technique did not damage the substrate at all, although it left traces of metal on the surface, and a few small nicks were accidentally made in the one strip which was left. What was left was, however, substantially a single strip, and this technique required far less effort than redesigning the mask and having another mask made and devices made from that mask.

With a single strip it was, of course, then possible to vary the frequency of the input wave to observe how the reflection coefficent varied as the length of a reflector relative to a wavelength was changed. With the banks of strips, quantitative measurements could only be made at discrete frequencies where the

periodicity of the strips in the banks was the same as that of the incident wave.

The modification described was applied to the two widest strips in the test banks, which when tested at frequencies in the passband of the higher frequency transducers allowed measurements to be made of the reflection coefficents of single strips over a relative strip length of from about 0.6 to about 1.3 wavelengths. The narrower strip had an effective length which varied from 0.6 to about 1 wavelength, through its nominal value of .75 wavelengths, this being the prime region of interest, where the previously-obtained results had differed most drastically from the predictions. The longer strip varied in length from about 0.9 to 1.3 wavelengths around the nominal value of 1 wavelength. At the shorter effective lengths its results overlapped with those of the other strip, giving a useful check on the results, and at the longer effective lengths it covered the whole of the region of the next peak and down into the next predicted trough, and part of the way towards the next peak.

Figure 5.3 shows the results obtained by this experiment. The full curve shows Milsom's prediction. The crosses show the experimentally obtained points. The signal levels available were quite low, especially at the edges of the response region, and this is what is mainly responsible for the scatter of the points. The resolution with which the signal amplitudes could be measured was not very good because of this. A narrow-band bandpass filter was used to clean up the observed traces, removing any out-of-band signals or noise which might be picked up by the amplifiers. This filter

tended to distort the received pulses somewhat as well, adding slightly to the problems of measurement, especially near the nulls of the responses, where the effective broadening of the signal bandwidth by the gating appeared to tend to upset the response, leading to distorted pulse shapes on reflection. These errors would be expected to add up to toal errors of prehaps around 20% in the calculated reflection coefficents, which would generally be consistant with what was observed. The dotted lines on figure 5.3 were 'best fit' curves which were estimated by eye for the results for the two reflectors.

It can be seen that the results agree with those of Milsom within the expected errors. Where they overlap the curves for the two reflectors, although distinct, also agree quite well. The dips predicted by Milsom are well in evidence. The theoretical curves do not go exactly to zero because they were obtained by joining up a series of discrete points, which appeared to fall around the nulls without ever quite falling on them, so that the actual depth of null which Milsom would predict is unknown, only an upper bound being available. The results of Cambiaggio and Cuozzo, however, predict accurate nulls, although at slightly different places. The experimental data still do not show accurate nulls, but the residual reflection coefficent in the dips is now compatible with what would be expected for the mass-loading due to the finite thickness of the strips.

This experiment would then appear to have achieved two things. It has confirmed the general predictions of the theories for

the electrical reflection effects for metal strips on lithium niobate, especially around the predicted dips which the earlier experiment had not shown. It has, by comparision with the results for banks of strips, also shown up dramatically the importance which inter-strip capacity can have on the reflection coefficent.

The quantitative results for the banks of strips should, therefore, be regarded with suspicion if it is hoped to extrapolate from them to the behaviour of isolated strips, even when the results are in qualitative agreement with the theory. The results for the single strips would seem to support Milsom's predicted amplitude responses rather than Cambiaggio and Cuozzo's, although there is evidence that the nulls occur at slightly higher strip-lengths than Milsom has predicted. This seems clearer for the second null than for the first. The placing of the first null would seem to agree better with the results of Cambiaggio and Cuozzo rather than with Milsom. Unfortunatly no predictions from the latter model are available for the second dip, where the disagreement between Milsom's model and the experimental result is more clear-cut.

The results for banks of strips with lower effective widths, as far as they can be trusted to be applied to single strips, would also support Milsom's calculations of the amplitude responses rather than Cambiaggio and Cuozzo's.

This section of the work has, then, generally confirmed the predictions of Cambiaggio and Cuozzo and of Milsom for the one--dimensional problem of the 180 degree reflection of a surface wave from a thin metal strip. The measurements were not, however, sufficently accurate to be able to ascertain which of the two models was more accurate where their predictions differed.

The experiments have also shown up the unexpected deviation from the predicted response by the three-quarter wavelength strips when grouped together in banks, and a possible explanation for this has been suggested in the mutual capacity of the strips.

This work has formed a foundation upon which a model for the behaviour of the dots could be formed, if such a procedure is found more worthwhile than the gathering of further empirical data on their behaviour. In order for this to be done the effects of mass loading would have to be considered, and the models expanded to cope with a two-dimensional problem.

5.3: Experimental Values of Dot Reflection Coefficents

This section will gather together the results obtained for the reflection coefficents of dots in arrays, which have been deduced from measurements made upon the arrays. Many of these results have been presented previously, in chapter 4, but they are grouped together here, in table 5.1, below.

Table 5.1: Reflection Coefficents of Dots in Close-Packed Arrays

Dot Type	Dot Size (Wavelengths)		Reflection Coefficent (per cent per dot)			
	'A'	'B'	Metal Thicknesses (Angstroms Al)			
			1000		4400	
			r_{zz}	r_{zx}	r_{zz}	r_{zx}
A1/S1	$\frac{1}{4}$	$\frac{1}{4}$	1.25	0.05	-	0.15
A2	$\frac{1}{8}$	$\frac{1}{8}$	-	-	-	0.05
S2	$\frac{1}{4}$	$\frac{3}{4}$	1.0	0.8	-	-
S3	$\frac{1}{4}$	$\frac{1}{2}$	-	-	1.2	0.9

The 'Close Packed' in the title of the table is a reminder that these were the values obtained from such arrays, and that the results obtained from the type A1 and A2 arrays with reduced dot density provide evidence that the reflection coefficent can change as the dot density is changed.

The first column of the table names the dot type by reference to the type of array in which it was used (see figure 4.1) . The

second column gives the size of the dot. Figure 5.4 shows to what the dimensions 'A' and 'B' refer. The last four columns give the reflection coefficents, 'r' for the two thicknesses of aluminium which were used in the dot array experiments. The first subscript of 'r' indicates the direction of the incident wave, and the second that of the reflected wave. 'r_{zx}' is therefore the scattering coefficent for the dot from a Z-propagating wave into an X-propagating wave, all the waves, of course, travelling on Y-cut lithium niobate.

The methods by which the various coefficents have been estimated have mostly been mentioned before, in chapters 3 or 4, but will be summarized here for completeness.

The 'zx' reflection coefficents for the type A1/S1 and type A2 dots were obtained from fitting equation 4.5 to the measured U-path responses of the devices. They are probably accurate within about 10%. The 'zz' reflection coefficents for the type S1 and S2 arrays were measured directly by putting a short burst of r.f. energy into the array and seeing the reflected wave on one of the other transducers, 5 to 8 in figure 4.2a. The corresponding measurement for the type S3 array was made using a single transducer, with the 3dB coupler to try to isolate the input and output signals. These measurements were probably made to about 20% accuracy. No measurement of r_{zz} was possible for the type A2 dot as no array was made which used these dots and which could reflect energy through 180 degrees.

The 'zx' reflection coefficents for the type S2 and S3 arrays were estimated from the U and Z path insertion losses. The insertion

loss was measured and it was then assumed that the array was simply reflective (which is, of course, a dubious assumption, but necessary). The device was then probed to determine over how much of its length power was reflected, in order to estimate the number of active reflectors. The reflection coefficent per dot could then be estimated to within about 25%. A similar estimate was made with the S1 array to see whether the method was at all accurate, and it appeared to work within the suggested accuracies

It is noticable that inspite of the fact that the dots will, in general, scatter energy in all directions, the structure of the arrays, with their distinct reflecting planes, and the positioning of the input and output transducers means that the reflection coefficents of the dots can only be measured in discrete directions. The use of U-path measurements relies upon the fact that, of course, $r_{zx} = r_{xz}$. Any attemt to use Z-path measurements would furthermore require the dots to have $r_{zx} = r_{z,-x}$, so that scattering upwards or downwards (with reference to figure 4.1) would be equally efficent, which is clearly a greater assumption. Comparisions of the U and Z path responses of the type S2 and type S3 arrays have shown, however, that this appears to be substantially the case for even these asymmetrical dots.

There are clearly a number of points about the results shown in table 5.1 upon which comment could be passed. One of these is its incompleteness, in as much as that the type A1/S1 dot was the only one which was used in both metal thicknesses, and that the thick type A1/S1 dot and the type A2 dot were only used in asymmetric arrays, the properties of which were such that the value of 'r_{zz}' could not be obtained from them.

These gaps in the table have occured because the experimental devices were designed and made firstly for the investigation of the effects of array patterns and array angle on their behaviour, in order to derive the results presented in the previous chapter. The data on the reflection coefficents of the dots which was gathered from these investigations were in some ways secondary results, despite their importance in the observed behaviour of the devices.

The results which have been gathered do, however, show several interesting points which are significaant for the design of dots for use in dot arrays.

The data shows that the ninety degree reflection coefficent, r_{zx}, varies as the dot size is increased towards a wavelength, which is what might be expected from simple assumptions about the scattering. The extent of this increase would also suggest that as the dot size is increased between the A1/S1 and S3 dots another reflection mechanism, electrical shorting, becomes important. There is evidence to show that the reflection mechanism in the smaller dots is predominantly mass-loading, whereas in the larger, electrical shorting is predominant.

The type A1/S1 is the only dot for which direct evidence is available to compare the reflection coefficents of dots with both 1000 and 4000 angstroms of aluminium. The great variation in the reflection coefficent, which is almost proportional to the thickness of the metal, is what would be expected if mass-loading dominated the reflection process. This is what Solie has said is the case for small dots[13], and which might be expected to apply to the type A2 dot,

but its occurence in the type A1/S1 dot, which is half a wavelength across the diagonal, is prehaps unexpected.

It was discussed in section 2 of chapter 4 how the type S3 dot would be expected to have $r_{zz}=0$ if its reflection mechanism were mass loading. Its value of r_{zx} would also be expected to be strictly twice that of the type A1/S1 dot if that assumption were true. The failure of both these predictions implies strongly that electrical shorting is an important reflection mechanism in that larger dot type. Although no model is available for electrical shorting, it could be expected that its behaviour would not be as simple as that of an almost purely local reflection mechanism such as mass loading.

The results for these two dot types therefore provide clear evidence for the contention that the dominant reflection mechanism in small dots is mass loading, whereas in larger dots electrical shorting becomes dominant. It also allows the statement that this change-over occurs with dot sizes between those of the A1/S1 and S3 dots.

The very high anisotropy of the reflection coefficents of the thin type A1/S1 dot is also worthy of note. It explains the preference of the type S1 array to scatter energy through 180 degrees rather than through ninety, but is in itself unexpected, especially given the physical isotropy of the dot. It prehaps provides an indication that while mass loading dominates r_{zx} for this dot, electrical shorting dominates r_{zz}. There are two reasons why this might be the case. One is that the wave will 'see' a physically isotropic dot such

as the type A1/S1 as longer than it is wide, because the wave which is reflected through 180 degrees travels both forewards and backwards under the dot, doubling its path length under it. Hence if there is a certain dot size at which electrical shorting begins to become significant, it will, other things being equal, tend to be physically less for r_{zz} than for r_{zx}.

Other things are not, however, equal. The strength of the electrical reflection by a dot will be proportional to the strength of the electrical shorting ,$\Delta v/v$, of the wave which it is reflecting. The value of this coefficent in the Z-direction for Y-cut lithium niobate is 2.35%, whilst for the X-direction it is only 0.88%. The electrical shorting would thus contribute more to r_{zz}, which employs only the Z-propagating wave than to r_{zx} which employs both Z- and X-propagating waves, if the lengths of the dots were equivalent. It is on this basis and upon the extreme anisotropy of the reflection coefficents that the electrical nature of the r_{zz} reflection of the S1/A1 dot is suggested.

In general these results confirm what would be expected, that the reflection coefficent of the dots increases as the dots get larger, and what Solie has suggested, that for sufficently small dots the predominant reflection mechanism is mass loading, and that electrical shorting only becomes important as the dots get larger.

This work has provided quantitative evidence to support these contentions, together with indications of the size of dot for ehich electrical shorting can be expected to be significant. It has also provided data on values of reflection coefficent which can be expected

from dots of different sizes. It will be observed that no regard has been paid in this work to the effects upon the reflection coefficent of changing the shape of the dots. This is because it was reckoned that, as the dots are mostly smaller than a wavelength across, the effect of changing the shape of the dot would be of second order, and that, for instance, changing the shape of the type A1/S1 dots between circular, square, or diamond would not have affected their reflection coefficents to any great extent,

This last idea, that of the relative unimportance of the effect of changes in the actual shape of the dots, is, however, without any evidence to support it, and this is one of several aspects of the behaviour of the dots into which further investigations should be made. More evidence should be gathered about the effects of using different metal thicknesses in different sized dots.

It would also be useful to have further information about the behaviour of dots of still other sizes, including, prehaps, seeing whether it is indeed possible to make dots with zero reflection coefficent in specified directions, as was tried without sucess in the type S3 dot.

In order to do this however, it would probably be necessary to have a relatively good model for the behaviour of the dots. Such a model would be of great general use in this work, and if such a model could be developed it could elegently reduce the number of experiments which must at present be undertaken to gather empirical information about the reflection coefficents of the individual dots. Such a model would, however, appear to be quite difficult to set up, if it were to be able

to deal accurately with all the reflection mechanisms involved in the problem of reflection on a two-dimensional, anisotropic substrate, and it may prove more effective, for the amount of information about the dots which is wanted to aquire it experimentally, rather than to try to develop a model for the problem.

Another aspect of the behaviour of the dots which is worthy of further attention are the results reported in chapter 4 of the apparent anomolous variations of reflection coefficent with the density of the dots in the arrays. These results should be extended by further work with even less dense arrays. This is also a factor which one would wish to incorporate into any model of the behaviour of the dots, although it might be thought that this could add considerably to the complexity of any such model.

This work has indicated various aspects of the behaviour of reflective dots which are worthy of investigation and of understanding, and has suggested the usefulness of a model of the behaviour of the dots. It has also lain the foundation for any such study by having gathered some experimental information about the refelction coefficents of dots. From the data which this work has made available, however, the expected insertion losses of dot array devices and the extent to which multiple reflections within the arrys need to be considered can both be estimated.

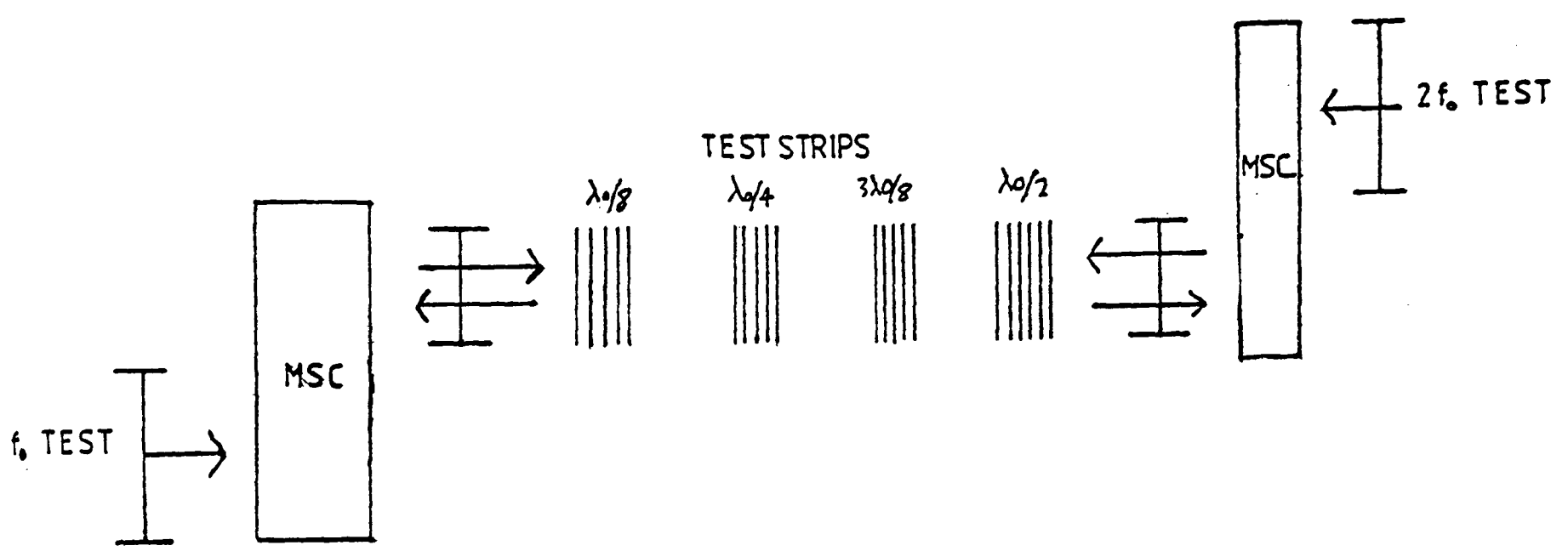

Figure 5.1: Layout of Experimental Device to Investigate Reflection by Metal Strips

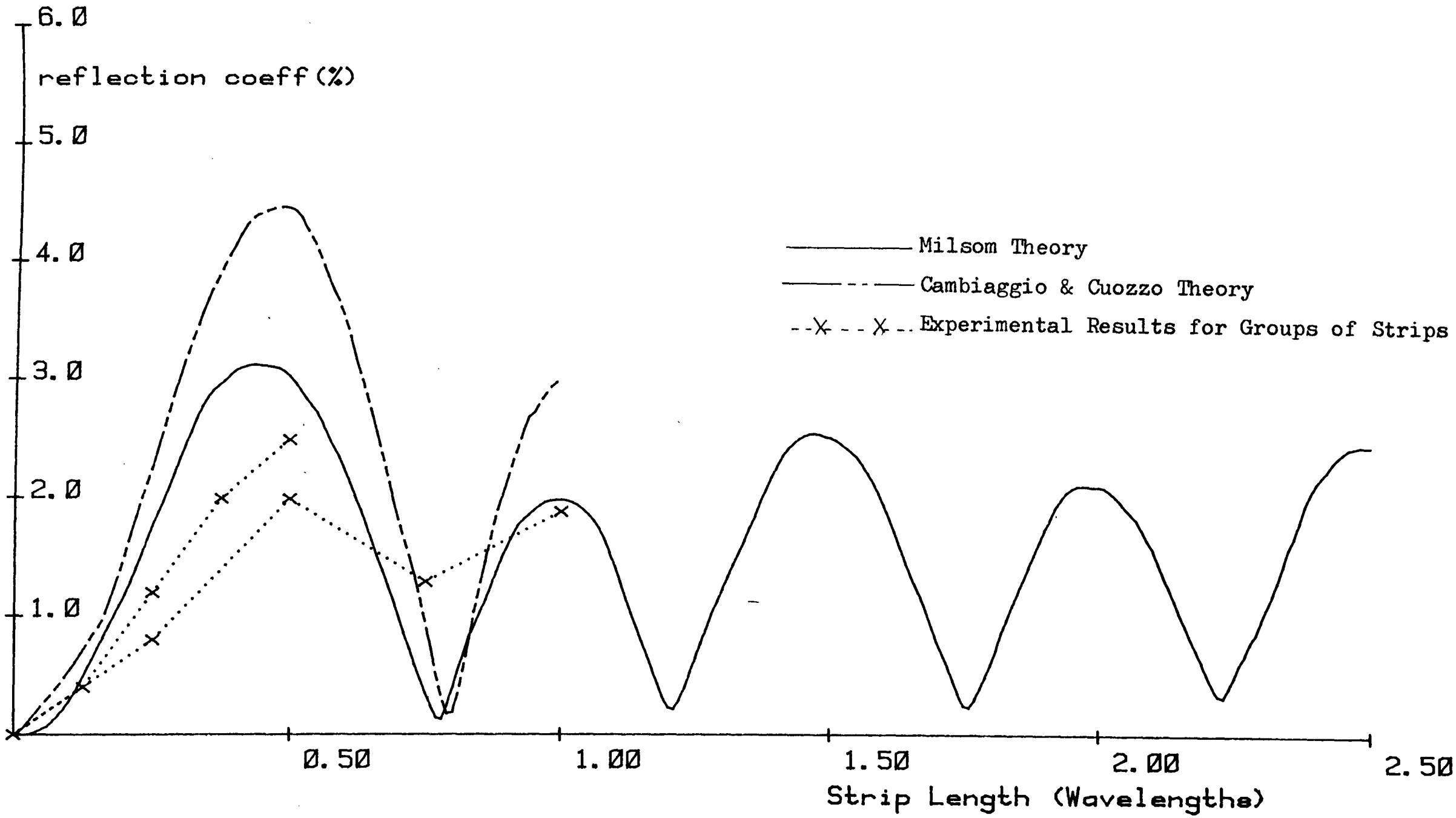

Figure 5.2: Comparision of Theoretical and Experimental Results For Reflection of Surface Waves by Metal Strips

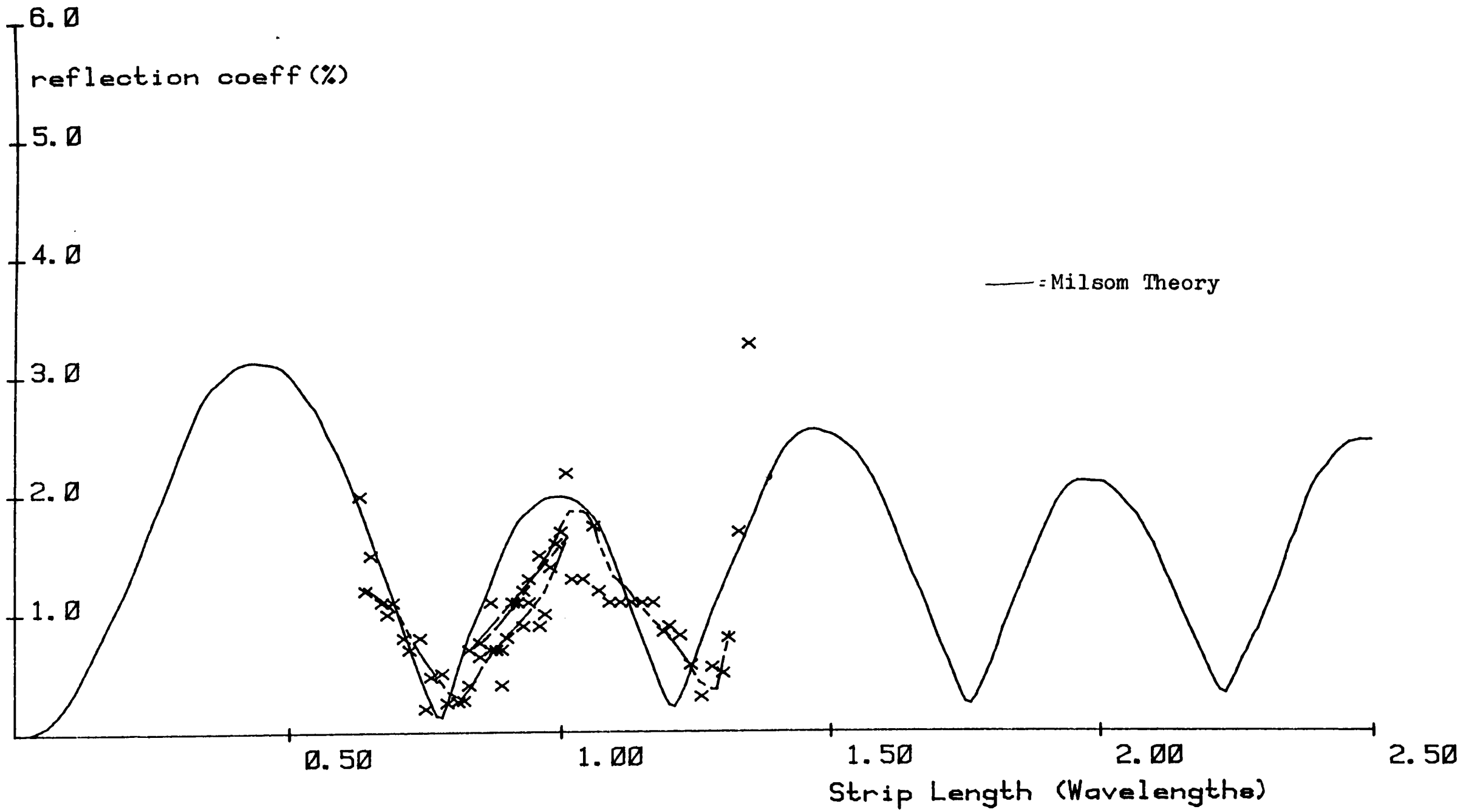

Figure 5.3: Reflection Coefficents for Single Metal Strips

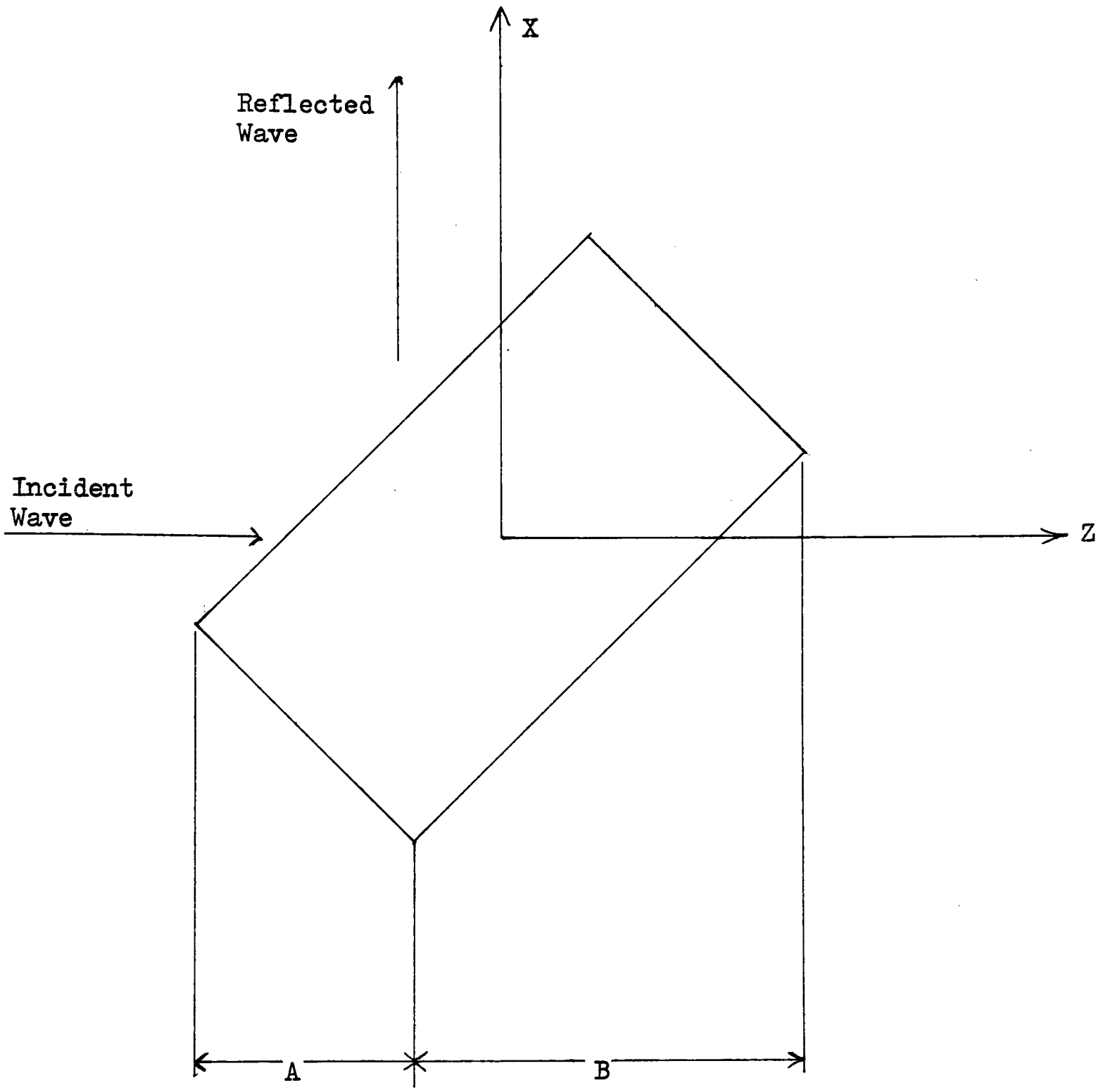

Figure 5.4: Dot Dimensions Used in Table 5.1

CHAPTER 6

INLINE DEVICES

Two inline reflective dot array devices were made, as part of this work, to the general design shown in figure 2.4d. As was said in chapter 2, the inline device is a relatively new idea, and no such devices had then been made using dot arrays, other than those desscribed below.

The first inline device which was made was a disperser which was designed to be as near as possible identical with one described by Chapman et al.[19]. The transducers and multistrip coupler designs for this device were taken straight from those used in the device described by Chapman et al.. The other inline device was a test-piece which consisted of a series of rectangular patterns of dots, each group having a different periodicity.

The disperser was designed to have a dispersion of 20μs over a 50MHz bandwidth centred on 150MHz. It was designed with the lowest frequency reflectors farthest from the transducers, so that the dealy time was inversely proportional to frequency, making it a down--chirp device. This was so that, ideally, the wave should be reflected before it could reach any reflectors designed for a lower freqeuncy than its own. This would remove the problem of a high-frequency wave intercepting a low-frequency array and coupling to bulk waves. Because inline arrays have no angle selectivity they will tend to be more sensitive to bulk wave effects than are U-path devices. In fact the effectiveness of this precaution in reducing bulk wave effects, at any

rate from a pseudo-continous response was limited because the arrays used were only weakly reflecting, so that most of the incident energy would still pass further down the array and intercept the lower-frequency structures.

The device was weighted along the array so that when the array weighting was combined with the tuned frequency response of the transducers the result should correspond to a 6-term 40dB sidelobe-level Taylor weighting [32]. The reflective arrays were extended by 1μsec (2.5MHz) at each end so that they had cosine-squared weighted tapers rather than abrupt ends, because this was intended to be able to give the device an improved performance in any actual pulse compression system.

The grooves used in the groove device of which this was a metal-dot copy were 1650Å deep. At 150MHz this corresponds to a reflection coefficent of 0.5% amplitude per groove. The metal dot device used dots a quarter-wavelength wide of 1000Å aluminium. From the data on metal strip reflectors which was presented in chapter 5 a full strip of that width should have a reflection coefficent of about 1.2% or so. The dots were thus spaced across the aperture of the reflectors to fill 42% of its width at maximum weighting in order to give the device an insertion loss which should be the same as that of its prototype.

The dot positions were randomized by up to a quarter-wavelength across the aperture, and the weighting was effected by reducing their density. The standard weighting unit used contained 4 dots, and the number of these units across the aperture was varied to give the weighting.

At maximum density there were 20 of these units across the aperture. This number was chosen as the maximum which could be used without increasing the amount of data required by the mask-making machine beyond

beyond that with which the processing programmes could cope. The calculation of the positions of the rows of dots made a first-order allowance for the piezoelectric slowing of the wave by the metal reflectors. This was done because inline devices cannot use phase--plates to compensate for any errors in the assumed velocities of the waves through the arrays.

The device had two arrays of 3301 reflecting planes each. Each array contained about 97000 groups of dots, a total of about 390,000 dots in each array. The two arrays were identical and they were made simultaneously on the mask by using a reticle plate containing one group of dots in each array.

The computer programming necessary to generate the data to produce the job was a major piece of work. The mask itself was made on an Electromask machine at R.S.R.E. Malvern, and took 10 hours continuous running by the machine to produce. This highlights one of the incipient problems with large dot array devices - the extreme complexity of the manufacture of the masks from which they are made, which is caused by the large number of individually-positioned dots which they contain.

The device was sucessful in as much as it showed the main features expected of it. The dispersion characteristics were approximately as expected, but accurate measurements were not made. The dispersion was observed by watching the behaviour of the end of a psuedo-continous long pulse on an oscilloscope. The delay time of the device changed smoothly as the frequency of the input was changed. The characteristic was accurate to within better than half a microsecond delay time. More accurate measurements were not made because there was too much electromagnetic breakthrough present for this to be done on the available

phase measurement equipment, which could only be operate in a purely continuous-wave mode.

Another problem with the device was that of spurious reflections from the multistrip coupler. These were about 10dB below the level of the desired signal at the peak of the latter's response. The problems of the criticallity of the coupler had been reported before[42], and its ends had been weighted to reduce such reflections. They can still occur, sometimes quite strongly, from faults in the coupler, broken strips or strips shorting together for instance. The amplitude response of the device is also dependent on the correct phasing of the two reflected signals coming into the coupler, and this could prehaps also be upset by coupler faults.

The amplitude response of the device is shown in figure 6.1, together with a dotted curve showing the intended weighting shape. The pulsed insertion loss measurement technique was used to obtain this result to eliminate not only electromagnetic breakthrough but also the reflections from the coupler, which had less time delay than did the response from the reflecting arrays. The agreement between the intended weighting and what what was actually achieved is not very good. When it is considered that of the 20dB or so weighting across the frequency band 125MHz to 175MHz, about 10dB is predicted to be provided by the transducers, the effect of the array weighting is seen to be almost random. The notch at around 130MHz and the response at around 170MHz can be associated with apparent faults in the mask, which would have been caused by errors in the programme which was created to generate the data for the mask-making machine, but the other irregularities are at present inexplicable. The overall minimum insertion loss of the device is around 40dB, which corresponds quite well with the value expected from the results of

Chapman et al.[19] of 35dB, indicating that the calculation of the reflection coefficent of the dots was approximately correct. The source of the 5dB or so inconsistancy is unknown.

Overall this device has shown that inline dispersive devices using RDAs should be feasible, but it cannot be said in itself to have been more than a first step to the design of such a device, if it is intended to try to be able to predict the amplitude responses of such devices.

Further work on this sort of device should include the accurate measurement of its dispersion characteristics, and the determination and elimination of the sources of the errors in the amplitude response.

The other inline device was designed to test the linearity of the relationship between the dot density and the reflection coefficent of the inline array, in view of the doubts expressed in chapter 4 about the linearity of this relationship for some ninety-degree dot arrays.

The device consisted of a series of rectangular blocks of dots, each of which should have a sine(x)/x -like frequency response as an inline reflector, centred at the synchronous frequency of the block and with an amplitude determined by the dot density. The width of the response was of course determined by the length of the block. The dots were arranged in a pattern similar to that which was used for the Taylor-weighted device. The device was designed so that with the transducers tuned it should have had a series of nine passbands, eight at the same level, over a bandwidth of 58 to 82MHz, and the centre one, at 70MHz, being some 22dB stronger. No velocity compensation was used in calculating the periodicity of the array.

The device contained two extra transducers so that the response of the

transducers alone could be measured, to remove one further cause of uncertainty in the calculation of the actual array responses from the overall device insertion loss characteristic. In the end the devices were used untuned to remove a possible cause of disparity between the different transducers.

The insertion loss response of the device is shown in figure 6.2. The superimposed dotted curve shows a prediction of the device's response. This prediction made use of the measured untuned frequency response of the transducers, and made four assumptions in predicting the device response:-

1) That there were no bulk-wave effects present;

2) That there was no piezoelectric slowing within the arrays;

3) That the reflection coefficents of the dots were independent of their packing;

4) That the effects of diffraction and of multiple reflections could be neglected.

The absolute level of the predicted response is arbitrary. The maximum dot density was about half that used in the dispersive device, the dots again being a quarter wavelength wide and rectangular. The blocks were fif-ty wavelengths long and the apertures were 120 centre--frequency wavelengths. The minimum expected insertion loss of the device was around 40dB. The extra loss observed in practice is due mostly to a mistake in the design of the multistrip coupler whereby its periodicity was made twice what it should have been. The response shown in figure 6.2 has been taken with the coupler reflections suppressed in the same way as was done for the Taylor-weighted device.

This fault in the coupler design increased the insertion loss of the

device by about 10 - 15dB, by reducing the coupler's efficency. This was the major factor contributing to the devices high insertion loss. This high insertion loss probably means that the measurement points near the top of figure 6.2 are unreliable. The displacements of the frequency responses at 58 and 70MHz from the predicted curve can be attributed to the piezoelectic slowing. Time domain observations of the shape of the psuedo-continuous signal has shown that the lack of agreement between the predicted and the practical results above 70MHz is due to the effects of bulk waves which were enhanced by the device's being an up-chirp, rather than a down-chirp like the disperser.

Despite these failings, it can be seen that the levels and positions of the responses at 58, 60, 62 and 70MHz are approximately as predicted. The 66MHz response does not agree with that which was predicted. The array weighting at this point is theore-tically -21.6dB. The response at 62MHz, corresponding to an array weighting of -17dB is, however, exactly as predicted, so that it is possible that the high insertion loss of the device at 66MHz has introduced significant errors into the measurements.

The centre fequency of the nominal 70MHz section is at 69.6MHz.This corresponds to a slowing of about 0.6%. The block is 25% metallized, so the expected slowing on YZ lithium niobate would be 2.35% x 25%, that is 0.6%, so that the simple assumption about the slowing being proportional to the amount of metallization would appear to be true for this inline array, at least to within the accuracy of the measurement.

The lower frequency response of this device is encouraging, especially in the apparent linearity of the weighting with dot density. In itself however, this device can yield little reliable quantitative

data. A necessary next step in the design is to rectify the error in the coupler and to remake the device as a down-chirp to try to reduce the level of the bulk wave responses. Quantitative measurements of the amount of slowing present and of the linearity of the weighting could then be made for all the different dot densities in the device.

Both the inline dot array devices described show considerable shortcomings in their performances, but they show that they can be made to work, and it is to be expected that when the shortcomings have been eliminated they could make useful devices. This work has been a first step in the design of such devices.

The main problem facing the long-term sucess of inline array devices lies in the use of the multistrip coupler. Although Chapman et al. have reported that troubles with the coupler have been largely eliminated, the fact remains that the inline devices have introduced a structure which is not tolerant of faults, the coupler used in this way, into reflective array devices, which are usually very tolerant of faults. This will always leave them at a disadvantage in commercial production compared with ninety-degree devices, except in specialized fields where the ability to change their weighting and dispersion characteristics very sharply give them other advantages over these latter. The fact that this work has shown a procedure for finding or calculating the correct array angle for a ninety-degree device means that in that respect the inline array has no long-term advantage over the ninety-degree array.

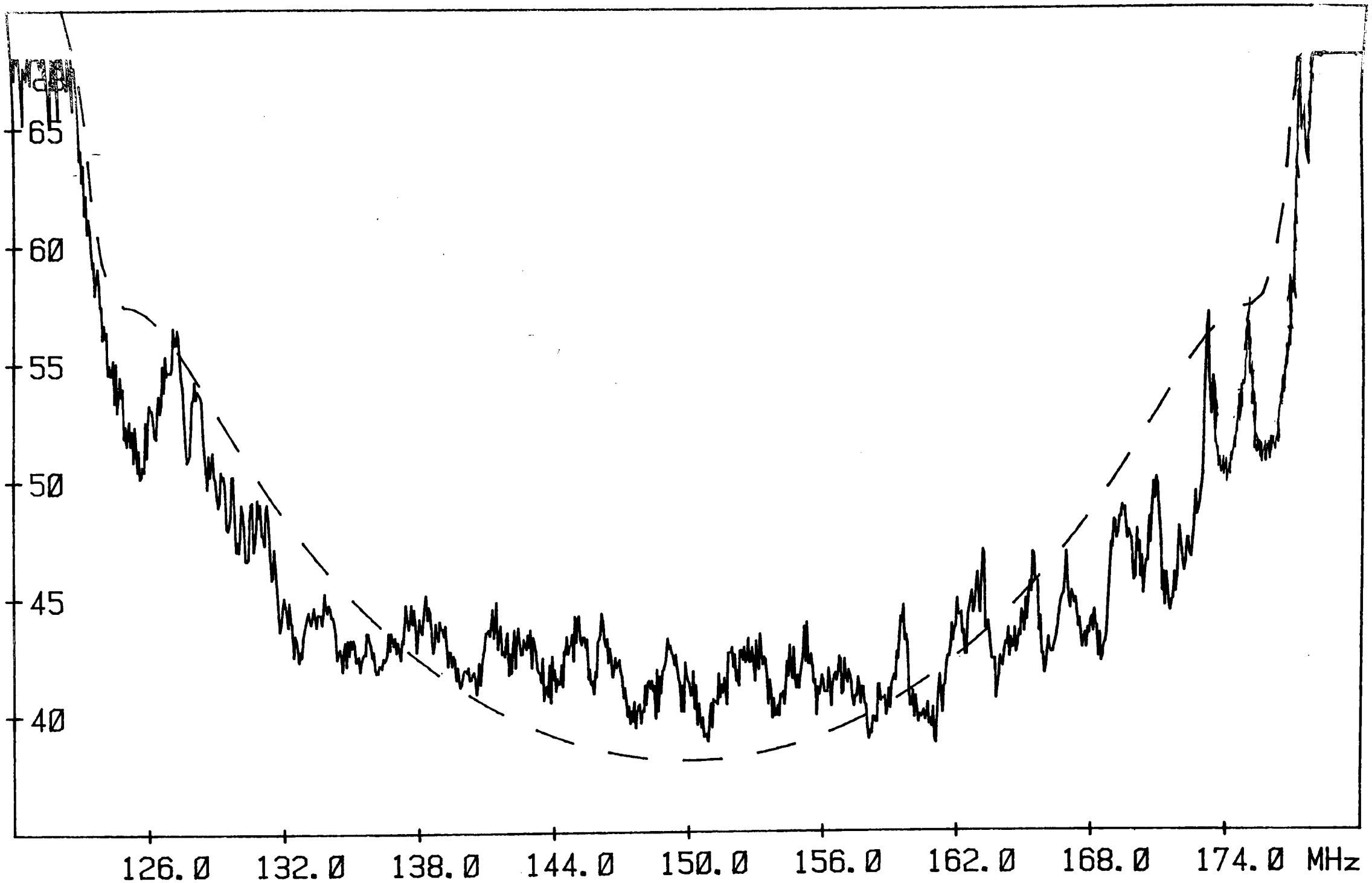

Figure 6.1: Frequency Response of Dispersive Inline Dot Array Device.

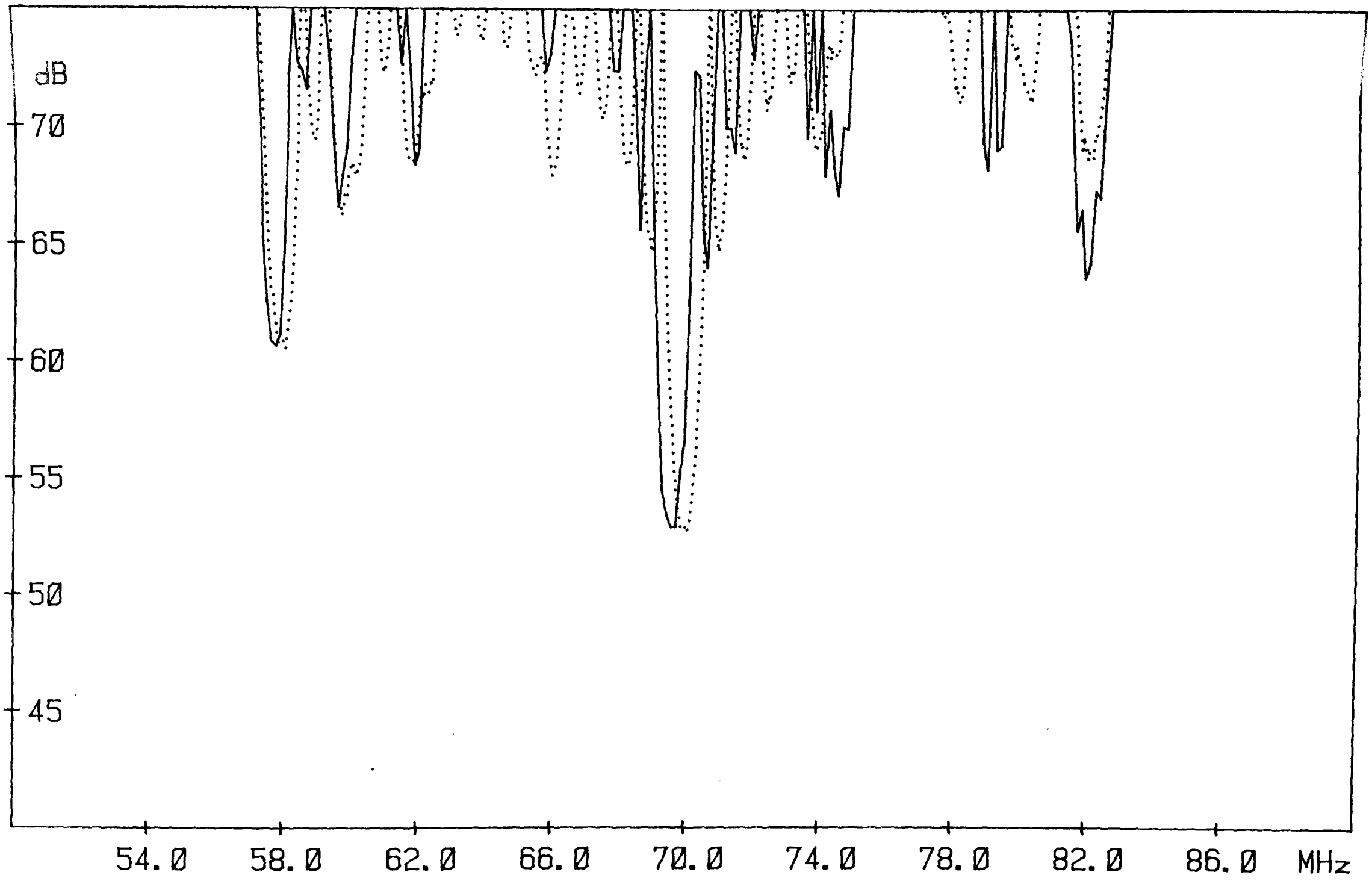

Figure 6.2: Response of Inline Test-Piece Dot Array Device.

CHAPTER 7

CONCLUSIONS

It was stated at the end of the first chapter of this thesis that in order to be able to design sucessful surface acoustic wave devices which used reflective dot arrays it would be necessary to know the velocities of the waves used, in order to get the angle of the reflective arrays correct and in order to be able to set the operating frequencies of the device correctly.

The results presented in chapter 4 have shown that this has been sucessfully done for the commonest substrate material and wave directions, Z and X propagation on Y cut lithium niobate.

Experimental results have been presented which have been obtained by the sucessful application of a simple analytic model of a regular dot array. For the substrate material chosen, these velocities, and hence the the correct angle for the reflecting planes, have been shown to vary as the proportion of metal in the array has been changed, as illustrated in figures 4.17- 4.19. The velocities have been shown to vary linearly with the proportion of the area of the array which has been covered with metal. The effect of the use of varying metal thicknesses has begun to be investigated for the type A1 array, and its effect on the dot reflection coefficent has been shown to be important for that array type, but its effect on the wave velocities has been shown to be small. A procedure has been developed which would enable further measurements to be made in a relatively simple and systematic manner if

they are needed. Evidence has been produced to show that at low proportions of metallization, akin to those which must be used in most dot arrys, the reflection angle becomes almost independent of the proportion of metal, so that when an array with a relatively low degree of metallization is itself weighted, the variations in the correct reflection angle which this would introduce would be negligible.

Different patterns for arranging the dots have been investigated, with the intention of exercising careful control over the directions into which the incident surface wave can be scattered. The results of the type S1 and type A1 arrays, when compared, have also shown the necessity for the exercise of such care.

A simple model has been sucessfully used to analyse weakly reflecting arrays, and has been shown to applicable to uniform arrays presenting device insertion losses of down to 12dB per array.

The existance of multiple reflections within more strongly reflecting arrays has been suggested, and its deleterious effects upon the performance of devices made with such arrays has been demonstrated, as have the difficulties in analysing effects within such arrays (type S1 and S3 arrays).

The simple theory that the reflection angle of an array should vary linearly with the frequency of the incident wave near the correct reflection angle has been shown to be adequate in describing weakly reflective arrays. It has also been shown to be wrong for strongly reflective arrays, where Otto's more complicated theory[31] has been shown to be more sucessful in explaining the variations of reflection angle with frequency.

The simple model for the behaviour of dot arrays has also yielded

accurate values for the reflection coefficents of the dots within the arrays.

It was also said in chapter 1 that data on the reflection coefficents of the individual dots should be available if a reflecting dot array suitable for use in a device to implement some signal processing function were to be able to be synthesized.

A series of measurements of reflection coefficents have been made using different-shaped diamond dots, and the results of these measurements have been discussed in chapter 5. These measurements have revealed several aspects of the properties of the dots which would not be expected from simple geometric consideration of their properties. Chief amongst these are the anisotropy of the type A1/S1 dot and the failure of the type S3 dot to suppress 180-degree reflections. These effects have been attributed to piezoelectric shorting, shorting, and it has been suggested that a quite complex model of the dot would be needed if these effects were to be fully understood.

A variation of the reflection coefficent of the dots with their density in the arrays has also been suggested. If this result is confirmed it could be of great significance if it is desired that amplitude weighting should be included in a reflective dot array. This effect imposes a limitation on the applicability of the simple theory. It is a factor which it would be useful to be able to model, or else the importance of the effect should be determined by experiment for any given case.

Experimental results relating to the reflection of surface waves by strips normal to the propagation path of the waves have

been obtained. These results have been compared with the results of computer-aided analyses of the problem. The results of two analyses have been shown to be in relatively good agreement with each other and with the experimental results for isolated metal strips. The effects of the mutual capacity of the strips has, however, been shown to be extremely important if a series of strips is set close together in an attempt to make their reflections reinforce.

Inline reflective array devices using metal dot arrays have been made, and preliminary results have been reported appertaining to the performance of such devices. The principle of such devices has been shown to work, although it is clear that more work is needed if such devices are to fulfil their promise.

In all, this work has obtained experimental results which should help to give a better basis to the study of reflective dot arrays, by having experimented with new dot types and patterns.

A sucessful model for simple dot arrays has been developed, and the importance of the use of the correct angle for the reflecting planes of dots has been shown, and that angle has been evaluated for several useful cases.

Some experimental data on the reflection coefficents of the individual dots has been obtained, this being the first time that such data has been obtained. The desirability of a model for the behaviour of the dots has been discussed, together with some problems with which such a model would be faced.

Some experimental results have, furthermore, been obtained for the reflections of surface waves by metal strips at normal incidence,

which results have been compared with different models for the problem, with some sucess.

There is one further problem which has been encountered in the design of surface acoustic wave dot arrays, but which has not yet been discussed.This is the problem of the number of dots in the arrays.

In the regular arrays discussed in this thesis, the number of dots was not a significant problem, because the arrays themselves were not particularly big. The masks from which the devices were made were made themselves on a step-and-repeat camera system, at the Royal Signals and Radar Establishment, which could expose several dots at once because of the regularity of the array.

The dot pattern in a dispersive, weighted, array, however, is irregular in both directions on the plane of the substrate, and requires each dot to be exposed individually onto the mask. The inline disperser was of this form, and the problem has recurred in some other devices designed during the course of this work but not reported here. The inline device required over 90,000 exposures on the step and repeat camera to make its mask, which required the mask-making machine to be run for ten hours for its manufacture. Such devices take up large amounts of time on such machines, and constitute very large jobs for them. If the jobs are to become much larger further problems begin to appear with the computer systems which are required to produce the data to drive the mask-making machines.

The use of electron-beam lithography has the potential of easing the problem of the time taken to make devices, and it is theoretically possible to fit very large jobs indeed into the computer systems if they can be broken up into smaller sections.

The whole job, however, remains extremely cumbersome and time-consuming. The potential limitations imposed upon the complexity of dot array devices by these problems were mentioned in passing by Solie on one occasion[14], and must be a factor in any consideration of the future of dot array devices. The complexity of the devices must be constrained by the potential size of the market for them, and by the price which the user is prepared to pay for them. The complexity of the dot array devices and the size of the potential market for them will also affect the point at which dot array devices become competitive with etch-groove array devices. The latter have the advantage of simpler masks, which is important for small runs where the original mask cost could be a significant proportion of the total cost of the device, whereas the dot array is much easier to make from its single mask, and will thus become more competitive for larger runs where the cost of the mask is reduced as a proportion of the overall cost of the device.

The introduction of a generation of mask-making machines in which the computer which actually controls the machine has some ability as a calculator would greatly ease such problems, because the calculating abilities of a four-function calculator within the pattern-generator would reduce the bulk of the data with which it would have to be provided by at least ten-fold for a dispersive RDA. Machines exist with the ability to add and subtract, but to make a disperser the ability to multiply and divide within the mask-maker would be most useful.

The total market for non-uniform masks is, however, so small compared with the integrated-circuit market that the mask-making

machines which are used for surface wave devices should be considered as 'spin-off's from the former, which would have little or no use for such calculating facilities in their mask-makers, so that the development of such machines would itself probably not be a worthwhile venture.

If such mask-making problems do not hamper their development, however, surface acoustic wave dot array devices show considerable promise for the development of relatively cheap devices capable of performing complicated analogue signal processing which cannot be done by other means.

REFERENCES

1: Lord Rayleigh , "On Waves Propagating Along a Plane Surface of an Elastic Solid," Proc. London Math. Soc., 17, pp 4-11, 1885.

2: White, R.M., "Surface Elastic Waves , Propagation and Amplification," IEEE Trans. on Electron Devices, ED-14, pp 181-189, 1967.

3: Maines, J.D. and Paige, E.G.S., "Surface Acoustic Wave Components, Devices and Applications," IEE Review, 120, pp 1078-1110, 1973.

4: Maines, J.D. and Paige, E.G.S., "Surface-Acoustic-Wave Devices for Signal Processing Applications," IEEE Proceedings, 64, pp 639-650, 1976.

5:White, R.M. and Voltmer, F.W., "Direct Piezoelectric Coupling to Surface Elastic Waves," App. Phys. Lett., 13, pp 314-316, 1968.

6: Hartmann, C.S., Bell, D.T. and Rosenfeld, R.C., 'Impulse Model Design of Acoustic Surface-Wave Filters," IEEE Trans. on Microwave Theory and Techniques, MTT-21, pp 162-175, 1973.

7: Milsom, R.F., Reilly, N.H.C. and Redwood, M., "Analysis of Generation and Detection of Surface and Bulk Acoustic Waves by Interdigital Transducers," IEEE Trans on Sonics and Ultrasonics, SU-24, pp 147-166, 1977.

8: Paige E.G.S., "Dispersive Filters: Their Design and Application to Pulse Compression and Temporal Transform," Proc. International Seminar on Component Performance and System Applications of SAW Devices (Aviemore, Scotland), IEE Publication No. 109, pp 115-129, 1973.

9: Heighway, J., Tarrent, D.W. and Oxley, C.H., "Simple Approach to Design of Interface Networks for Surface-Acoustic-Wave Transducers," El. Lett., 8, pp 642-643, 1972.

10: Gerrard, H.M., Jones, W.R., Smith, W.R. and Show, P.B., "Development of Low-Loss 1000:1 Dispersive Filter," Proc. 1972 IEEE Ultrasonics Symposium, pp 253-262.

11: Williamson, R.C., "Properties and Applications of Reflective Array Devices," IEEE Proceedings, 64, pp 702-710, 1976.

12: Gerrard, H.M., Otto, O.W., and Weglein, R.D., "Development of a Broadband Reflective Array 10000:1 Pulse Compression Filter," Proc. 1974 IEEE Ultrasonics Symposium, pp 197-201.

13: Solie, L.P., "A Surface Acoustic Wave Reflecting Dot Array," App. Phys. Lett., 28, pp 420-422, 1976.

14: Solie, L.P., "The Development of High-Performance Reflective Dot Array Devices," Proc. 1979 IEEE Ultrasonics Symposium, pp 682-688.

15: Nash, J.H., "Reflective Dot Array Structures," Annual Report to Ministry of Defence CVD, M.E.S.L., 1977.

16: Solie, L.P., "A Filter Using a Reflecting Dot Array (RDA)," Proc 1976 IEEE Ultrasonics Symposium, pp309-312.

17: Matthai, G.L., O'Shaughnessy, B.P. and Barman, F., "Relations for Analysis and Design of Surface Acoustic Wave Resonators," IEEE Trans. on Sonics and Ultrasonics, SU-23, pp 99-107, 1976.

18: Matthai, G.L. and Barman, F., "SAW Resonators Using Low-Loss 'Waffle Iron' Reflectors," Proc. 1976 IEEE Ultrasonics Symposium, pp 415-418.

19: Chapman, R.E., Chapman, R.K., Morgan, D.P. and Paige, E.G.S., "Weighted In Line Reflective Array Devices," Proc. 1979 IEEE Ultrasonics Symposium," pp 696-700.

20: Matthews, H., Editor, "Surface Wave Filters," Wiley, 1977, pp28-30.

21: Munasinghe, H. and Farnell, G.W., "Surface Scattering at Vertical Discontinuities," Proc. 1972 IEEE Ultrasonics Symposium, pp 267-270.

22: Li, R.C.M. and Melngailis, J., "Second Order Effects Due to Stored Energy at Step Discontinuities," Proc. 1973 IEEE Ultrasonics Symposium, pp503-505.

23: Cambiaggio, E.L. and Cuozzo, F.C., "SAW Reflection from Conducting Strips on LiNbO3," IEEE Trans. on Sonics and Ultrasonics, SU-26, pp 340-344, 1979.

24: Milsom, R.F., Private Communication, 1978.

25: Borges, J.L., Editor, The Anglo American Cyclopedia, 16, pp 918-921, 1917.

26: Marshall, F.G., Paige, E.G.S. and Young, A., "Amplitude Weighted Surface Acoustic Wave Reflective Array Structure," Proc. 1974 IEEE Ultrasonics Symposium, pp 202-204.

27: Gerrard, H.M., and Judd, G.W., "500MHz Bandwidth RAC Filter with Constant Groove Depth," Proc. 1978 IEE Ultrasonics Symposium, pp734-737.

28: Solie, L.P., "Reflective Dot Array Devices," Proc. 1977 IEEE Ultrasonics Symposium, pp 579-584.

29: Otto, O.W. and Weglein, R.D., "SAW Oscillator Using Reflective Gratings," Proc. 1975 IEEE Ultrasonics Symposium, pp 255-260.

30: Marshall, F.G., Newton, C.O. and Paige, E.G.S., "Theory and Design of the Surface Acoustic Wave Multi Strip Coupler," IEEE Trans. on Microwave Theory and Techniques, MTT-21, pp 206-215, 1973.

31: Otto, O.W., "Multiple Reflections in Acoustic Surface Wave Reflective Arrays," IEEE Trans. on Sonics and Ultrasonics, SU-22, pp 251-257, 1975.

32: Cook and Bernfeld, "Radar Signals an Introduction to Theory and Application," Academic Press, 1967, pp 180-182.

33: Richardson, B.A., and Kino, G.S., "Probing of Elastic Surface Waves in Piezoelectric Media," App. Phys. Lett., 16, pp 82-84, 1970.

34: Williamson, R.C., "Improved Electrostatic Probe for the Measurement of Elastic Surface Waves," IEEE Trans. on Sonics and Ultrasonics, SU-19, pp 436-441, 1972.

35: Moreau, J.B., Hashan, R. and Nieu, J.C., "New Electrostatic Probe for Absolute Measurement of Amplitude of Surface Acoustic Waves," El. Lett., 15, pp 155-156, 1979.

36: IEEE Standard 488-1975.

37: Burroughs, W.S., "Junky," Pengiun Books, 1977, p 158.

38: Akcakaya, E., and Farnell, G.W., "Reflection of Acoustic Surface Waves From a Row of Dots," Wave Electronics, 4, pp 49-55, 1979.

39: DeVries, A.J., Miller, R.L. and Wojcik, T.J., "Reflection of Surface Waves from 3 Types of I.D. Transducers," Proc. 1972 IEEE Ultrasonics Symposium, pp 353-358.

40: Ameri, S., Ash, E., Htoo, U., Murray, D. and Wickramasinghe, H., Private Communication.

41: Kogelnik, H., "Bragg Diffraction in Holographic Gratings with Multiple Internal Reflections," JOSA, 57, p431, 1967.

42: Chapman, R.E., Chapman, R.K., Morgan, D.P. and Paige, E.G.S., "Inline Reflective Array Devices," Proc. 1978 IEEE Ultrsonics Symposium, pp 728-733.